

Respiratory Rate Estimation using a Pressure Sensor Mattress

Primo Relatore: *Prof. Domenico Sorrenti*

Secondo Relatore: *Prof. Cristiano Alessandro*

Correlatore: *Prof. Robert Riener*

Tesi di Laurea Magistrale di:
Artemisia Sarteschi
Matricola 829677

Anno Accademico 2021-2022

*Quando la vita si fa dura sai che devi fare Marlin?
Zitto e nuota, nuota e nuota, zitto e nuota e nuota e nuota?
E noi che si fa?
Nuotiam, nuotiam. . .
Dory*

Eidgenössische Technische Hochschule (ETH) Zürich

Department of Health Sciences and Technology

Sensory-Motor Systems Lab

ETH zürich



Sensory-Motor Systems Lab

Contents

1	Introduction	3
2	State of Art	9
2.1	Sleep Stages	9
2.2	Respiratory System	11
2.3	Polysomnography	13
2.3.1	Cardiorespiratory Polysomnography	14
2.4	Unobtrusive sensors	16
2.4.1	Textile Pressure Mattress	17
3	Methods	19
3.1	Instruments	19
3.1.1	Sensomatique	19
3.1.2	SensingTex	21
3.1.3	Nox A1, polysomnography	22
3.1.4	Somnomat Casa	24
3.2	Data Collection	25
3.2.1	Normal Bed	26
3.2.2	Rocking Bed	27
3.2.3	Data processing	28
4	Data Analysis	29
4.1	Preliminary Study on Sensomatique Mattress	29
4.2	Pipeline	31
4.2.1	Weighted and binary method	32

4.2.2	Excluding criteria	32
4.2.3	Denoised Signals	36
4.2.4	Multiresolution Overlap Discrete Wavelet Transform	37
4.2.5	Savitz-Golay filter	40
4.2.6	Subsequent analyses of the filtered signal	43
4.2.7	Compute the Respiratory Rate	45
4.2.8	Result of the Pipeline (visual)	46
5	Result	48
5.1	Evaluation Metrics	49
5.1.1	Mean absolute error	49
5.1.2	Mean absolute percentage error	49
5.1.3	Bland–Altman Plot	50
5.2	Result for MODWTMRA	51
5.2.1	Normal Bed	51
5.2.2	Rocking Bed	64
5.3	Result for Savitzky–Golay filter	77
5.3.1	Normal Bed	77
5.3.2	Rocking Bed	89
5.4	Final Remarks on the Results	100
6	Conclusion	103

Chapter 1

Introduction

This work aims to investigate the possibility of estimating a patient's respiratory rate using a sensor pressure mattress and whether its usage with a rocking bed could hamper reaching this objective. Initially, the possibility of extracting the breath and heart rate from pressure sensors has been investigated using a dataset already available from previous studies. The work, therefore, will focus on respiratory rate. Since the necessary data are not available, data collection has been conducted using an innovative textile pressure sensor mattress and cardiorespiratory polysomnography as ground truth: the primary objective has been to collect data in order to understand the feasibility of determining breath rate from the mattress in case of stationary bed; the second goal has been to understand if the movement of the rocking bed could influence the measurement of the breathing rate. Then a pipeline has been created to analyse the extracted data: from each mattress sensor, the signals are processed to exclude the ones without meaningful information, such as those where the person is not present. Metrics have been designed to assess the confidence that a respiratory pattern could be extracted from a sensor. The selected signals are filtered to eliminate noise using multiresolution analysis of the maximal overlap discrete wavelet transform and Savitz-Golay filter to obtain a clean wave from which the number of breaths a person has in a minute could be counted. As a result, the respiration rate per minute of the person has been obtained and compared with the cardiopulmonary polysomnography to assess the error. The influence of the rocking bed on the mattress has been obtained by comparing the mattress's performance with the stationary bed. As a result of the

pipeline, a heatmap, has been made available to visualise where the best sensors are positioned with respect to the body and mattress.

Sleep is one of the most important physiological functions. Sleep quality can affect physical and mental wellness; for this reason, it is crucial to monitor vital signs and sleep stages without interfering with natural sleep. The state-of-the-art in sleep monitoring technology for physiological data is polysomnography [1], which involves recording sleep stages, respiratory and heart rate, and other parameters. However, this procedure is time-consuming, complicated, expensive, invasive for the patient and often unavailable in hospitals. Even in its simplified version, cardiorespiratory polysomnography [2], where only nose cannulas, chest belts and electrocardiogram (ECG) electrodes are involved and neurophysiological variables are not tracked, the patient is subjected to physical discomfort throughout the night.

Breathing monitoring is also crucial because the population presents a higher percentage of sleep-related breathing disorders that can be studied and monitored with this instrument, like sleep apnoea/hypopnoea syndrome (SAS)[3], where the individuals experience a collapse of the airway in deeper sleep states: the ability to monitor it allows for a faster and closer intervention in severe cases.

Also, in the study of sleep stages [4], it is known that different muscle tones, brain wave patterns, eye movements and heart and breathing rate alterations characterise every phase and stage. In particular, the respiratory rate slowly becomes more stable in the Non-Rapid Eye Movement (NREM) phase and increases during the Rapid Eye Movement (REM) phase, giving the possibility to understand at which stage a person is just by focusing on the respiratory signal[5].

Nowadays, it is possible to achieve this goal using different unobtrusive methods, such as radar technology [6]. The limitation of this approach lies in the fact that the presence of another person in the room, in a hospital condition like a nurse or doctor, or even from fans or oxygen concentrators, could be a source of noise for the radar that could lead to an incorrect prediction; it can also be disturbed by the movement of the patient itself [7]. Another possibility is to use video cameras with infrared filters [8]; even if this approach seems promising, it leads to personal privacy concerns. Currently, it is possible to buy smartwatches, like Garmin[9], that

can estimate multiple vital signs with good precision[10], but they need to be worn all night, which could lead to discomfort for some people. Moreover, these devices do not allow raw data extraction, and tracking is lost if the batteries run out. It is also possible to find under-mattress ballistocardiography-based sensors[11], like Emfit [12], that in case of multiple people inside the bed need to be placed in half of it and the wrong position can lead to inaccurate data.

In this thesis, it has been decided to use unobtrusive methods not to cause discomfort to the user, which could also give us the possibility to track vital signs.

However, the decision of which type of method to use has been influenced by the availability, in the lab where this thesis has been carried out, of a rocking bed part of the *Somnomat*[13] project. This rocking bed aims to interact with the person and study how to improve sleep quality via vestibular stimulation. Also, in this case, the possibility of tracking vital signs could be significant, so the possibility of integrating unobtrusive methods with the Somnomat is part of this thesis. Given all those considerations, the choice fell to pressure sensor mattresses (hereafter referred to as “pressure mattresses”). They can be installed over the standard mattress and are now available as textile-sensor, which means that they can be very thin and lead to negligible discomfort, but at the same time, can be used to track the respiratory rate and, depending on the sensor area density and sampling frequency of the sensors, even heart rate.

In this project, at first, it has been decided to use pressure-sensor textile mattresses from *Sensomatique* [14] that have 14 x 28 sensor elements for a total sensor area of 40cm x 80cm that can cover a width of a regular bed with a sampling rate of 50Hz. Due to the small area of this pressure mattress, it needs to be placed in a specific position and in case the patient moves, it is not possible to have any data. Previous studies have brought out the possibility of estimating breathing patterns; since the data from this mattress and the ground truth data from polysomnography are available, this possibility is explored.

After evaluating a possible valid approach to this data, it has been decided to use it on a second mattress, from *SensingTex* [15] that is already installed in a hospital ward of the *University of Bern* for the study research on movement disorders during sleep in patients with Parkinson’s disease. The ability to estimate breath and heart rate could be helpful for that study. This mattress has a sampling

frequency of 10Hz and 40 x 22 sensor elements for a total area of 192cm x 94cm that can cover a standard bed's area.

Raw data extracted from the mattress can be visualized to determine the person's position and movement, and it is shown as a heatmap since pressure sensors record the different pressures exerted by the presence/absence of a body or by its parts on it.

So it has been possible to create a heatmap to show the variation in colour of the intensity of the pressure, which can produce the shape of a person on the mattress. Looking closer into signals of single channels is possible to see a pattern that resembles a breathing rhythm, similar to the data that can be retrieved from the nasal pressure exerted on the cannula of cardiorespiratory polysomnography. This pattern was the key factor in deciding to use this pressure mattress.

Since there is no data on the rocking bed recorded before this project, it has been necessary to conduct a data collection with two main objectives: the primary has been to collect data to understand the feasibility of extracting breath rate from the mat; the second goal has been to understand if the movement of the rocking bed could influence the signal. Six people participated in the data collection, half male and half female, between 20 and 30 years old. Each participant wears a cardiorespiratory wireless and portable polysomnography device (Nox A1 PSG by Nox Medical[16]) that monitors nasal pressure, pulse, and heart rate with ECG and respiratory inductance plethysmography (RIP), which is a method of evaluating pulmonary ventilation by measuring the movement of the chest and abdominal wall.

The protocol has been divided into two phases:

- The setting for the first phase involved placing the pressure mat over a standard bed. During the night and through the different sleep stages, the breath rate increases or decreases, so it has been decided to insert a similar variability in the data. The participant had to perform a set of five jumps and then lie down in a specific position for four minutes. After this period, they had to stand up, repeat the five jumps and lie down again. The positions follow a pattern of supine, left side, prone, right side and with a total of twenty jumps.

- For the second phase, since the data needs to be collected while the Somnomat is moving, the period for the movement of the bed has been fixed at 4 seconds (15 periods in a minute) with an acceleration of 0.25 m/s^2 . Also, in this phase, the participants were asked to turn around following the specific pattern: supine, left side, prone, right side and remain in that position for 4 minutes.

This resulted in a recording of 32 minutes for each participant divided into 4 minutes in each of the four positions with a standard bed and with Somnomat.

The SensingTex has a total of 1056 sensors, but they are never all significant at the same time. A person's body can not cover the entire mattress and activate all the sensors (hereafter referred to as "Channels") simultaneously. Consequently, this leads to the necessity of an algorithm to discriminate the ones from where it has been possible to extract valuable information. Many of these channels are stationary on a value; others present just interference from the mattress. It has been possible to retrieve a respiratory pattern from just a few sensors and then extract the respiratory rate per minute (rpm). Therefore becomes necessary to design a metric that underlines these channels. This metric must be interpreted as confidence expressed in percentual of the goodness of the signal; at the same time, it is necessary to have a workflow that can estimate a person's respiratory rate from mattress data. This led to the creation of a pipeline that estimates the rpm based on the previous minute. The objective is to create a real-time pipeline in which the streaming of the sensors is simulated with a 60-second long moving window that slides with an interval of 10 seconds on the data collected in the project.

The first step of the pipeline excludes those signals for the entire window length that are either stationary or present only interference from the mattress. That interference appears as spikes but sometimes is present just in a percentage of the signal; the same could happen for stationarities that can be focused in just a subpart of the windows. In this case, the signal has been not excluded and has been assigned with confidence equal to the percentage of the signal that could have meaningful information. Another possibility is a noisy signal, excluded or weighted with a percentage of confidence with the same approach as the previous two.

After these preliminary analyses, the number of signals decreases drastically. It has been assumed to count as one breath the moment between inhaling and

exhaling, which can also be considered a peak in the signal wave. At this point, most of the signals are still noisy. To be better analysed, it has been decided to filter them using two different approaches: Multiresolution analysis of the maximal overlap discrete wavelet transform and Savitz-Golay filter.

The reconstructed signals are given as input to a peak finder algorithm to select both peaks and valleys of the signal. The channels with peaks greater than 30 rpm are excluded because the normal rpm during sleep is between 8-25rpm [17], but since a rate over 25rpm is predictive of cardiopulmonary arrest [18], it has been decided to keep only signals under 30rpm. The remaining signals are further analyzed in their structure to understand whether they represent a breath pattern.

In the end, to calculate the rpm, the channels with the highest confidence percentage are taken into account, and the rpm has been computed as the average of the number of peaks of the signals. A heatmap has also been visualized in the different moments to understand where the best channels are in respect of the body depending on the position.

**indice in forma discorsiva
lo compilo come ultime cosa**

Acknowledgement

The project is carried out in collaboration with *Sensory-Motor System Lab* of Prof. Robert Riener at *Eidgenössische Technische Hochschule (ETH) Zürich* and supervised by Dr. Alexander Breuss, Dr. Oriella Gnarra and Dr. Manuel Fujis[19].

Chapter 2

State of Art

2.1 Sleep Stages

Sleep is a fundamental physiological function that occupies one-third of everyday life and affects almost every type of tissue and system in the body from the brain, heart, and lungs to metabolism, immune function, mood, and disease resistance. The quality and the quantity also can affect mental wellness, for example, lack of sleep affects our memory and ability to think clearly or sleep deprivation can lead to neurological dysfunction such as hallucinations. Moreover, those who do not get enough sleep are at higher risk of developing high blood pressure, cardiovascular disease, diabetes, depression, and obesity [20].

The sleep cycle of a person is divided into two phases Non-Rapid Eye Movement (NREM) and Rapid Eye Movement (REM); this second phase is further divided into three other stages (N1-N3). Different muscle tones, brain wave patterns, eye movements, and heart and breathing rate alterations characterise every phase and stage. Each cycle is approximately 90 minutes long, over the course of the night a person goes through four to six sleep cycles[21]. The composition of each cycle, so time spent in each sleep stage, changes as the night goes along and depending on other factors such as age, recent sleep patterns, and alcohol consumption. During an interrupted sleep, the stages progress as follows, also visible in Fig 2.1:

- Awake to NREM stage 1 sleep.
- NREM stage 1 progresses into NREM stage 2.

- NREM stage 2 is followed by NREM stage 3.
- NREM stage 3 to REM sleep.

Then the cycle comes back to NREM stage 1.

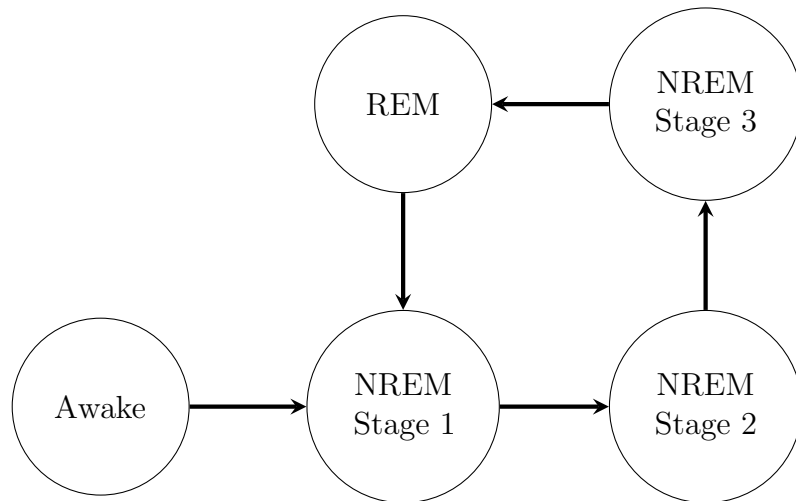


Figure 2.1: Sleep Cycles

NREM sleep is composed of three stages [22]:

- N1: the first stage happens when a person first falls asleep, it last between one and seven minutes. The body has not fully relaxed and body and brain activities start to slow with periods of brief movements. If there are no external events a person can go into stage 2, during the night an uninterrupted sleeper may not spend much more time in stage 1 as they move through further sleep cycles.
- N2: During the second stage the body has a drop in temperature, muscles start to relax, and slowed breathing and heart rate. Simultaneously, brain activity slows, even if they still present some short bursts of activity and eye movement stops. This stage can last for 10 to 25 minutes during the first sleep cycle, and each N2 stage can become longer during the night. Jointly, half of the sleep time is in N2 sleep.

- N3: The last stage of NREM or deep sleep is when the body is more relaxed: muscle tone, pulse and breathing rate decrease. The brain activity during this period has an identifiable pattern of what is known as delta waves. For this reason, stage 3 may also be called delta sleep or slow-wave sleep (SWS). This stage is critical for restorative sleep, allowing for the body to recover and grow. Even though brain activity is reduced, there is evidence that deep sleep contributes to insightful thinking, creativity, and memory[23]. The duration of this stage is 20 to 40 minutes, overnight the other stages became shorter and more time gets spent in REM sleep instead.

REM sleep is characterised by brain activity near levels of awakeness, due to this at the same time the body experience atonia, which is a temporary paralysis of the muscles, with two exceptions: the eyes and the muscles that control breathing. Even though the eyes are closed, they can be seen moving quickly, which is how this stage gets its name. This sleep phase is essential to cognitive functions like memory, learning, creativity and emotions [24]. REM sleep is known for the most vivid dreams, which is explained by the significant uptick in brain activity, this is why the body experiences a temporary atonia as it prevents from acting out inside dreams. Dreams can occur in any sleep stage, but they are less common and intense in the NREM periods. The first REM stage could last only a few minutes, and later stages can last for around an hour.

Both NREM and REM are important because they allow the brain and body to recuperate and develop. Sleepers who are frequently awoken during earlier stages, such as people with sleep apnea, may struggle to properly cycle into these deeper sleep stages. People with insomnia may not get enough total sleep to accumulate the needed time in each stage.

2.2 Respiratory System

Respiration is the physiological process[25] of our body to exchange carbon dioxide (CO_2) with oxygen (O_2). This process has an external phase that consists of the exchange of gases with the environment and the transfer of gas across the blood-gas barrier, and an internal phase that begins with the loading of oxygen onto the haemoglobin molecule and is followed by the transportation, delivery, and transfer

of O₂ to the tissue. CO₂ is delivered back to the lung and ventilated out to the environment with the reversed process.

Normal tidal breathing is comprised of inspiratory and expiratory phases and occurs with the synchronous movement of the thorax and abdomen. In particular, during inhalation (Fig.2.2.a), when we have the loading of O₂ into haemoglobin, the diaphragm moves downward toward the abdomen, and the rib muscles pull the ribs upward and outward making the chest cavity bigger and pulling air through the nose or mouth into the lungs. In exhalation,(Fig.2.2.b), when the CO₂ leave the body, the diaphragm moves upward and the chest wall muscles relax, causing the chest cavity to get smaller and push air out of the respiratory system through the nose or mouth.

This movement can be automatic or can be controlled voluntarily and it is adjusted based on the activity performed at that moment like coughing, sneezing, yawning, or speaking if a person is eating it is coordinated to chew and swallow to avoid choking. It could also increase as a response to physical activity, like running or climbing stairs[26].

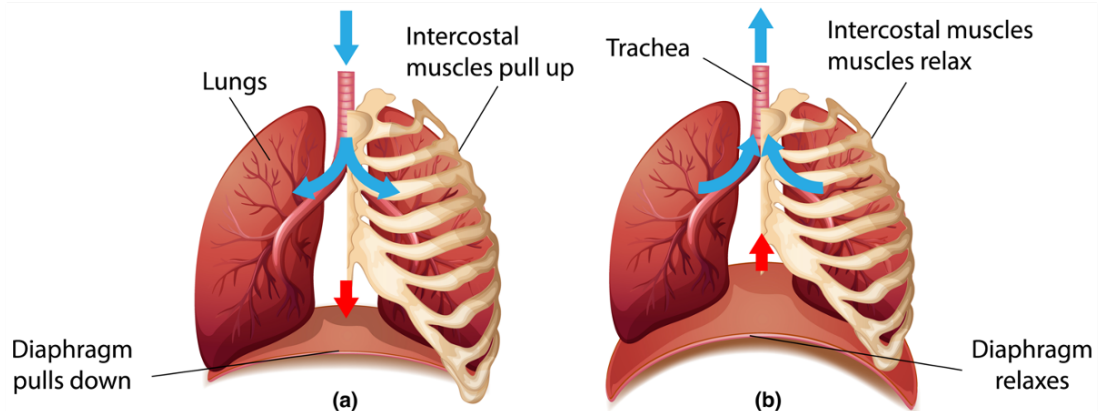


Figure 2.2: Respiratory sistem

The respiration and the tidal volume vary in response to metabolic demand or diseases such as infection. Patients with elevated respiratory rates, reflected by the

magnitude of the metabolic demand, often have a more serious illness.

The respiratory rate per minute (rpm) varies by age, focusing on healthy adults the average respiratory rate at rest is between 12 and 15 breaths per minute[27].

Some studies found that a respiratory rate greater than 20 breaths per min was predictive of cardiopulmonary arrest within 72 hours and death within 30 days[28]; greater than 27 breaths per minute was predictive of cardiopulmonary arrest within 72 hours [29]; also a prospective observational study of acute medical admissions, patients with a composite outcome of cardiopulmonary arrest, intensive care admission, or death within 24 hours had a mean respiratory rate of 27[30].

2.3 Polysomnography

Polysomnography (PSG) is the state-of-art to monitor physiological data during sleep and is used to diagnose sleep disorders [1, 31], such as obstructive sleep apnea (OSA), sleep-related hypoventilation/hypoxia, nocturnal seizure, or periodic limb movement disorder. PSG require a complex monitor system because it consists of several instruments that the patient has to wear, visible in Fig 2.3.

This procedure involves:

- electroencephalogram(EEG)[32]: this test measures electrical activity in the brain using electrodes, small metal discs with wires pasted on the scalp.
- electrooculogram(EOG)[33]: this test measures the corne-positive stain potential relative to the back of the eye, it is performed using skin electrodes outside the eye.
- electromyogram(EMG)[34]: this diagnostic procedure can reveal nerve dysfunction, muscle dysfunction or problem with nerve-to-muscle signal transmission since is used to assess the health of muscles and the nerve cells that control them.
- electrocardiogram(ECG)[35]: this test can be used to check the heart's rhythm and electrical activity.
- pulse oximetry[36]: this electronic device measures the saturation of oxygen carried in red blood cells, it is used to understand how well the oxygen is being sent to the part of the body furthest from the heart.

- cannula: this instrument via nasal pressure monitor the airflow and respiratory effort[37].
- respiratory inductance plethysmography(RIP)[38]: which is a method of evaluating pulmonary ventilation by measuring the movement of the chest and abdominal wall.

As part of PSG are also monitored limb movement, body position and as derived data sleep stages. After the test is completed a “score” analyzes the data by 30-second “epochs”.

2.3.1 Cardiorespiratory Polysomnography

The state-of-the-art to monitor physiological data during sleep is polysomnography (PSG) [1], described in Chapter (2.3, which involves recording sleep stages, respiratory rate, heart and other parameters. However, this procedure is time-consuming, complicated, expensive, invasive for the patient and only sometimes available in hospitals. Focusing on sleep-related breathing disorders, like sleep apnoea/hypopnoea syndrome (SAS), there is the possibility to use cardiorespiratory polysomnography instead of full PSG. This type of PSG involves fewer instruments, as shown in Figure2.4, and in particular, does not record neurophysiological variables avoiding using EEG electrodes that can cause high discomfort for the patient. Even if this method compared to full PSG can collect less parameters, it is used to diagnose SAS [39] and Obstructive sleep apnea(OSA) and other breath-related disturbs or also to track the effectiveness of other treatments during sleep.

Focusing on one of the vital signs that characterise the different sleep stages, respiratory rate (as discussed in Chapter 2.1). It is described by becoming slowly and more stable going from the awake to the REM phase and increasing its rate going to the NREM phase. This fluctuation characterizes the different stages and gives the possibility to understand in which stage a person is based on the parameter extracted via cardiorespiratory PSG [40], such as respiratory inductance plethysmography and nasal pressure. In some studies, the sleep stages, are often classified using a combination of respiratory signals and heart rate [41], that cardiorespiratory PSG monitor.

This instrument is increasingly used in a medical context, for the reasons

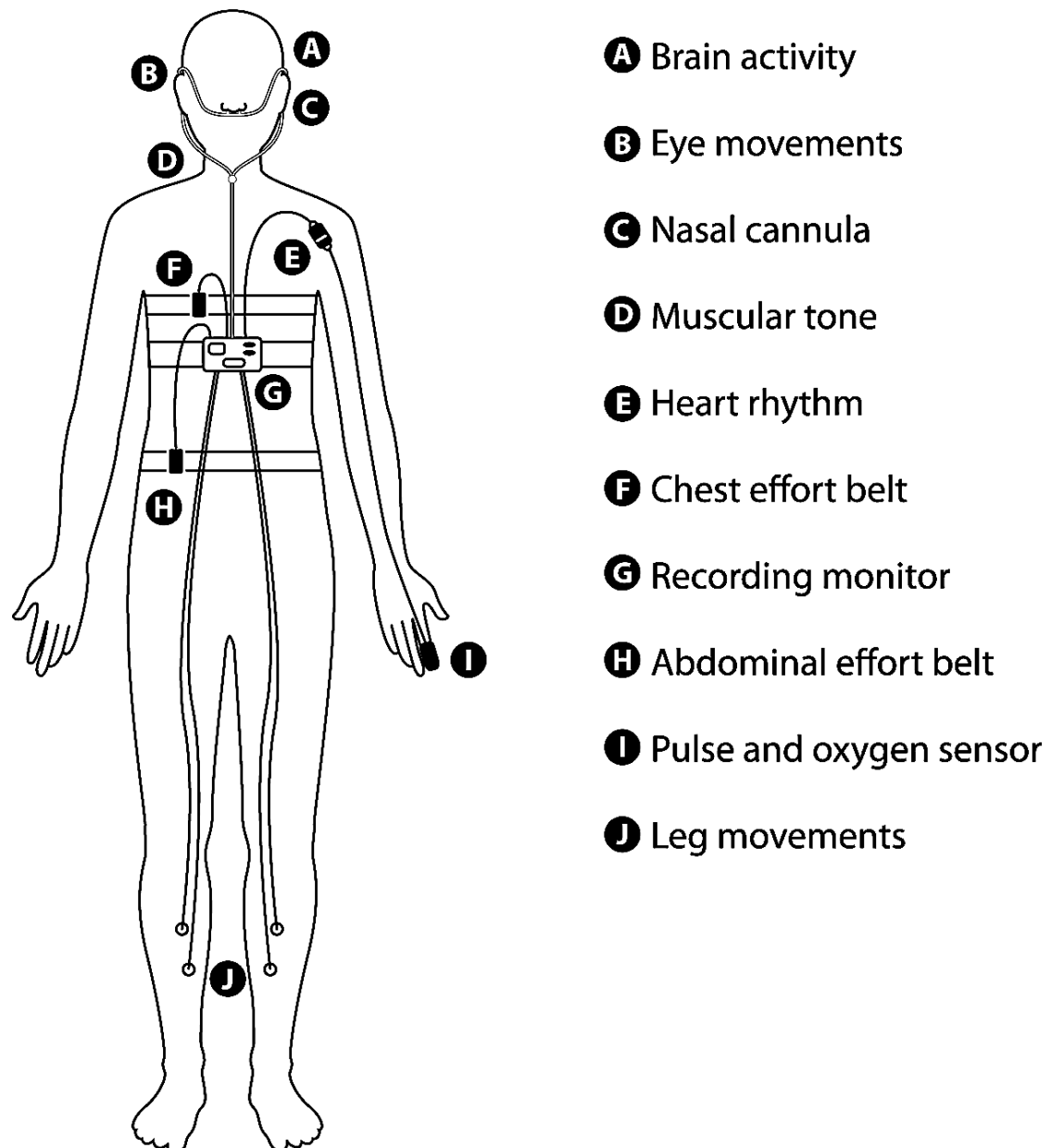


Figure 2.3: Polysomnography

mentioned above and because cardiorespiratory PSG devices are becoming smaller and more portable, such as NOX A1 described in Chapter 3.1.3, with accuracy and user-friendliness that allow being used in a home environment.

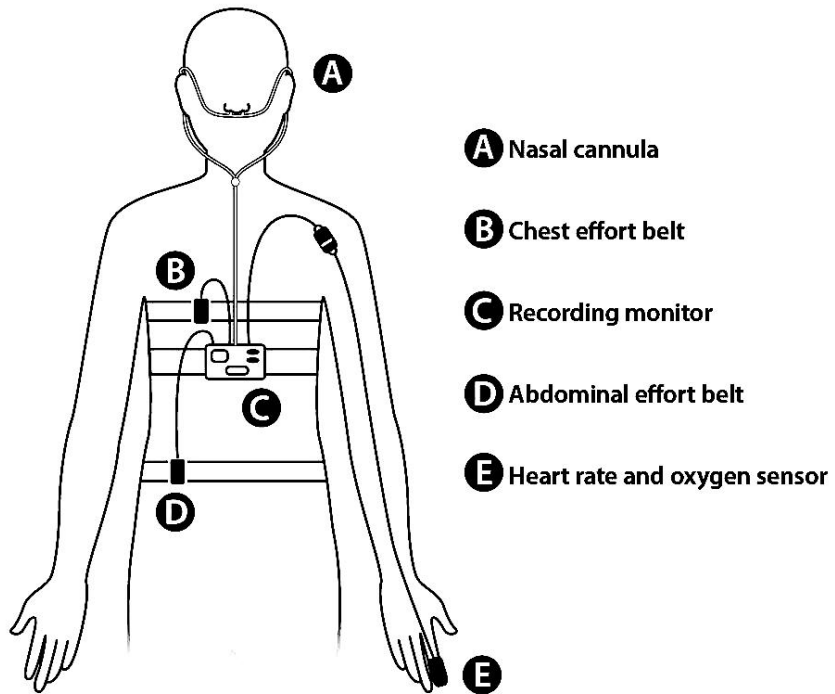


Figure 2.4: Cardiorespiratory Polysomnography

2.4 Unobtrusive sensors

As said before, the state-of-art is a cumbersome device that requires cables attached to the users' bodies and often interferes with natural sleep. To avoid it, in literature is possible to find new instruments such as video cameras, which lead to privacy concerns; radar technology, which could have problems in case there are more than one person inside the room; or smartwatches, which are also able to track respiratory rate but involve to have something on the arm that for some person can lead to discomfort.

The research field focused on discovering unobtrusive sensors to track vital signs

has proposed bed pressure sensors as a possible solution to these concerns. The pressure sensors used today are different and with different kinds of sensors like piezo-electric, inductive and capacitive. As an instrument, in literature is possible to find: pneumatic sensor array [42], as shown in Figure 2.5, that can be placed between the mattress and bad base; micro bend optic fiber sensors mattress [43], shown in Figure 2.6, that are small, lightweight and affordable and also immune to electromagnetic and radio frequency interference, that can be placed directly under body's person; air-mattress [44], shown in Figure 2.7, that measure changes in air pressure inside single air compartment of an inflatable mattress.

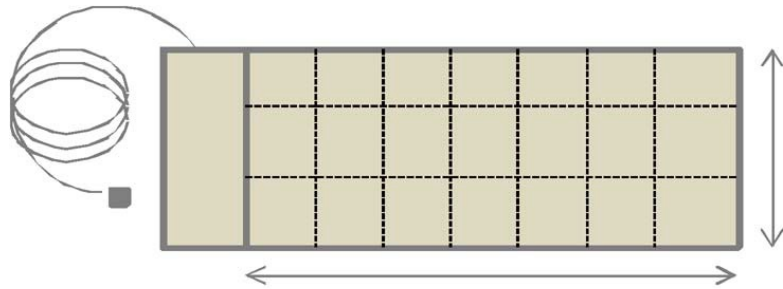


Figure 2.5: Pressure Sensor Array

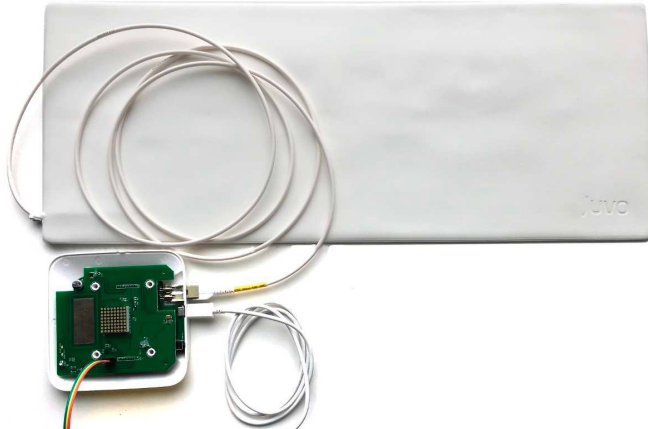


Figure 2.6: Sensing Mat (optic fiber sensors)

2.4.1 Textile Pressure Mattress

A particular type of pressure mattresses available nowadays are textile pressure sensor mattresses, based on piezoelectric sensor, where each sensor appears as shown

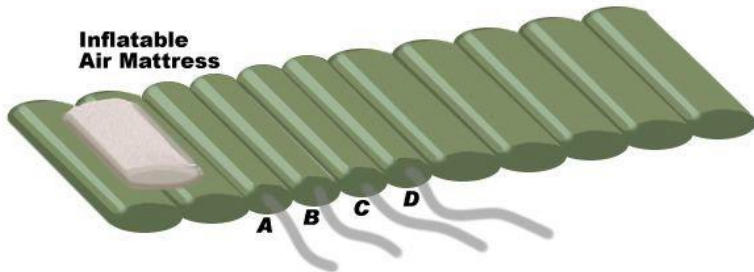


Figure 2.7: Inflatable Mattress

in Figure 2.8. This project involved two of these kinds of mattresses: Sensomative[14] described in Chapter 3.1.1 and SensingTex[15] described in Chapter 3.1.2.

These particular sensor mattresses appear like thin mattresses similar that can be easily installed with adjustable straps over a standard mattress. Due to their small height, they are completely unobtrusive and allow to monitor of both physiological and positional data without interfering with the patient's comfort.

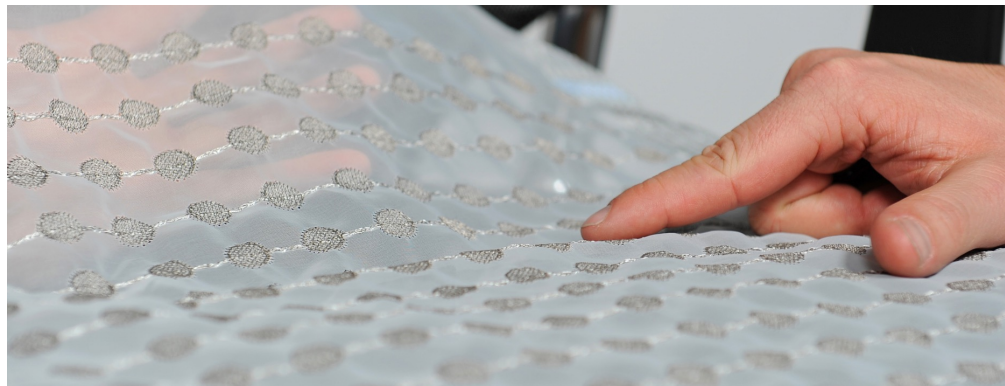


Figure 2.8: Sensomative textile sensors

Chapter 3

Methods

3.1 Instruments

The project involved two textile sensor mattresses: Sensomative and SensingTex (described in Chapter 3.1.1 - 3.1.2) and a rocking bed Somnomat Casa described in Chapter 3.1.4.

The chosen instrument to collect the ground truth, cardiopulmonary polysomnography, is Nox A1, described in Chapter 3.1.3.

3.1.1 Sensomative

Sensomative (Rothenburg, Switzerland)[14] is a start-up company, founded in 2015 in Switzerland, which produces textile pressure-measuring mats. These are based on the same principle as resistive touchpads. The sensor mass consists of two layers of conductive textile which are separated from each other by a spacer grid.

The sensor seen in Fig.3.1 is composed of 14 x 28 sensor elements with a sampling frequency of 50Hz. The sensing area is 40 cm x 80 cm and thus stretches almost over the entire width of a standard-sized bed. Each sensor element is round and has a diameter of 2 cm. This mattress is commonly used to investigate position since it is possible to have the pressure distribution (example visible in Fig.3.2). This mattress is used, for example, to control the sitting posture of office chairs and wheelchairs, analysing the pressure distribution is possible to discover posture

errors and uneven loads.



Figure 3.1: Sensomative over a bed

However, its dimension of 40 cm x 80 cm does not allow it to cover the entire mattress so it is crucial to find the correct position to detect the desirable data. In this project, the aim is to estimate the respiration rate so the position chosen is under the lungs, so from just above the shoulder to the middle of the abdomen.

This is to be able to track the movement of the thorax during respiration. The movement is extracted and evaluated from the single sensor channel of the mattress, for the inhalation phase it has been seen an increase in pressure and during the exhalation phase a decrease. Following a pattern, as shown in Figure 4.1, similar to nasal pressure or respiratory inductance plethysmography, recorded by the cardiopulmonary polysomnography, described in section 3.1.3.

The data for this mattress are a subsection of the entire data and come from a previous data collection of one of the supervisors of this thesis, Manuel Fujis [19], who kindly make them available to inspect further the possibility to estimate respiratory rate from this mattress and also to have the data to do a preliminary study of the general feasibility to extract this physiological data.

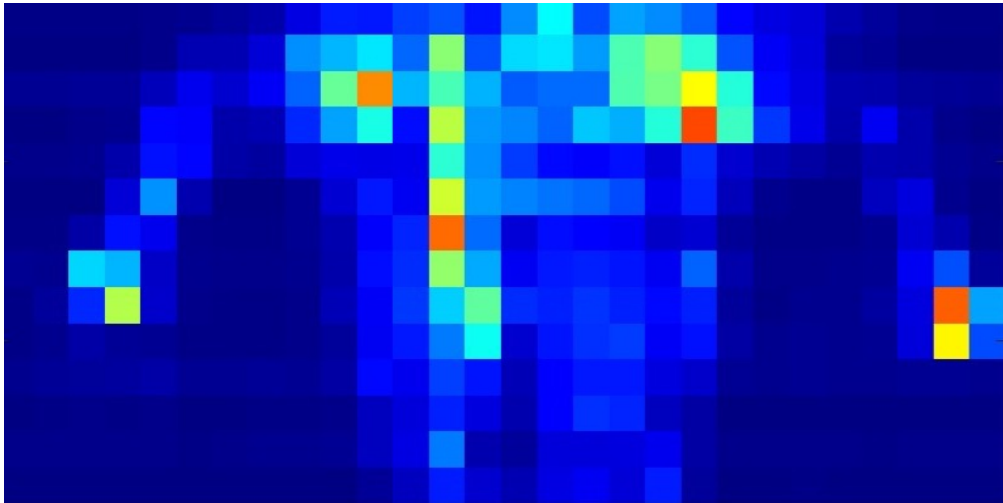


Figure 3.2: Sensomative data

3.1.2 SensingTex

The instrument on which this thesis is focalised then is SensigTex [15], visible in Fig 3.3 this is a commercially available textile pressure sensor mattress. The Mattress Mat Dev Kit is capable to cover the entire area of a bed measuring 192cm x 94cm, with 48 x 22 sensor elements and a sampling rate of 10Hz. This means that is five times slower than Sensomative (Chapter 3.1.1), but that is already installed in a hospital ward of the *University of Bern* for the study research on movement disorders during sleep in patients with Parkinson's disease. The ability to estimate breath could be helpful for that study and then this project focused on this possibility.

This mattress is already implemented in the context of position classification because as shown in Figure 3.4, is possible to retrieve the position of the person on it. The raw data has a scale in the range of 0-256 (minimum-maximum).

Looking closer into signals of single channels is possible to see a pattern that resembles a breathing rhythm, similar to the data that can be retrieved from the nasal pressure exerted on the cannula of cardiorespiratory polysomnography, as

shown in Figure 4.13.



Figure 3.3: SensigTex over a bed

3.1.3 Nox A1, polysomnography

As explained in Chapter 2.3.1 cardiopulmonary polysomnography is an accepted method to monitor physiological data during sleep.

Since in the data collection conducted during the thesis, further explained in Chapter 3.2, it has been necessary to have a gold standard to track the respiratory rate and validate estimated respiratory rate from the pipeline, described in Chapter 4.2.

The instrument chosen has been Nox A1 of NoxMedical, shown in Figure 3.5, a wireless and portable PSG recording the following physiological parameters:

- Nasal pressure and Nasal Flow via nasal cannula.
- Chest and Abdomen Movement with respiratory inductance plethysmography (RIP) gathered together in a parameter called "RIP Flow"

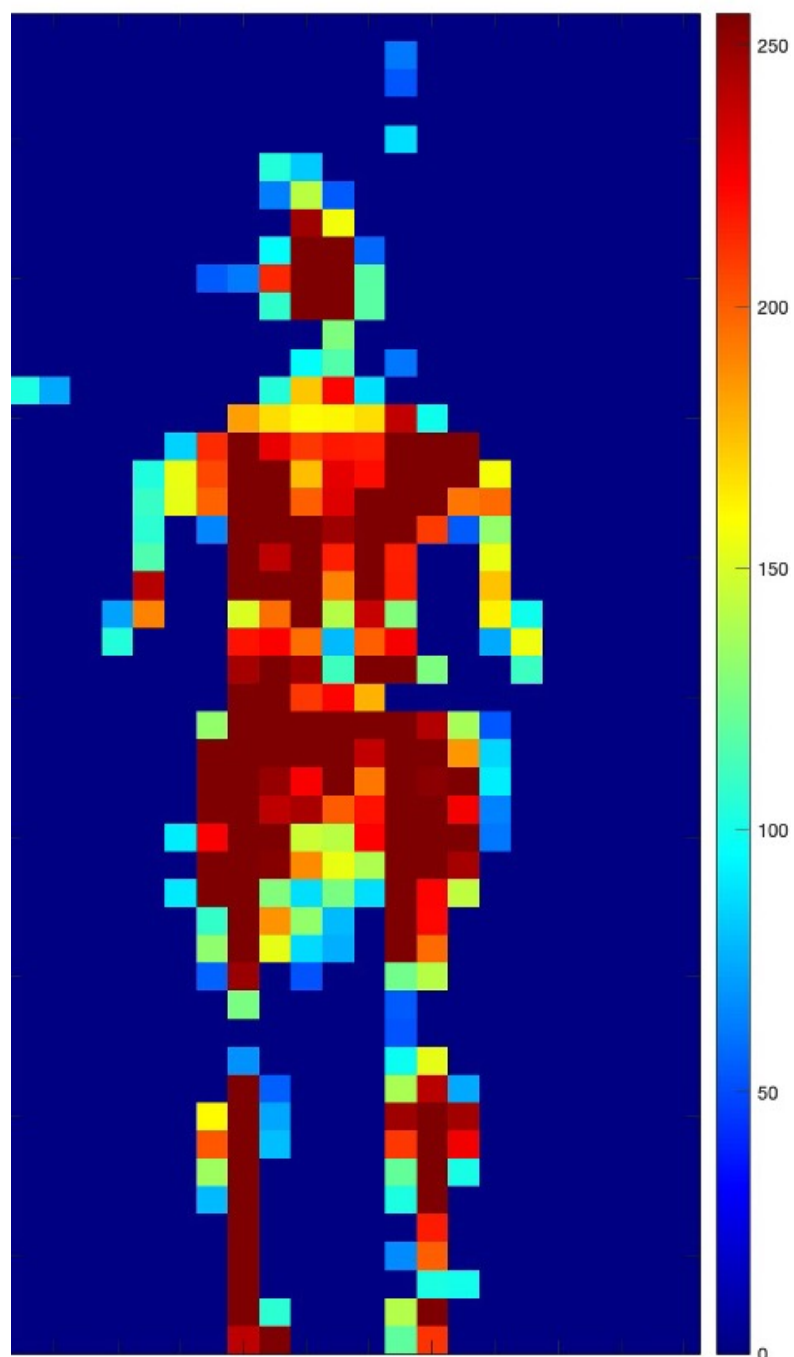


Figure 3.4: SensigTex Data

- Heart Rate (ECG)
- SPO2 and Pulse with a fingertip

In the pipeline (Chapter4.2) it has been decided to use the Resp Rate (respiratory rate) calculated by the NOX A1 and displayed as respirations per minute or [rpm] based on RIP Flow data. However, to further understand if the channels in the mattress represent the correct respiratory rate also used Nasal pressure and Nasal Flow.



Figure 3.5: Nox A1™ PSG System device of NoxMedical

3.1.4 Somnomat Casa

The lab, where this thesis is carried out, has one of the main focuses on sleep robotics. Inside the Somnomat project, there are two research domains: one covers controlled positional therapy and the other investigates the potential benefits of rocking movements on sleep.

The second research domain aims to replicate the rocking movement made by the mother to help babies to fall asleep, replicating back-and-forth motions. The Somnomat Casa, shown in Figure3.6, looks like a conventional bed but fits into private bedrooms and can be operated by the push of a button. Rocking movement

has determined suitable motion parameters and mechanical adaptations to have an inaudible rocking mechanism.

The possibility to estimate the respiratory rate of a person while the rocking bed is moving could be important to discover how this movement could help to fall asleep, based also on the respiration rate. As discussed in Chapter 2.1, breathing is one of the parameters that highlight the sleep stage in which the person is in that moment. This knowledge could be used to further implement the intervention.



Figure 3.6: Somnomat

3.2 Data Collection

In the course of the thesis project been conducted data collection because the data from Sensingtex where not has been collected yet. However, the availability of a rocking bed gives this data collection a second objective. The primary objective

has been to collect data from SensingTex to understand the feasibility of extracting breath rate from the mat; the second goal is to understand if the movement of the rocking bed could influence the signal.

The participant involved were 6, half male and half female, between 20-30 years old, who were asked to lie on a standard mattress covered with the sensor mattresses in a specific position, for the first part of the data collection (described in Chapter 3.2.1), and on a rocking bed while it is moving, for the second part of the data collection (described in Chapter 3.2.2). Each participant wore a cardiorespiratory wireless and portable polysomnography device (Nox A1 PSG of Nox Medical), described in Chapter 3.1.3. The total length of the data collection for each participant is 36 minutes long divided into 4 minutes in each of the 4 positions with normal bed and with Somnomat.

3.2.1 Normal Bed

The first part of the data collection aims to understand the feasibility of extracting breath rate from the mat, so the setting involves the pressure mat over a standard bed.

During the night and through the different sleep stages, the breath rate increase or decreases, so we decide to insert a similar variability in our data. Since this study is performed in a laboratory condition to recreate this it has been asked to the participant to perform a set of five jumps before lying down, so it is expected to find in the data this variability that is firstly checked with the data coming from the ground truth.

The participant performs the jumps and then lies down on a mattress in a specific position for 4 minutes. After that, they were asked to stand up, perform the other 4 jumps and go down again. This is done for each of the positions of the pattern: supine, left side, prone, and right side. The total number of jumps performed is 20 and the Toal time for this part is about 18 minutes (including getting in and out of bed and jump time).

PLACE HOLDER PER INSERIRE WORKFLOW DI QUESTA PARTE DELLA DATA COLLECTION

Figure 3.7: Place holder normal bed

3.2.2 Rocking Bed

The second part of the data collection aims to understand if the movement of the rocking bed could influence the signal.

Since the data are collected while the Somnomat Casa is moving, it has been fixed the period for the movement of the bed at 4 seconds (15 periods in a minute) with an acceleration of 0.25 m/s^2 . The participant has not been asked to perform any jumps, to have less variability in breath patterns and see the possible interference from the mattress. They have been asked to lie down in a supine position for 4 minutes, and after that, they have been asked to turn around on the left side. This has been asked to perform for all the positions: supine, left side, prone, and right side. The total time for this part is about 18 minutes, including the necessary time to turn around on the bed and stop the movement between each position.

PLACE HOLDER PER INSERIRE WORKFLOW DI QUESTA PARTE DELLA DATA COLLECTION

Figure 3.8: Place holder rocking bed

3.2.3 Data processing

After the data collection, it has been necessary to clean the data in order to remove the moment when the participant was getting in and out of the bed.

For each recording, based on different data extracted from the PSG and pressure mattress, is possible to retrieve when the person stands up to perform the jumps or to turn around in another position. As shown in Figure 3.9, based on nasal pressure data, is possible to recognize the different moments. In the left part of the plot the four positions on the stationary bed and in the right part the four positions on the moving bed. In the end, for each participant are available eight different recordings, 4 minutes long, one for each position of the different phases in which the data collection is divided.

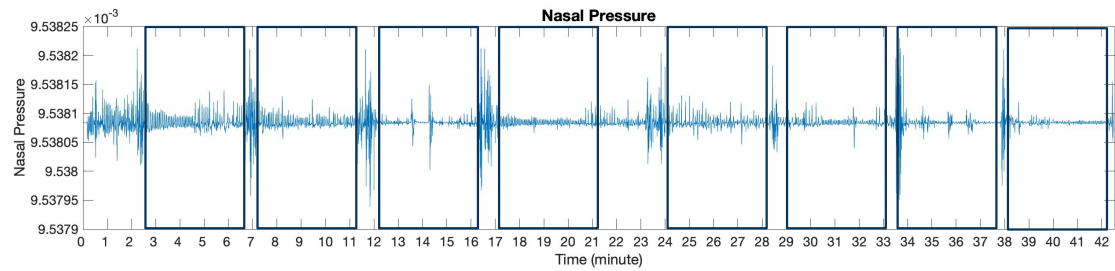


Figure 3.9: Full recording of a participant - 42 minutes long

Chapter 4

Data Analysis

The data analysis focuses, in the first section 4.1, on the preliminary study conducted to understand the feasibility to estimate respiratory rate from a pressure sensor mattress. The data involved in the first part belong to the Sensomative mattress (Chapter 3.1.1), collected by a supervisor of this thesis, Manuel Fujis [19], who kindly make them available. During the second section 4.2 is presented the pipeline to analyse the data extracted with the data collection. This pipeline aims to find the best channels, that represent a respiratory pattern, in the mattress and from them estimate the respiratory rate per minute.

4.1 Preliminary Study on Sensomative Mattress

A preliminary study on the feasibility of estimating breathing rate from a mattress is conducted on a subsect of the available data belonging to Sensomative mattress (Chapter 3.1.1).

From the comparison of raw mattress data and nasal pressure (PSG), as shown in Figure 4.1, is possible to retrieve a respiratory pattern. This is the starting point of the preliminary study.

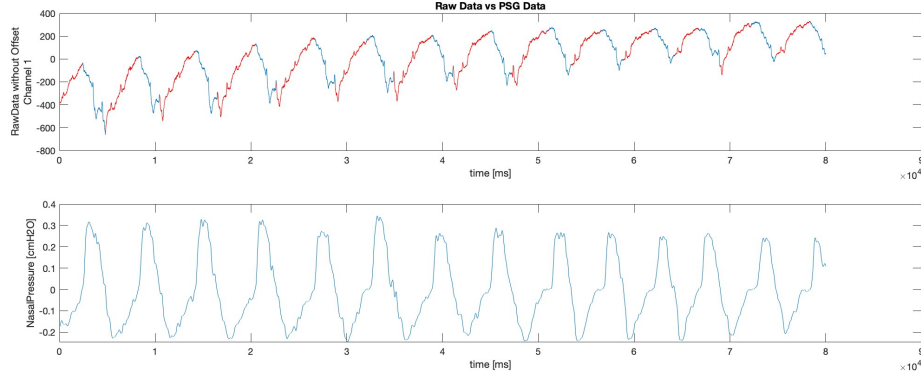


Figure 4.1: Breath pattern

The moment between inhaling and exhaling, visible as a peak in the raw data and the PSG data, is counted as a breath. The raw data are too noisy to be given as input to a peak finder, for this reason, is applied a multiresolution overlap discrete wavelet transform, explained later in Chapter 4.2.4.

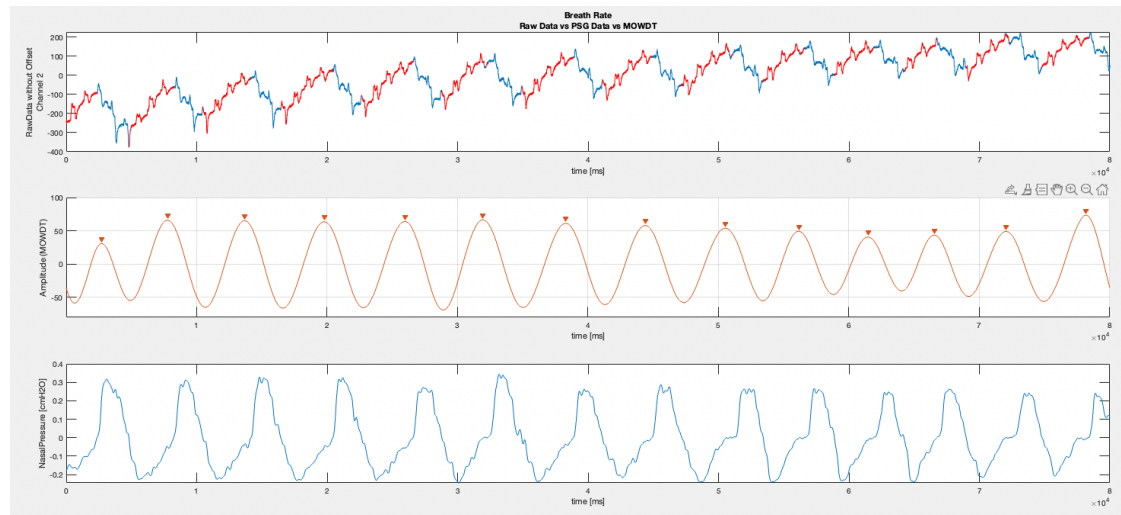


Figure 4.2: MODWTMRA reconstruction

The so reconstruct signal is given as input to a peak finder that allows counting them and obtaining the respiration rate per minute (rpm).

4.2 Pipeline

The designed pipeline aims to replicate a semi-realtime analysis using the data obtained from the SensingTex mattress, during the data collection.

The SensingTex has a total number of sensors of 1056, and consequently, the same number of signals from the mattress; this leads to the necessity of an algorithm to discriminate the ones from whom it is possible to extract valuable information about the respiratory rate of the person on the mattress. A person's body can not cover the entire mattress and activate all sensors (hereafter referred to as "Channels") simultaneously. Many of these channels present a signal that is stationary on a value; others present just interference from the mattress. From just a few sensors, it is possible to retrieve a respiratory pattern and extract the respiratory rate per minute (rpm). Therefore becomes necessary to design a metric that underlines these channels. The meaning of this metric must be interpreted as confidence expressed as the goodness of the signal in percentual.

Since the designed pipeline aims to replicate a semi-realtime analysis, it takes in input a sliding window of 60 seconds that is moving, for each position, through the 4-minute recording obtained after the cleaning of the data (Chapter 3.2.3). Figure 4.3 shows a 4-minute recording with a highlighted window of 60 seconds, which can be consulted in more detail in figure 4.4.

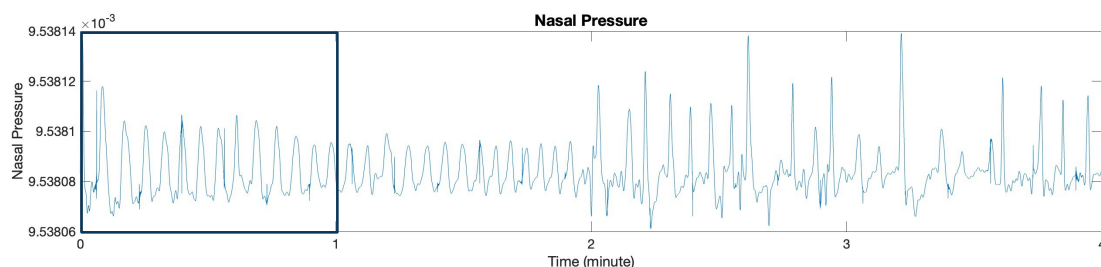


Figure 4.3: 4 minute

In Figure 4.5 it is possible to visualize a scheme of the entire pipeline.

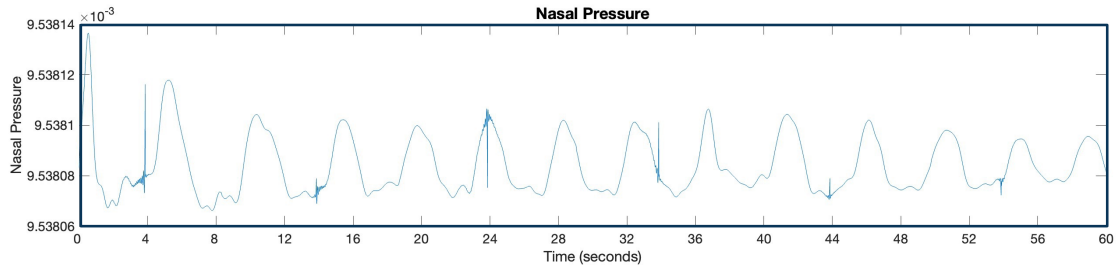


Figure 4.4: 1 minute

4.2.1 Weighted and binary method

The metric has been designed as a confidence expressed as the goodness of the signal in percentual. To create this percentual has been decided to use create a series of criteria that each signal has to follow.

Some of these criteria, such as in Chapter 4.2.2, are excluding criteria, that are referred to particular phenomena that if present for the entire length lead to having an unusable signal. If one of these criteria is not passed the signal is not further analysed, but if they present the phenomena but not for the entire length, it has been decided to keep them and understand if in another part they could be meaningful. So they can express the percentage of the signal that follow those criteria or just that they present a possible meaningful part.

For this reason, it has been implemented a version of the pipeline where the criteria are binary, they can be passed or not (1 passed, 0 not passed), and a version where some criteria give as an answer the percentage of the channel that could contain valuable information (hereafter also referred to as "weighted method"). For each criterion, the following section will explain the different outputs of the metrics, in the case of binary or weighted approach. In both cases, the final confidence is the mean of percentages of each criterion.

4.2.2 Excluding criteria

The first step of this pipeline excludes those signals for the entire window length that is stationary on value, with small amplitude, or present only interference from the mattress. So channels do not have meaningful information, in case this behaviour is present in a part of the signal the output for the metric is different

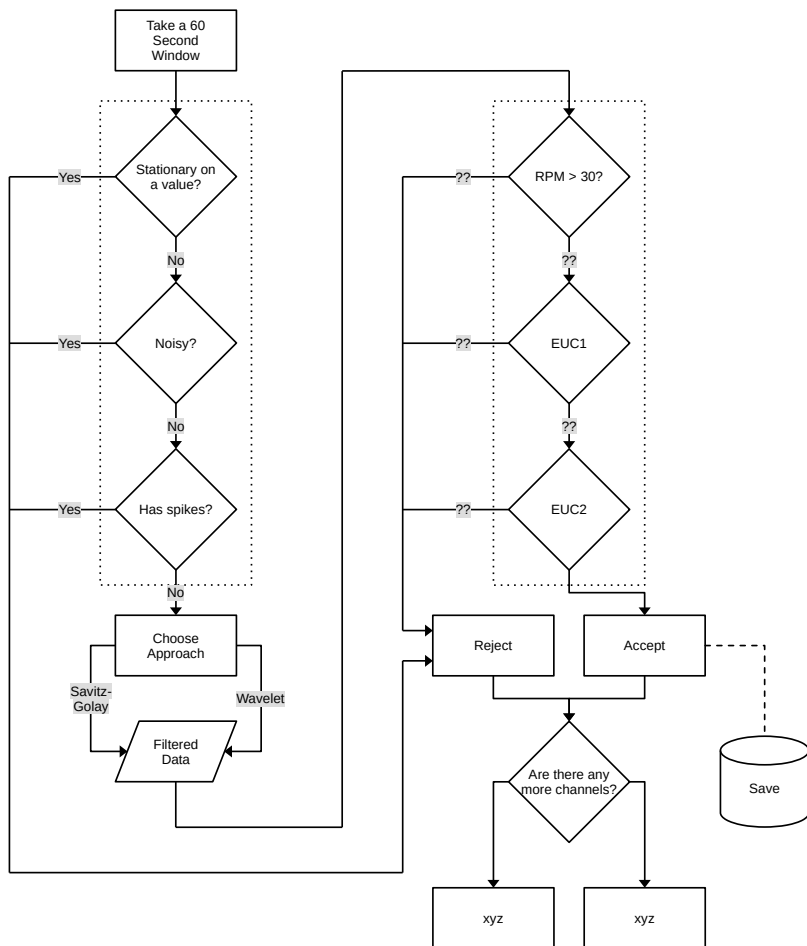


Figure 4.5: Pipeline

based on the binary or weighted approach. Artefacts are the only excluding criteria.

Stationary signals on a value

A stationary signal on a value is defined as a signal that remains on the same value for the entire length of the window.

An example of the stationary signal on a value is shown in Figure 4.6, in this case, the channel, for this window, is excluded and not further analysed. However, since it is used as a moving window it will take again into account in the next window and, if it presents a different behaviour, it maybe is considered. Nevertheless, If the channel presents only a part of the signal stationary on a value as in Figure 4.7, the channel is given as a percentage of confidence, the percentage of the non-stationary on a value signal for weighted approach or 1 for binary if the non-stationary value is more than 20%.

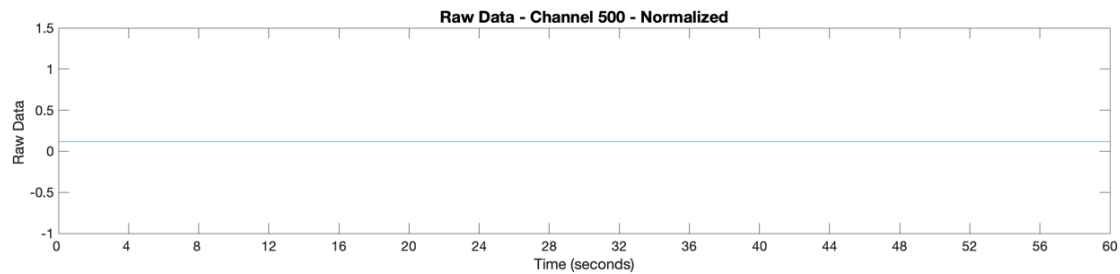


Figure 4.6: Raw Data - Channel 500 - Stationary on a Value

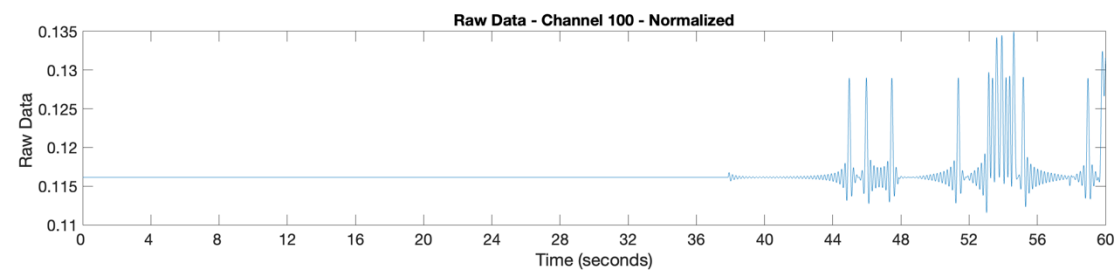


Figure 4.7: Raw Data - Channel 100 - Partial Stationary Signal

Signal with small amplitude

Several channels present a signal with a small amplitude, between [intervall], an example is visible in Figure 4.8, so after verifying if they are not stationary on a value case (Chapter 4.2.2), if the signal presents a small amplitude for the entire length of the window that could not represent a respiratory pattern is excluded. Otherwise, if part of the signal does not have a small amplitude: for the weighted approach, the percentage of confidence in output is equal to the percentage of a signal without a small amplitude.; for the binary approach, the criteria is passed if the small amplitude is present in less than 20% of the signal. As in the previous case, due to the moving window nature of the pipeline after the shift of 10 seconds, the channel could have a different behaviour and be further analysed.

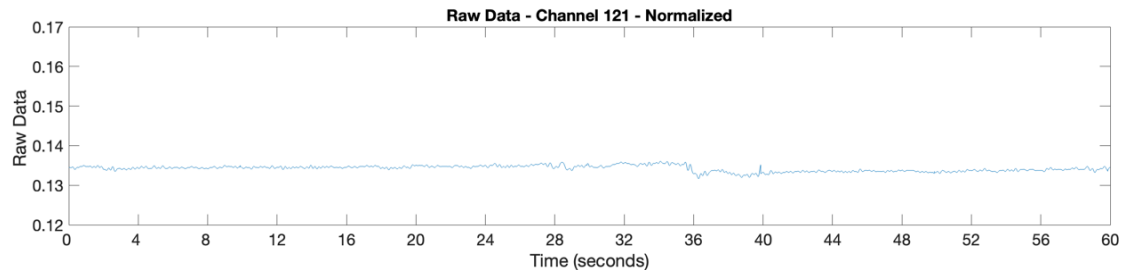


Figure 4.8: Raw Data - Channel 121 - Small amplitude

Spikes Signals

The mattress can produce artefacts, that are visible in the channels as spikes as in Figure 4.9. Since these artefacts are visible also in channels that present a good respiratory pattern (Figure 4.10), after evaluating different thresholds it has been decided to accept the channel that has a percentage of spikes under 30%. In this case, both methods (binary and weighted), has the same output 100% or 1 in case of passed criteria, 0 otherwise.

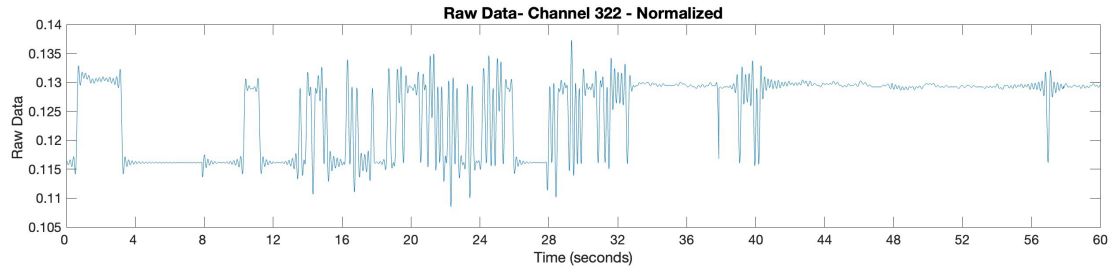


Figure 4.9: Raw Data - Channel 322 - Massive presence of Spike

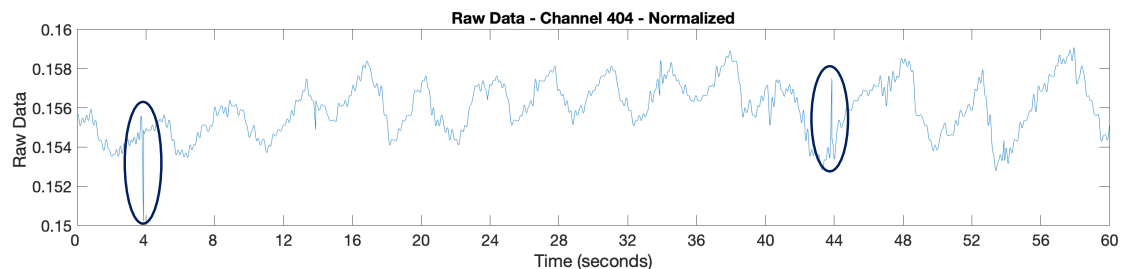


Figure 4.10: Raw Data - Channel 404 - Small presence of spikes

4.2.3 Denoised Signals

After these preliminary analyses, the number of signals decreases drastically; as a result, has been obtained signals that could contain valuable information and the relative percentage of confidence. To be able to estimate the number of breaths it has been assumed to count as one breath the moment between inhale and exhale, which can also be considered a peak in the signal. At this point, most of the signals are still noisy. To be better analysed has been decided to filter them. In general, filtering consists of replacing each point of a signal with some combination of the signal values contained in a moving window centred at the point, on the assumption that nearby points measure nearly the same underlying value.

In this pipeline two different kinds of approaches are involved: Multiresolution analysis of the maximal overlap discrete wavelet transform (Chapter 4.2.4), and Savitz-Golay filter (Chapter 4.2.5). It is possible to choose which approach to use in the context of the data, in this project are both used rather than compare them.

4.2.4 Multiresolution Overlap Discrete Wavelet Transform

The Multiresolution Overlap Discrete Wavelet Transform (hereafter also referred to as "MODWTMRA") is based on wavelet analysis (MOWDT) that transforms the original signal into a time-frequency domain to be analysed and processed, the multiresolution analysis (MRA), which cuts the signal into components, can produce the original signal exactly when added back together.

The input data of MOWDT are samples of a function $f(x)$ evaluated at N time points, this function can be expressed as the linear combination of the scaling function $\phi(x)$ and wavelet $\psi(x)$ at varying scales and translations:

$$f(x) = \sum_{k=0}^{N-1} c_k 2^{-J_0/2} \phi(2^{-J_0}x - k) + \sum_{j=1}^{J_0} f_j(x)$$

where

$$f_j(x) = \sum_{k=0}^{N-1} d_{j,k} 2^{-J/2} \phi(2^{-J}x - k)$$

and J_0 is the number of levels of wavelet decomposition calculated as $\text{floor}(\log_2(N))$.

The first sum represents the first approximation of the signal and then the successive scales. MODWT returns the N coefficients $\{c_k\}$ and the $(J_0 \times N)$ detail coefficients $\{d_{j,k}\}$ of the expansion.

Since it has been used the MODWTMRA, instead of just MODWT, the returns are the projections of the function $f(x)$ onto the various wavelet subspaces and final scaling space. That is, MODWTMRA returns

$$\sum_{k=0}^{N-1} c_k 2^{-J_0/2} \phi(2^{-J_0}x - k)$$

and the J_0 -many $\{f_j(x)\}$ evalutaed at N time points. It is then obtained a projection of $f(x)$ onto a different subspace, the original signal can be recovered by adding all the projections.

For our approach, we choose the Daubechies wavelet with two vanishing moments (Figure 4.11) that better represent the breath signal present in our data.

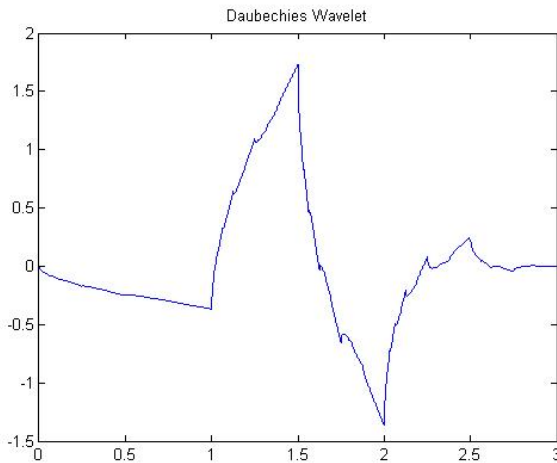


Figure 4.11: Daubechies wavelet with two vanishing moments

The decomposition of the signal of channel 404 (Figure 4.13), is shown in Figure 4.12. The raw data has been decomposed into 13 levels to obtain our denoised signal, it has been decided to sum only a subset of this scale, which allowed us to reconstruct a clear signal where the peaks could be underlined and counted.

Application in the Pipeline

To show the application of the MOWDTMRA in the pipeline, the signal in Figure 4.13, which has not been excluded by the criteria explained in Chapter 4.2.2 is taken as an example.

The signal is decomposed into 13 levels, as shown in Figure 4.12, and choose the levels that are added together to reconstruct the signal of breath rate, in the context of this project the 9th and 10th level. The levels are chosen to recreate a wave that best fits the original wave of the signal but excludes the noise. The resulting wave is given as input to a peak finder to point out the moment between inhaling and exhaling, visible as a peak in the wave and counted as a breath. Since the window is 60 seconds long, these peaks are interpreted as rpm. The resulting plot is shown in Figure 4.14.

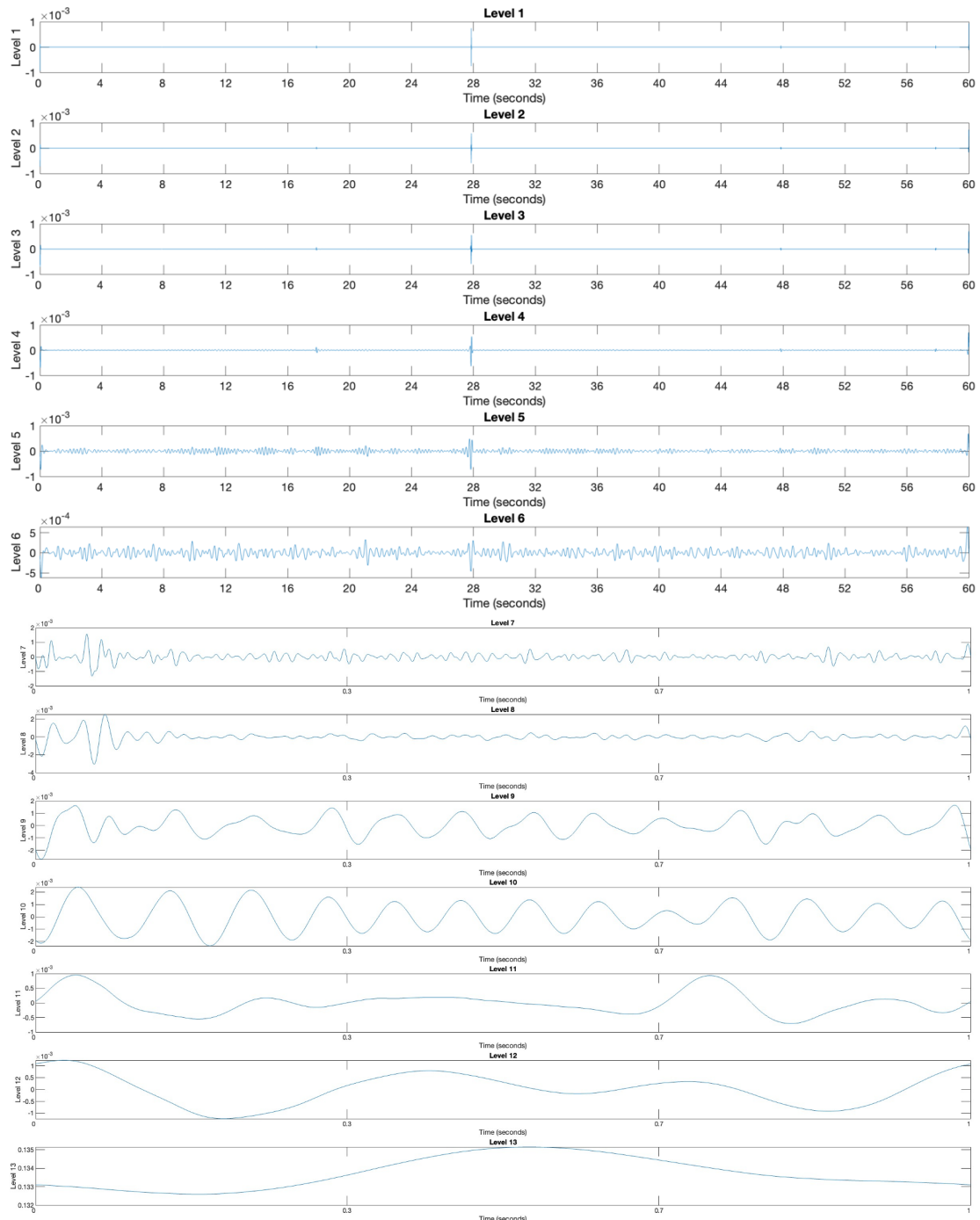


Figure 4.12: Stationary Signal

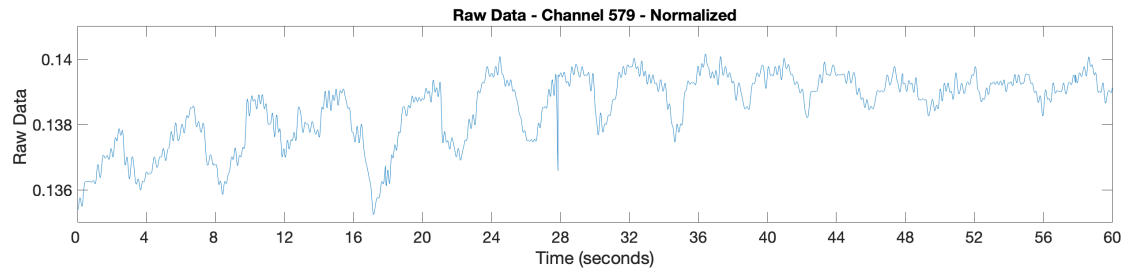


Figure 4.13: Raw Data - Channel 579 - Massive presence of Spike

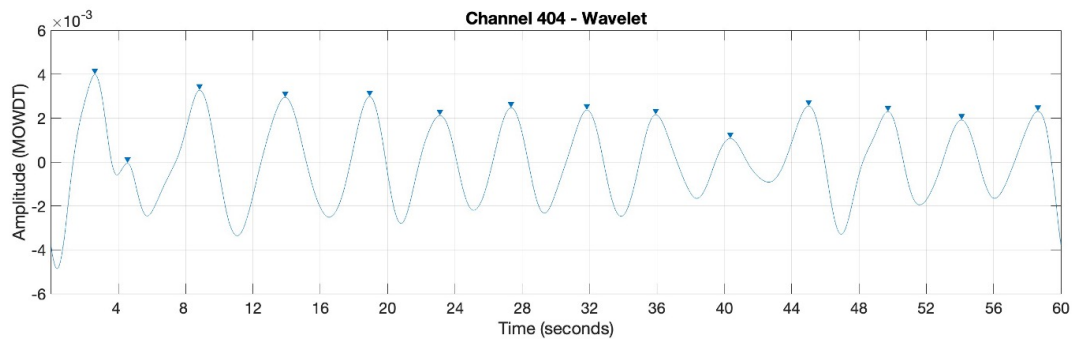


Figure 4.14: Channel 404 Filtered - with Wavelet

4.2.5 Savitz-Golay filter

The Savitz-Golay filter is a filter used to "smooth out" a noisy signal whose frequency span (without noise) is significant. They are also called digital smoothing polynomial filters or least-squares smoothing filters. Savitzky-Golay filters generalize the idea of filtering of replacing each point of a signal with a combination of the signal values contained in a moving window centred at the point, on the assumption that nearby points measure nearly the same underlying value, by least-squares fitting an n th-order polynomial through the signal values in the window and taking the calculated central point of the fitted polynomial curve as the new smoothed data point.

For a given point x that has k points to the left and k points to the right, for a

total window length of $L = 2k + 1$:

$$\mathbf{x} = \begin{bmatrix} 1 & -k & (-k)^2 & \cdots & (-k)^n \\ 1 & \vdots & \vdots & \ddots & \vdots \\ 1 & -2 & (-2)^2 & \cdots & (-2)^n \\ 1 & -2 & (-1)^2 & \cdots & (-1)^n \\ 1 & 0 & 0 & \cdots & 0 \\ 1 & 1 & 1^2 & \cdots & 1^n \\ 1 & 2 & 2^2 & \cdots & 2^n \\ 1 & \vdots & \vdots & \ddots & \vdots \\ 1 & k & k^2 & \cdots & k^n \end{bmatrix} \begin{bmatrix} a_0 \\ \vdots \\ a_n \end{bmatrix} \equiv \mathbf{H}\mathbf{a}$$

To find the Savitzky-Golay estimates, use the pseudoinverse of \mathbf{H} to compute \mathbf{a} and then premultiply by \mathbf{H}

$$\hat{\mathbf{x}} = \mathbf{H}(\mathbf{H}^T\mathbf{H})^{-1}\mathbf{H}^T\mathbf{x} = \mathbf{B}\mathbf{x}$$

An example of how the Savitzky–Golay filter works is shown in Figure 4.15.

Application in the Pipeline

To show the application of the Savitz-Golay filter in the pipeline, the signal in Figure 4.13, which has not been excluded by the criteria explained in Chapter 4.2.2 is taken as an example.

For the filter is chosen a 9th order polynomial, that allows for obtaining a wave similar to the one in MODWTMRA form. The resulting wave is given as input to a peak finder to point out the moment between inhaling and exhaling, visible as a peak in the wave and counted as a breath and since the window is 60 seconds long,

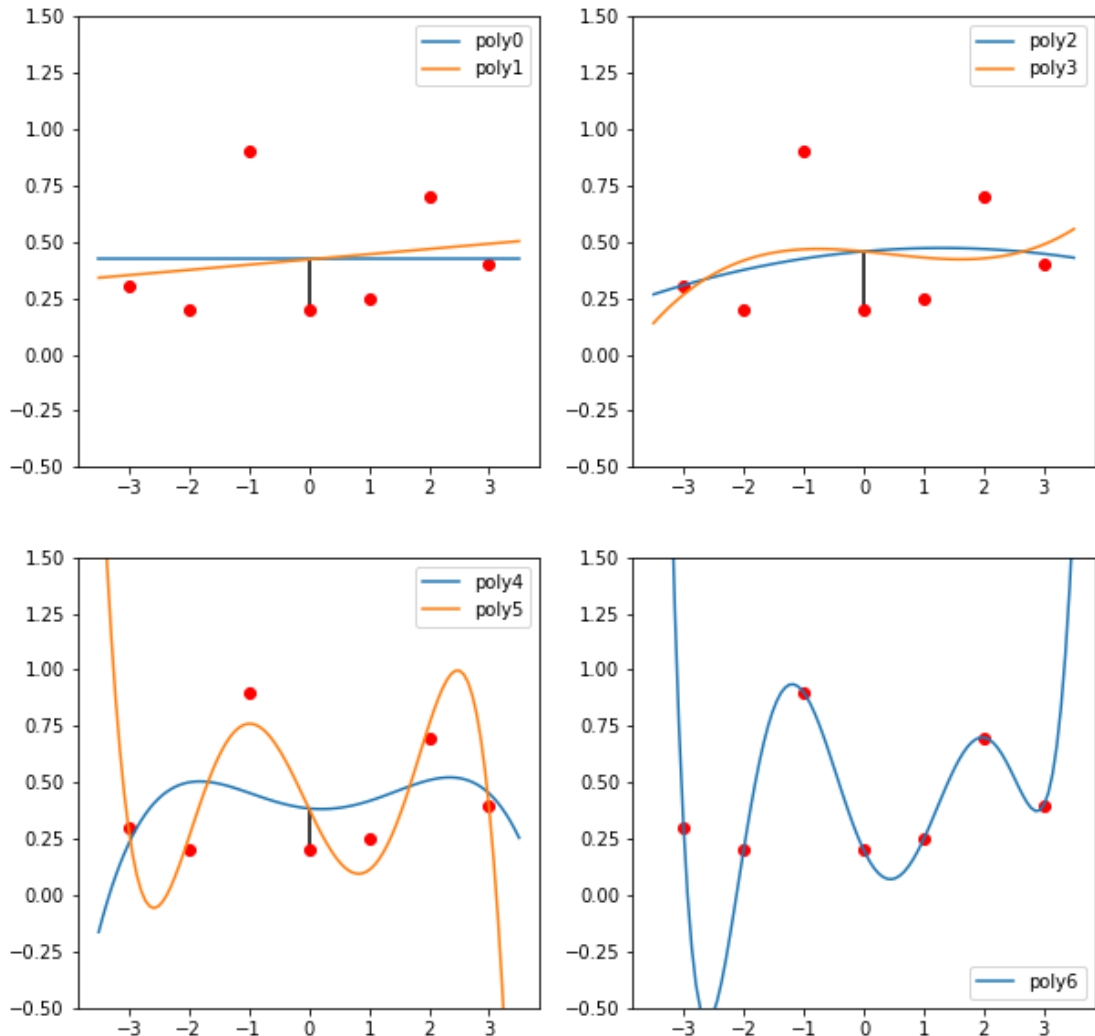


Figure 4.15: Savitzky-Golay filter

these peaks are interpreted as rpm. The resulting plot is shown in Figure 4.16.

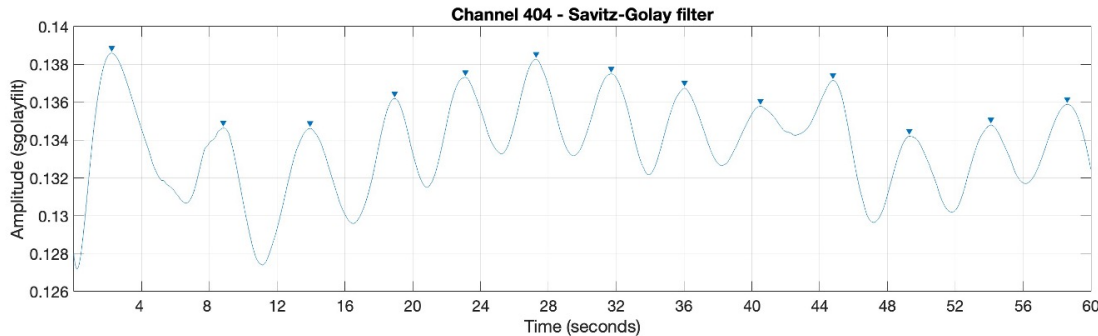


Figure 4.16: Channel 404 Filtered - with Savitz-Golay filter

4.2.6 Subsequent analyses of the filtered signal

The reconstructed signal with MODWTMRA or Savitzky–Golay filter is then further analysed, based on physiological information. This criterion is considered binary, so the weighted approach follows the scheme 1000% in case of passed and 0% otherwise.

Respiratory Rate over a Threshold

Since this project is a preliminary analysis of the feasibility to use pressure sensor mattresses to estimate a respiratory rate per minute (rpm). It has been decided to choose a threshold over which a respiratory rate of a person should not go , threshold is 30rpm because as discussed in Chapter 2.2 an rpm greater than 20 breaths per min was predictive of cardiopulmonary arrest within 72 hours and death within 30 days[28]; greater than 27 breaths per minute were predictive of cardiopulmonary arrest within 72 hours [29]. So the channels with a signal with more than 30 rpm, to admit a part of the error in our reconstruction and arrive at the limit given by literature between healthy and problematic and lead to a 0% percentage of confidence.

Distance peaks valley

The signal is then given as input to an algorithm that points out the valley of the filtered signal and not only the peaks. The distance between the valley and peaks is calculated with Euclidean distance, if the value between the signal's valley and peaks should differ inside the interval of $\pm 20\%$ from the preceding breath the signal is considered to be meaningful and lead to a 100% percentage of confidence.

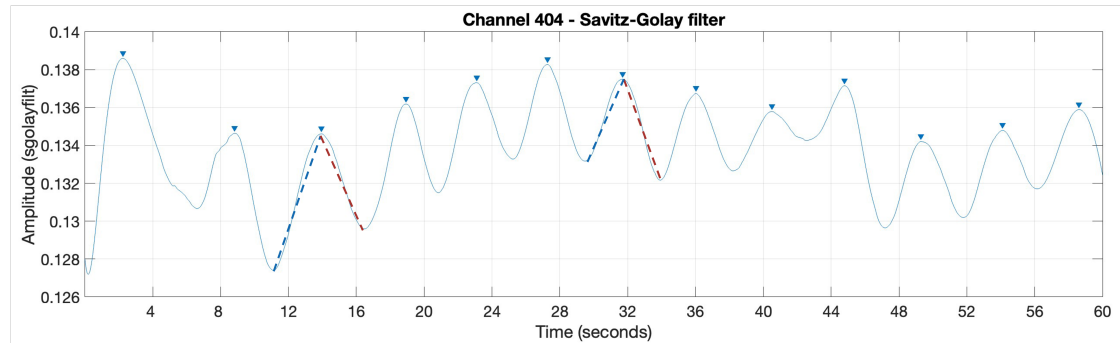


Figure 4.17: Euclidean

Lenght of breath

The valleys calculated in Chapter 4.2.6 are taken into account to calculate the distance between peaks and valleys on the time axis, to check the length of inspiration and expiratory phase. The difference should not vary between $\pm 20\%$ from the previous breath. If the signal is in this range the channel is considered meaningful and leads to a 100% percentage of confidence.

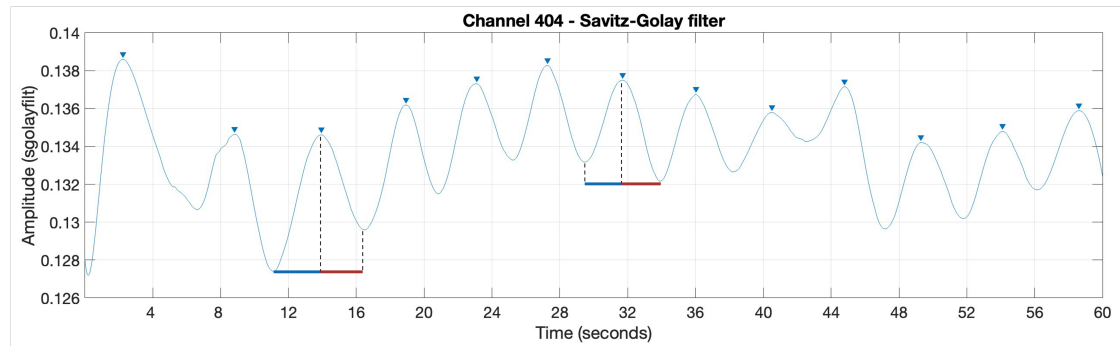


Figure 4.18: Length

4.2.7 Compute the Respiratory Rate

At the end of the pipeline, for each method: binary or weighted; for each approach: MODWTMRA and Savitzky–Golay filter, it has been saved the result of each of them. In case it is been decided to perform all the possible approaches and methods, there are a total of four combinations:

- MODWTMRA with binary approach
- MODWTMRA with weighted approach
- Savitzky–Golay filter with binary approach
- Savitzky–Golay filter with weighted approach

In the end, to calculate the rpm, the channels with the highest confidence, which can be chosen at the beginning of the pipeline, are taken into account, and the rpm is computed as the average of the number of peaks (hereafter referred to as "pks") of those signals.

As an example, if the chosen threshold for confidence is 80% and 5 channels are over it with the following value: 13pks, 14pks, 12pks, 13pks, 14pks; the result rpm is the average, so 13.2rpm.

The rpm value is computed for each position of both conditions (normal bed and rocking bed).

4.2.8 Result of the Pipeline (visual)

As a result, the pipeline is also available a heatmap that allows visualizing where the channels with the highest percentage of confidence, understand where are in respect of the body. Figure 4.19, is an example of the resulting heatmap, where the channels with the highest value are red and with lower are green up to blue when the channels have the 0% of representing a respiratory pattern.

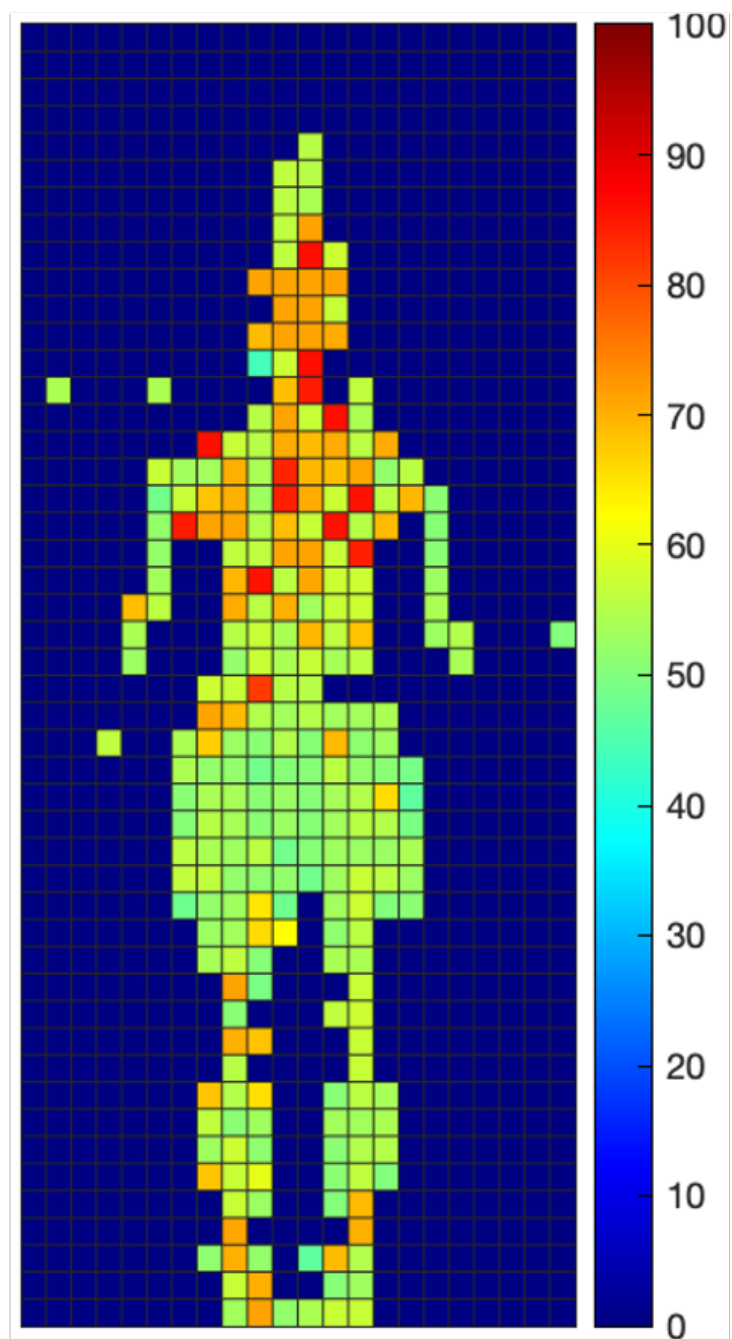


Figure 4.19: Heatmap of channels with the highest confidence

Chapter 5

Result

At the end of the pipeline, has been computed a respiratory rate per minute (rpm), for each position of both conditions (normal bed and rocking bed). This number is obtained as the average of the number of peaks of the channels with the highest confidence that outstrip the value of confidence set as a minimum, at the beginning of the pipeline, to accept the channels (in this case has been 80%), as discussed in Chapter 4.2.7. The following section 5.1 presented the metric used to assert the error between the estimated rpm resulting from the pipeline and the one given by the ground truth. These metrics are commonly employed to determine the difference between medical instruments [45, 46, 47]. To assert better how the pipeline works, it also shows visually the raw data of the channel with the highest confidence, his reconstruction or filtering and nasal pressure at that moment.

The results are divided into the different combinations of approaches and methods applied to the different positions and conditions. The result for the following combination can be found in the section:

- Multiresolution Overlap Discrete Wavelet Transform (MODWTMRA) with binary approach.
- Multiresolution Overlap Discrete Wavelet Transform (MODWTMRA) with weighted approach
- Savitzky–Golay filter with binary approach
- Savitzky–Golay filter with weighted approach

5.1 Evaluation Metrics

To evaluate the result of the pipeline has been chosen metrics that are on the same scale as the target prediction. This decision has been done to preserve the scale and has an estimation of the difference based on the number of breaths per minute, in our result from the actual value. The chosen evaluation metrics are: Mean absolute error (MAE), discussed in section 5.1.1 and Mean absolute percentage error (MAPE), discussed in section 5.1.2. These metrics are usually presented combined with the Bland–Altman plot, further discussed in section 5.1.3.

5.1.1 Mean absolute error

Mean Absolute Error (MAE) is the average absolute error between actual and predicted values. It is a measure of model accuracy given on the same scale as the prediction target, it can be seen as the average error that the model's prediction has in comparison with their corresponding actual targets.

$$MAE = \frac{1}{n} \sum_{i=1}^n |y_i - x_i|$$

where y_i is the prediction (pipeline's result), x_i the true value (ground truth respiration rate) and n sample size.

5.1.2 Mean absolute percentage error

Mean Absolute Percentage Error (MAPE) is the mean of all absolute percentage errors between the predicted and actual values. MAPE is the average percentage difference between predictions and their intended targets in the database.

$$MAPE = \frac{100}{n} \sum_{i=1}^n \left| \frac{y_i - x_i}{x_i} \right|$$

where y_i is the prediction (pipeline's result), x_i the true value (ground truth respiration rate) and n sample size.

5.1.3 Bland–Altman Plot

The Bland-Altman plot is highly employed in medical statistics to visualize the difference in measurements between two different instruments or two different measurement techniques. An example is shown in Figure 5.1.

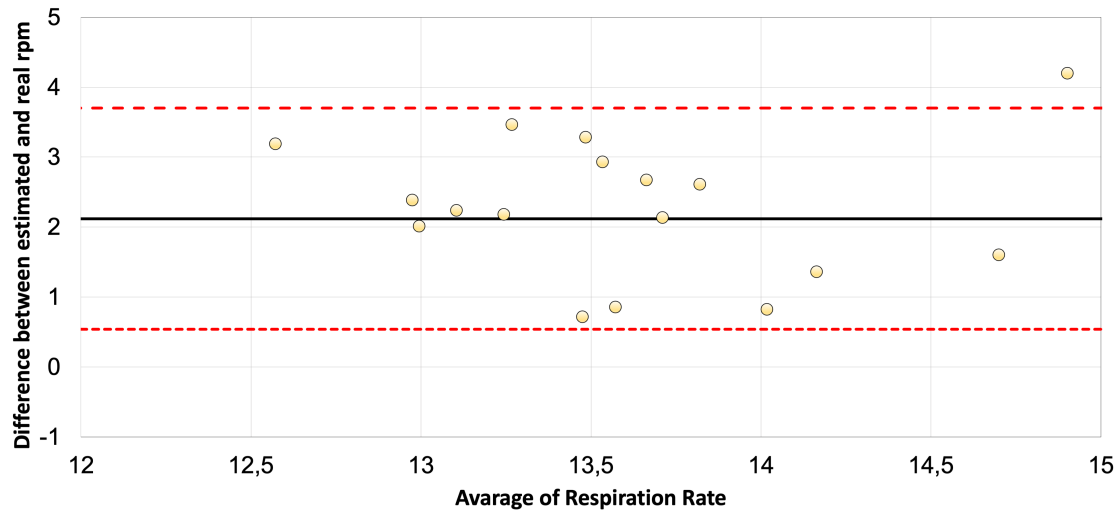


Figure 5.1: Example of Bland Altman Plot

The *x-axis* of the plot displays the average measurement of the two instruments and the *y-axis* displays the difference in measurements between the two instruments. In the plot are present also three lines, the central black represents the average difference in measurements between the two instruments also known as “bias” between the two measurements, as far from zero as large the average difference is large. The red dotted lines are the limits of the agreement, defined as the mean difference ± 1.96 standard deviation of the difference.

5.2 Result for MODWTMRA

This section of the result is divided into normal bed, section 5.3.1, and rocking bed ???. Inside both sections are presented the result for each position for the binary and weighted approach, the denoise method is MODWTMRA.

The estimated respiratory rate per minute (rpm) while the participants are on the mattress are further presented. Given the use of a moving window to simulate a real-time pipeline, the estimated rpm for each window is shown. The total number of windows for each position is 18 since the window is 60 seconds long and the entire recording for each position is 4 minutes long. First, is presented the table containing the estimated rpm using binary and weighted approaches compared with the rpm given by the ground truth. After is shown a table with the average rpm for both approaches and the relative mean absolute error (MAE) and mean absolute percentage error (MAPE). In the end, are presented the Bland–Altman plot to better visualize and understand the data in respect of the error and a plot of the best channel with its raw data and relative denoised wave.

5.2.1 Normal Bed

The participant in this phase has to perform a series of jumps before lying on the mattress due to recreating the increase or decrease of the breath rate between the different sleep stages. This phase aims to understand the feasibility of extracting breath rate from the mat. For this phase, the mattress is placed on a standard bed.

Result Normal Bed in Supine Position

The estimated respiratory rate per minute (rpm) while the participants are supine with the mattress placed on a normal bed is further presented. Table 5.17 presented the estimated rpm using binary and weighted approach compared with the rpm given by the ground truth. The approaches retrieve an almost identical rpm, this result may be due to the choice of the minimum confidence value at 80% that allows keeping only the best signal, maybe with higher confidence can be seen a higher difference between the two approaches.

Table 5.18 present the average rpm for both approaches and the relative mean

Binary	Weighted	RPM (NOXA1)
14.8438	14.7353	13.485
14	14	13.1443
15.125	15.125	12.5154
13.8333	13.8333	13.117
14.4286	14.4286	13.6077
15.5	15.5	13.8993
15	15	12.0681
11	11	11.4768
14.3333	14.3333	12.1549
17	17	12.8028
15	15	12.3275
14.1667	14.1667	10.9785
15.125	15.125	11.8441
14.7778	14.7778	12.6438
15	15	11.5351
14	14	11.99
14.2222	14.2222	11.9868
14.1667	13.8571	11.7824

Table 5.1: Estimated rpm using binary and weighted approach of the pipeline compared with the rpm given by the ground truth - Normal bed and supine position

absolute error (MAE) and mean absolute percentage error (MAPE). As just discussed in the previous paragraph there is no substantial difference between the two different approaches. The data on which to focus more is the number of breaths that the algorithm misses, represented by MAE and expressed in percentage by MAPE. The average number is 2rpm, which means that if we consider the estimated average of 14.5rpm the error is almost 20%, quite high for an approach that must be used in the medical field.

	Binary	Weighted
rpm mean	14.529	14.506
MAE rpm	2.1731	2.1499
MAPE	17.8104%	17.6198%

Table 5.2: Average number of breath for each approach with the relative mean absolute error (MAE) and mean absolute percentage error (MAPE) - Normal bed and supine position

Figure 5.32 show the Bland–Altman plot, presented in section 5.1.3, of the estimated rpm from the pipeline compared to the value of the ground truth. It helps to visualize the data from Table 5.18 in respect of the error. Since the result for the approaches is similar the data presented with this plot refers to the weighted approach only.

Figure 5.33 shows the denoised signal using MODWTMRA with the highest accuracy (92%) for the supine position with a normal mattress.

Result Normal Bed in Left Side Position

The estimated respiratory rate per minute (rpm) while the participants are on the left side with the mattress placed on a normal bed is further presented. Table 5.19 presented the estimated rpm using binary and weighted approach compared with the rpm given by the ground truth. The approaches retrieve an almost identical rpm, this result may be due to the choice of the minimum confidence value at 80% that allows keeping only the best signal, maybe with higher confidence can be seen a higher difference between the two approaches.

Table 5.20 present the average rpm for both approaches and the relative mean absolute error (MAE) and mean absolute percentage error (MAPE). As just discussed in the previous paragraph there is no substantial difference between the two different approaches. The data on which to focus more is the number of breaths that the algorithm misses, represented by MAE and expressed in percentage by MAPE. The average number is 2.5rpm, which means that if we consider the estimated average of 15.3rpm the error is over 24%, worst than in the supine position, probably due to the smaller contact area between the body and the mattress.

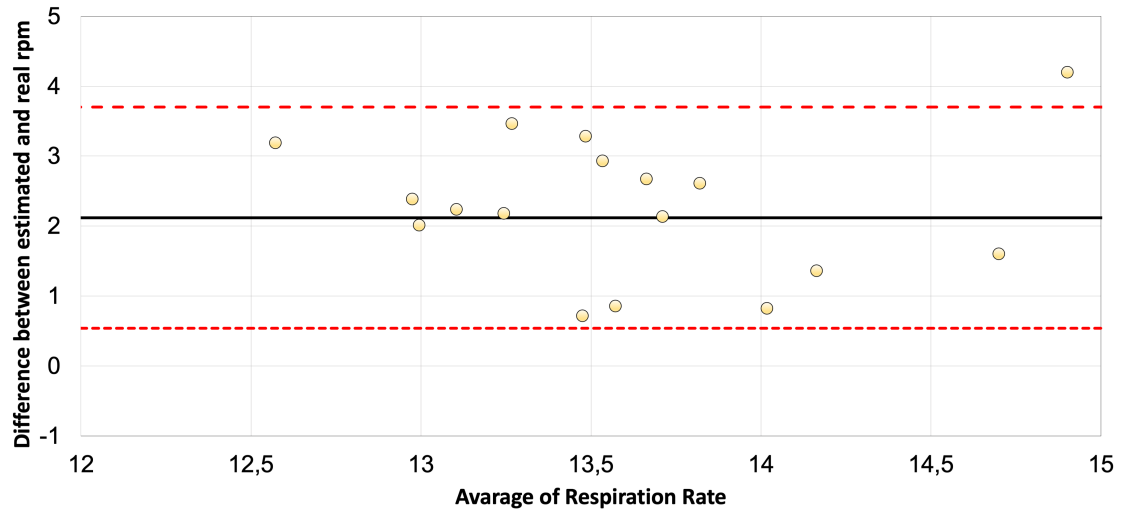


Figure 5.2: Bland Altman Plot of estimated rpm from the pipeline compared to the value of the ground truth - Normal bed and supine position

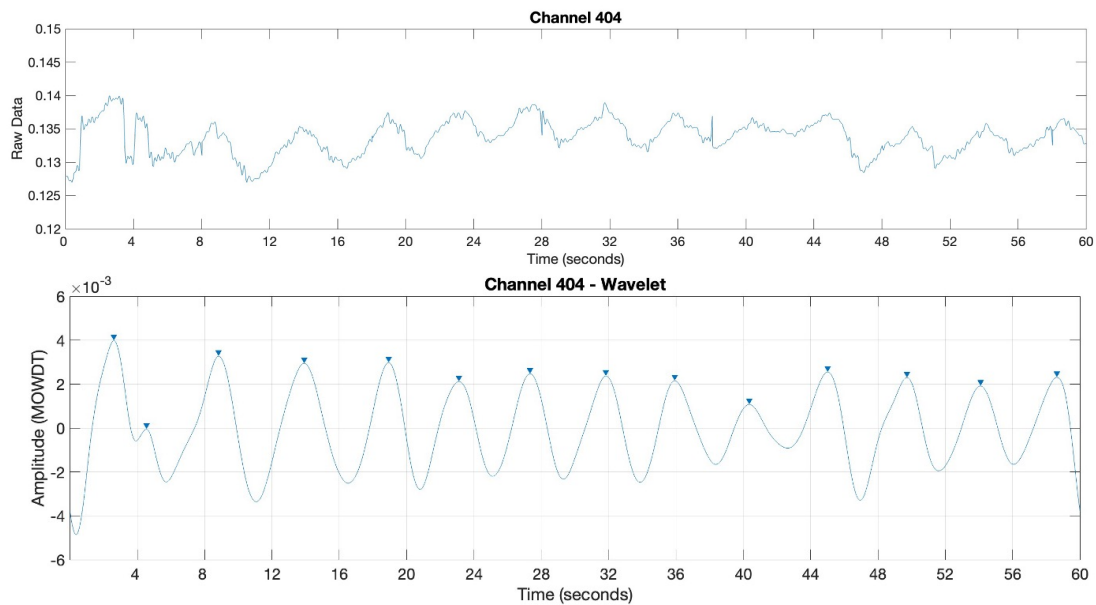


Figure 5.3: Raw data and denoised signal using MODWTMRA of the channel with the highest percentage of confidence (92%) - Normal bed and supine position

Binary	Weighed	RPM (NOXA1)
14.6364	14.6364	11.2045
15	15	12.7397
16	15.25	13.0613
14.2	14.2	12.2669
19	19	12.1628
15	14.5	13.6039
14.2222	14.2222	13.1398
15.6667	15.6667	11.5445
+ 14.7	14.7	10.77
15.8571	15.8571	14.2216
15.5556	15.5556	13.1656
16.5714	16.5714	12.9764
15	15	10.9055
15.125	15.125	13.2294
15.7143	15.5	12.8524
15.2	15.2	11.3824
14.6	14.6	13.5579
15.8889	15.8889	11.6069

Table 5.3: Estimated rpm using binary and weighted approach of the pipeline compared with the rpm given by the ground truth - - Normal bed and left side

	Binary	Weighed
rpm mean	15.441	15.360
MAE resp	2.4545	2.8934
MAPE	24.62%	24.0041%

Table 5.4: varage number of breath for each approach with the relative mean absolute error (MAE) and mean absolute percentage error (MAE) - Normal bed and left side

Figure 5.22 show the Bland–Altman plot, presented in section 5.1.3, of the estimated rpm from the pipeline compared to the value of the ground truth. It helps to visualize the data from Table 5.20 in respect of the error. Since the result for the approaches is similar the data presented with this plot refers to the weighted approach only.

Figure 5.33 shows the denoised signal using MODWTMRA with the highest

accuracy (92%) for the supine position with a normal mattress.

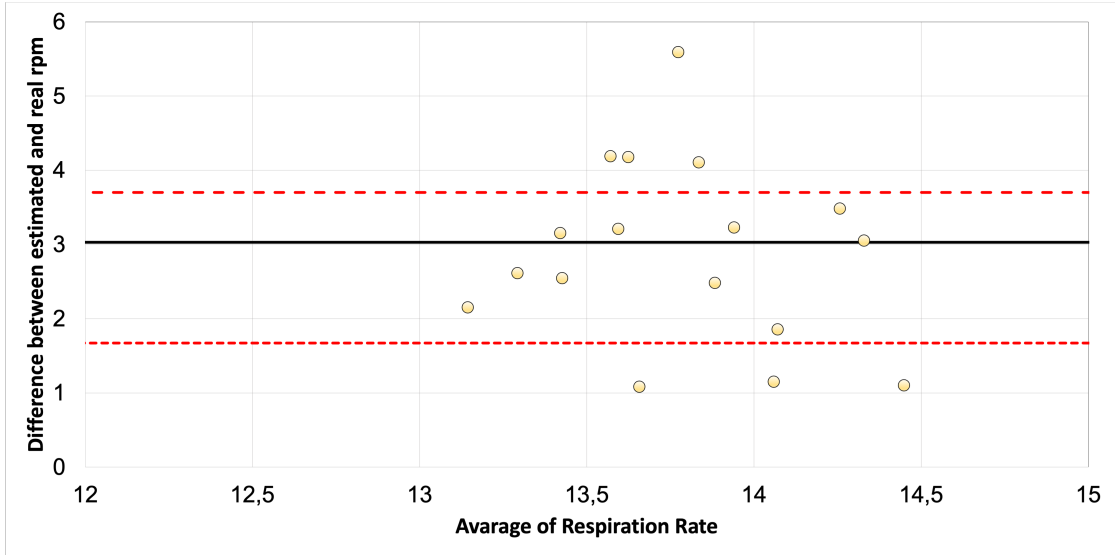


Figure 5.4: Bland Altman Plot of estimated rpm from the pipeline compared to the value of the ground truth - Normal bed and left side

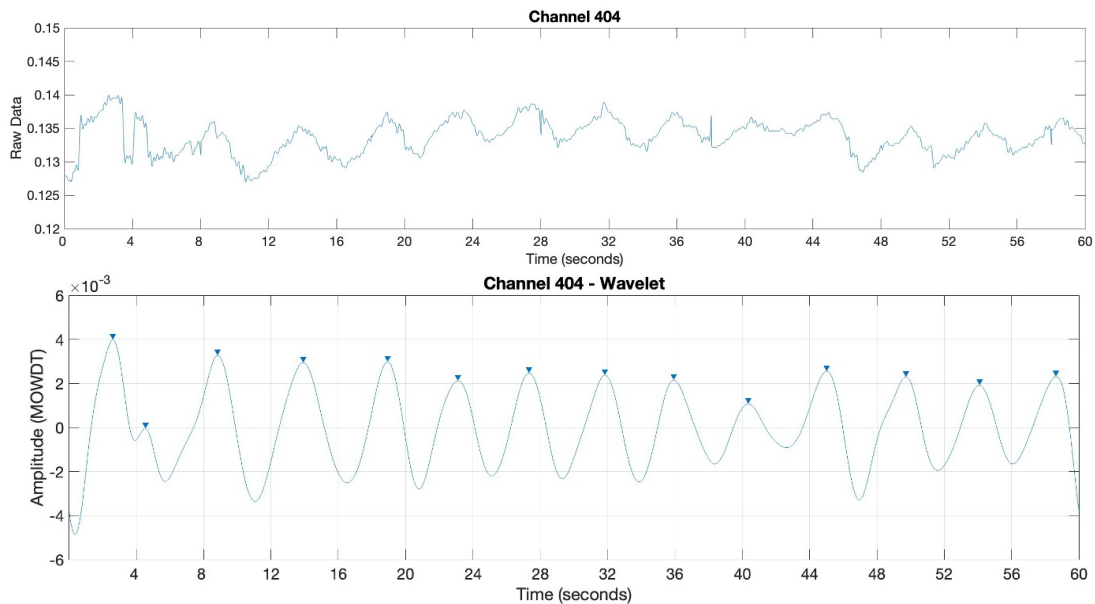


Figure 5.5: Raw data and denoised signal using MODWTMRA of the channel with the highest percentage of confidence (92%) - Normal bed and supine position

Result Normal Bed in Prone Side Position

The estimated respiratory rate per minute (rpm) while the participants are in the prone position with the mattress placed on a normal bed is further presented. Table 5.21 presented the estimated rpm using binary and weighted approach compared with the rpm given by the ground truth. The approaches retrieve an almost identical rpm, this result may be due to the choice of the minimum confidence value at 80% that allows keeping only the best signal, maybe with higher confidence can be seen a higher difference between the two approaches.

Binary	Weighed SGf	RPM (NOXA1)
15.7	15.7	11.5949
15.7333	15.7333	11.1628
16.1	16.1	11.0005
15.6667	15.6667	10.4762
15.25	15.25	10.4723
14.5714	14.5714	9.5345
15.5714	15.5714	9.5467
15.875	15.875	13.5758
14	14	11.1779
14.375	14.375	9.5345
14.4667	14.4667	9.5841
14.5	14.5	11.8196
14.2143	14.2143	11.8153
13.9474	13.9474	9.5223
15.037	15.037	10.8508
14.931	14.931	10.8876
15.25	15.25	10.9705
15.3333	15.3333	11.237

Table 5.5: Estimated rpm using binary and weighted approach of the pipeline compared with the rpm given by the ground truth - Normal bed and supine position

Table 5.22 present the average rpm for both approaches and the relative mean absolute error (MAE) and mean absolute percentage error (MAPE). As just discussed in the previous paragraph there is no substantial difference between

the two different approaches. The data on which to focus more is the number of breaths that the algorithm misses, represented by MAE and expressed in percentage by MAPE. The average number is 2.8rpm, which means that if we consider the estimated average of 15rpm the error is over 36%, worst worse than the two previous results it may depend on the movement of the chest in the prone position changes.

	Binary	Weighed
rpm mean	15.029	15.029
MAE rpm	2.8957 %	2.8957%
MAPE tool	36.5982	36.5982

Table 5.6: Metrics to evaluate the participant in belly position with moving mattress

Figure 5.22 show the Bland–Altman plot, presented in section 5.1.3, of the estimated rpm from the pipeline compared to the value of the ground truth. It helps to visualize the data from Table 5.22 in respect of the error. Since the result for the approaches is similar the data presented with this plot refers to the weighted approach only.

Figure 5.33 shows the denoised signal using MODWTMRA with the highest accuracy (92%) for the supine position with a normal mattress.

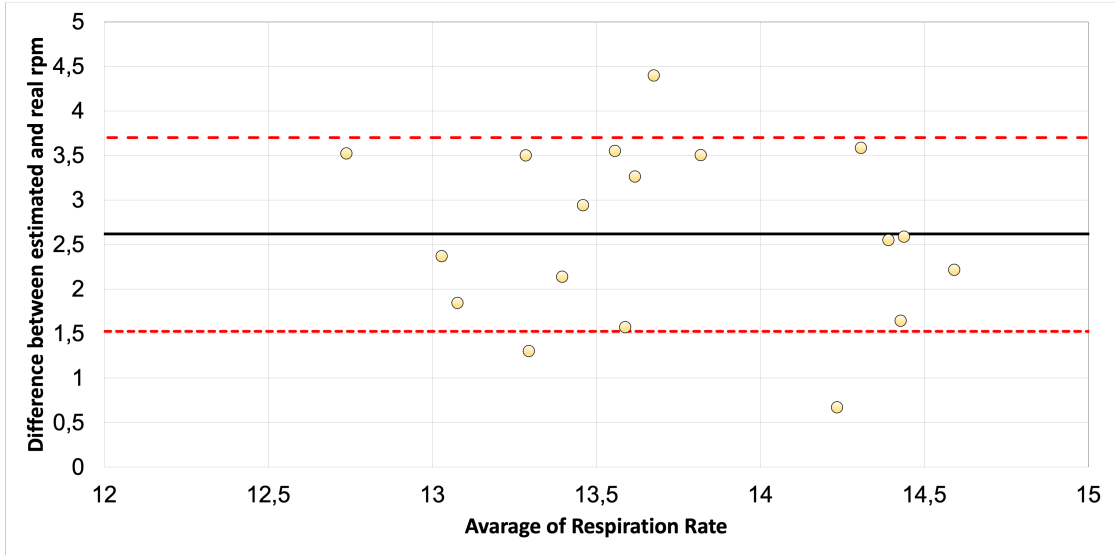


Figure 5.6: Bland Altman Plot of estimated rpm from the pipeline compared to the value of the ground truth - Normal bed and prone position

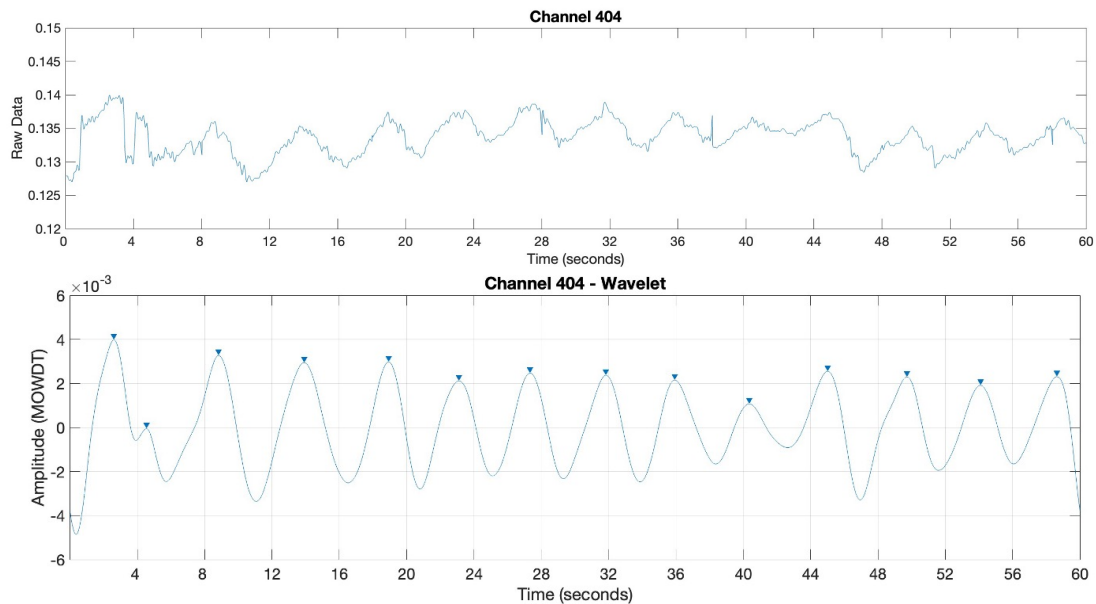


Figure 5.7: Raw data and denoised signal using MODWTMRA of the channel with the highest percentage of confidence (92%) - Normal bed and supine position

Result Normal Bed in Right Side Position

The estimated respiratory rate per minute (rpm) while the participants are on the right side with the mattress placed on a normal bed is further presented. Table 5.23 presented the estimated rpm using binary and weighted approach compared with the rpm given by the ground truth. The approaches retrieve an almost identical rpm, this result may be due to the choice of the minimum confidence value at 80% that allows keeping only the best signal, maybe with higher confidence can be seen a higher difference between the two approaches.

Binary	Weighed	RPM (NOXA1)
16.1667	16.1667	12.4771
17.75	17.75	13.0835
16.5	16.5	14.3858
15.25	15.25	12.7261
15.8333	15.8333	13.4867
15	15	12.9816
15.2353	15.2353	14.0566
15.1667	15.1667	12.038
15.5	15.5	11.4923
13	13	11.9625
13.3333	13.3333	11.0151
15.5	15.5	11.9016
14.3333	14.3333	11.4255
13.8333	13.8333	12.5227
15.2	15.2	11.5945
14.0909	14.0909	13.4141
14.5	14.4286	13.5282
15.2308	15.2308	12.9839

Table 5.7: Estimated rpm using binary and weighted approach of the pipeline compared with the rpm given by the ground truth - Normal bed and right side

Table 5.24 present the average rpm for both approaches and the relative mean absolute error (MAE) and mean absolute percentage error (MAPE). As just discussed in the previous paragraphs there is no substantial difference between

the two different approaches. The data on which to focus more is the number of breaths that the algorithm misses, represented by MAE and expressed in percentage by MAPE. The average number is 2.5rpm, which means that if we consider the estimated average of 15rpm the error is almost 20%, worst than in the supine position but better than in the prone position and left side.

	Binary	Weighed
rpm mean	15.015	15.020
MAE resp	2.4638	2.4691
MAPE	19.9146 %	19.9693 %

Table 5.8: Evarage number of breath for each approach with the relative mean absolute error (MAE) and mean absolute percentage error (MAE) - Normal bed and right side

Figure 5.24 show the Bland–Altman plot, presented in section 5.1.3, of the estimated rpm from the pipeline compared to the value of the ground truth. It helps to visualize the data from Table 5.24 in respect of the error. Since the result for the approaches is similar the data presented with this plot refers to the weighted approach only.

Figure 5.25 shows the denoised signal using MODWTMRA with the highest accuracy (92%) for the supine position with a normal mattress.

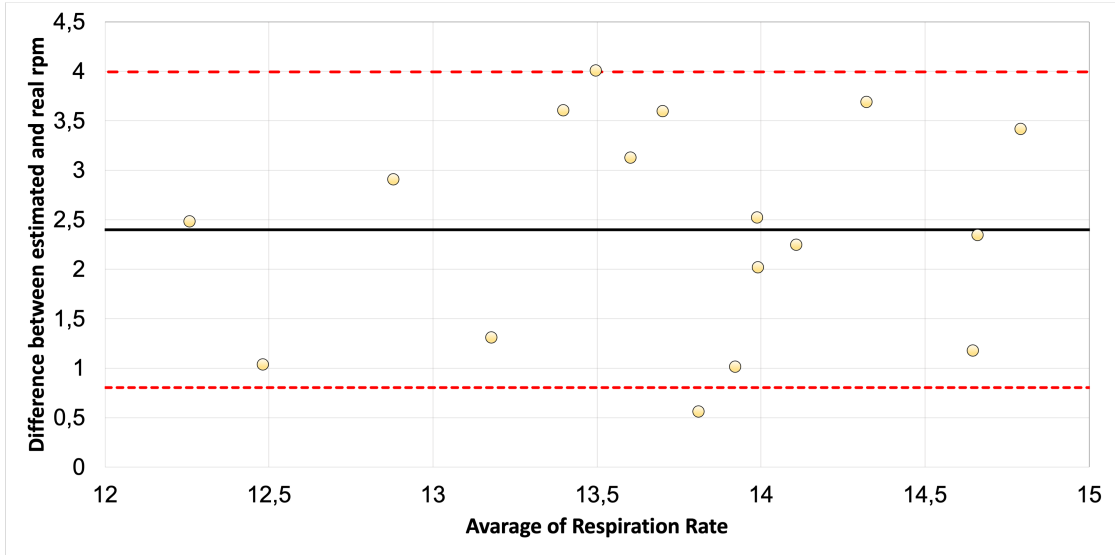


Figure 5.8: Bland Altman Plot of estimated rpm from the pipeline compared to the value of the ground truth - Normal bed and left side

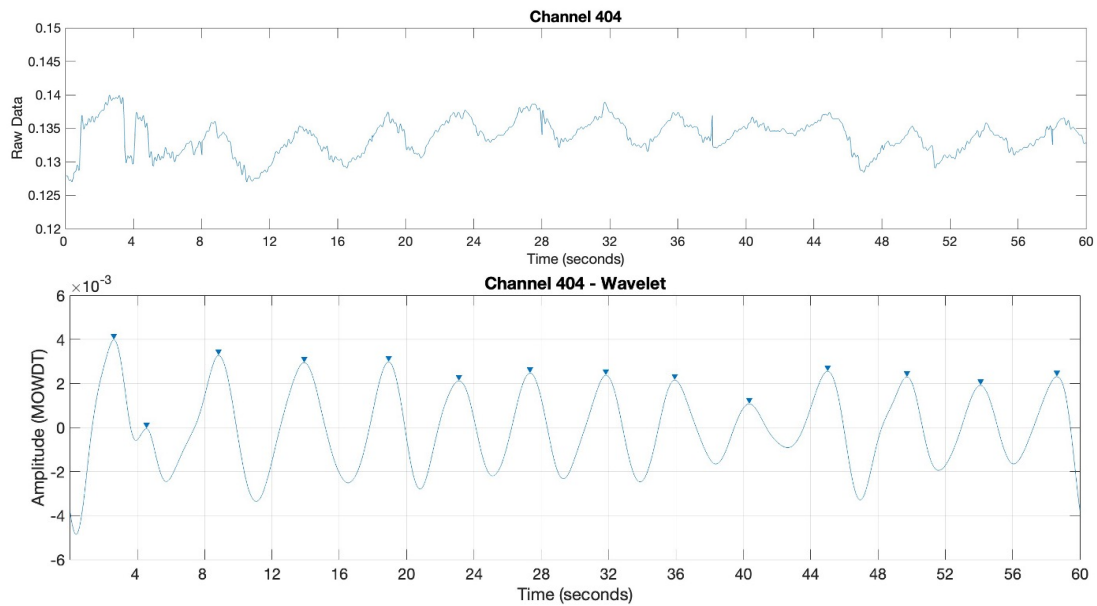


Figure 5.9: Raw data and denoised signal using MODWTMRA of the channel with the highest percentage of confidence (92%) - Normal bed and supine position

5.2.2 Rocking Bed

The second part of the data collection aims to understand if the movement of the rocking bed could influence the signal. The participant has to lie on the mattress without jumps, to have less variability in the data. For this phase, the mattress is placed on a rocking bed, which periods have been fixed at 4 seconds (15 periods in a minute) with an acceleration of 0.25 m/s^2 .

Result Rocking Bed in Supine Position

The estimated respiratory rate per minute (rpm) while the participants are supine with the mattress placed on a rocking bed is further presented.

Table 5.25 presented the estimated rpm using binary and weighted approach compared with the rpm given by the ground truth. The approaches retrieve an almost identical rpm.

Binary	Weighed	RPM (NOXA1)
15.5	15.5	10.7609
16.1333	16.1333	11.3077
15.3333	15.3333	13.1449
14.9474	14.9474	11.3366
15.1	15.1	12.7314
15.6364	15.6364	11.8892
14.6923	14.6923	11.42
15.2222	15.2222	13.0092
15.1667	15.1667	13.2539
14.6667	14.6667	11.6391
15	15	12.2165
14.75	14.75	11.9216
15	15	11.3091
14.625	14.625	13.8905
15.6154	15.6154	11.3344
15	14.8182	11.4474
15.1765	15.1765	11.6675
14.6154	14.6154	13.4799

Table 5.9: Estimated rpm using binary and weighted approach of the pipeline compared with the rpm given by the ground truth - Rocking bed and supine position

Table 5.25 present the average rpm for both approaches and the relative mean absolute error (MAE) and mean absolute percentage error (MAPE). As just discussed in the previous paragraph there is no substantial difference between the two different approaches. The data on which to focus more is the number of breaths that the algorithm misses, represented by MAE and expressed in percentage by MAPE. The average number is 3rpm, which means that if we consider the estimated average of 15.1rpm the error is almost 25%, is too high for an approach that must be used in the medical field.

Figure 5.32 show the Bland–Altman plot, presented in section 5.1.3, of the estimated rpm from the pipeline compared to the value of the ground truth. It helps to visualize the data from Table 5.26 in respect of the error. Since the result for the approaches is similar the data presented with this plot refers to the weighted approach only.

	Binary	Weighed
rpm mean	15.1211	15.1110
MAE resp	3.0234	3.0133
MAPE resp	25.7324%	25.6442%

Table 5.10: Evarage number of breath for each approach with the relative mean absolute error (MAE) and mean absolute percentage error (MAE) - Rocking bed and right side

Figure 5.33 shows the denoised signal using MODWTMRA with the highest accuracy (92%) for the supine position with a normal mattress.

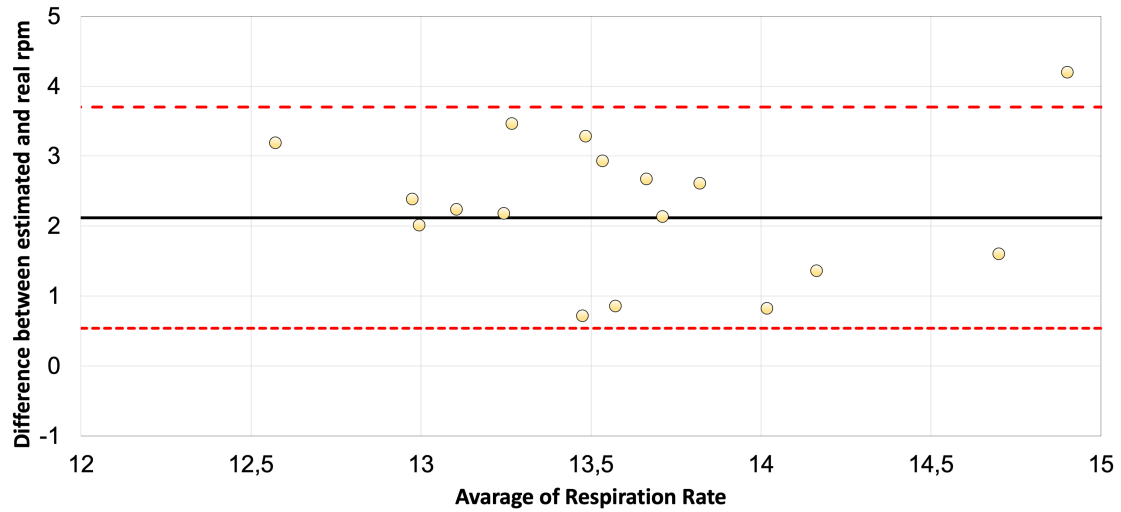


Figure 5.10: Bland Altman Plot of estimated rpm from the pipeline compared to the value of the ground truth - Rocking bed and supine position

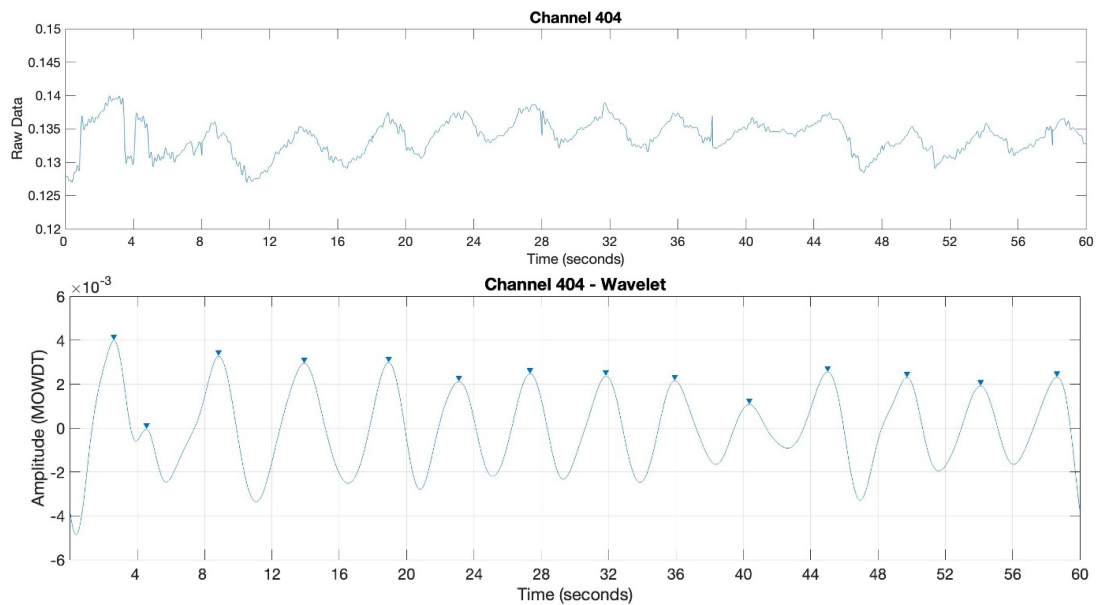


Figure 5.11: Raw data and denoised signal using MODWTMRA of the channel with the highest percentage of confidence (92%) - Normal bed and supine position

Result Rocking Bed in Left Side Position

The estimated respiratory rate per minute (rpm) while the participants are in left side position with the mattress placed on a rocking bed is further presented.

Table 5.27 presented the estimated rpm using binary and weighted approach compared with the rpm given by the ground truth. The approaches retrieve an almost identical rpm.

Binary	Weighed	RPM (NOXA1)
15.0625	15.0625	13.6613
15.5556	15.5556	11.4545
15.8824	15.8824	12.3288
16.1176	16.1176	10.8865
15.2083	15.2083	11.4082
15.3214	15.3103	12.2589
15.4583	15.4583	13.7093
15.4375	15.4375	12.7019
15.2353	15.2353	13.3305
15.5556	15.5556	13.7078
15.2143	15.2143	13.5674
15.2	15.1538	11.8694
15.5556	15.5556	13.4086
14.75	14.75	13.9781
14.5	14.5	12.4749
15.25	15.25	12.4049
14.625	14.7273	13.4108
14.2857	14.3333	13.4716

Table 5.11: Estimated rpm using binary and weighted approach of the pipeline compared with the rpm given by the ground truth - Rocking bed and left side

Table 5.27 present the average rpm for both approaches and the relative mean absolute error (MAE) and mean absolute percentage error (MAPE). As just discussed in the previous paragraph there is no substantial difference between the two different approaches. The data on which to focus more is the number of breaths that the algorithm misses, represented by MAE and expressed in percentage by MAPE. The average number is 2.5rpm, which means that if we consider the

estimated average of 15.2rpm the error is almost 20%, which is too high for an approach that must be used in the medical field.

	Binary	Weighed
rpm mean	15.2342	15.2393
MAE resp	2.4545	2.4597
MAPE resp	19.9605 %	19.9959 %

Table 5.12: Evarage number of breath for each approach with the relative mean absolute error (MAE) and mean absolute percentage error (MAE) - Rocking bed and left side

Figure 5.32 show the Bland–Altman plot, presented in section 5.1.3, of the estimated rpm from the pipeline compared to the value of the ground truth. It helps to visualize the data from Table 5.28 in respect of the error. Since the result for the approaches is similar the data presented with this plot refers to the weighted approach only.

Figure 5.33 shows the denoised signal using MODWTMRA with the highest accuracy (92%) for the supine position with a normal mattress.

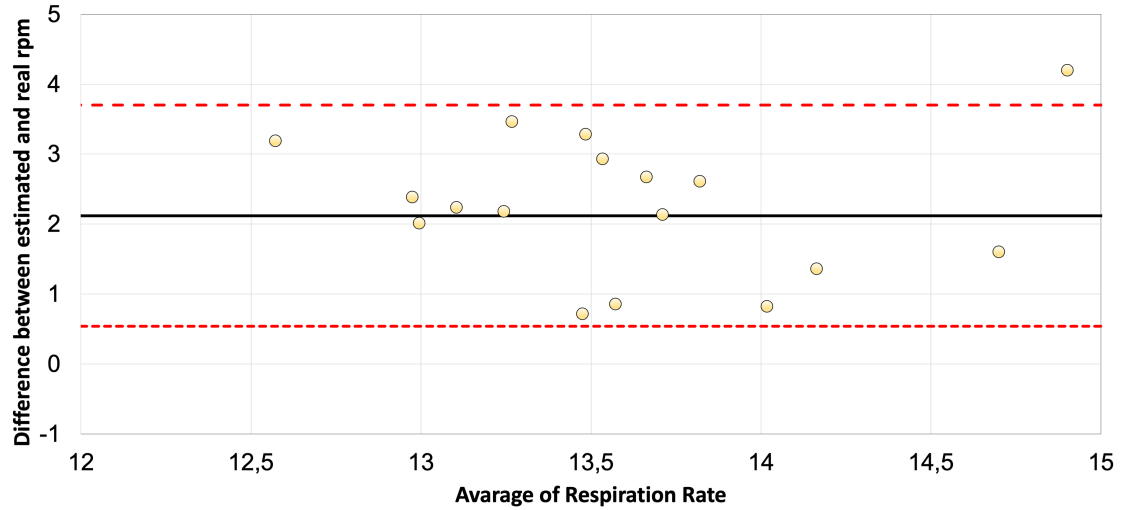


Figure 5.12: Bland Altman Plot of estimated rpm from the pipeline compared to the value of the ground truth - Normal bed and supine position

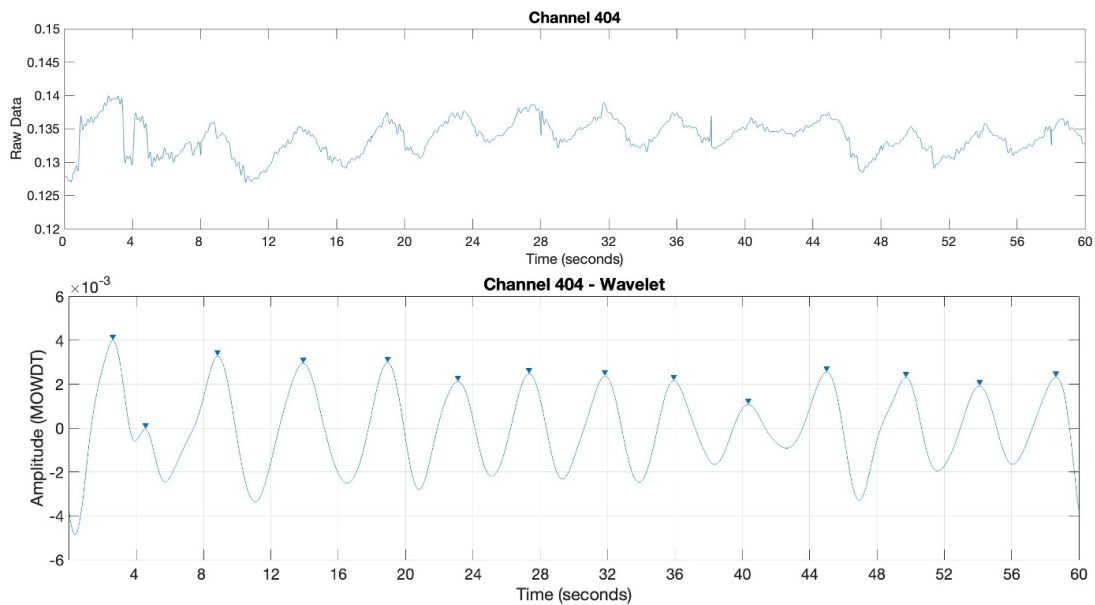


Figure 5.13: Raw data and denoised signal using MODWTMRA of the channel with the highest percentage of confidence (92%) - Normal bed and supine position

Result Rocking Bed in Prone Position

The estimated respiratory rate per minute (rpm) while the participants are in prone position with the mattress placed on a rocking bed is further presented.

Table 5.27 presented the estimated rpm using binary and weighted approach compared with the rpm given by the ground truth. The approaches retrieve an almost identical rpm.

Binary	Weighed	RPM (NOXA1)
16	16	12.6296
15.3684	15.3684	14.168
15.6818	15.6818	13.2588
15.5	15.4286	13.8107
15.8333	15.8333	13.485
16	16	12.6052
16	16	11.0417
15.7059	15.7059	12.9088
15.5333	15.5333	13.0502
16.3333	16.3333	11.1723
14.5625	14.5625	14.6869
15.5294	15.5294	11.3484
14.7273	14.7273	13.0399
14.7778	14.7778	9.54872
15.4444	15.4444	11.7918
14.9286	14.9286	12.8182
15.8333	15.8333	9.53453
14.619	14.619	9.5416

Table 5.13: Estimated rpm using binary and weighted approach of the pipeline compared with the rpm given by the ground truth - Rocking bed and prone position

Table 5.30 present the average rpm for both approaches and the relative mean absolute error (MAE) and mean absolute percentage error (MAPE). As just discussed in the previous paragraph there is no substantial difference between the two different approaches. The data on which to focus more is the number of breaths that the algorithm misses, represented by MAE and expressed in percentage by MAPE. The average number is 2.5rpm, which means that if we consider the estimated average of 15.2rpm the error is almost 20%, which is too high for an

approach that must be used in the medical field.

	Binary	Weighed
rpm mean	15.4655	15.4615
MAE resp	3.2326	3.2286
MAPE resp	28.5509	28.5221

Table 5.14: Evarage number of breath for each approach with the relative mean absolute error (MAE) and mean absolute percentage error (MAE) - Rocking bed and prone position

Figure 5.32 show the Bland–Altman plot, presented in section 5.1.3, of the estimated rpm from the pipeline compared to the value of the ground truth. It helps to visualize the data from Table 5.30 in respect of the error. Since the result for the approaches is similar the data presented with this plot refers to the weighted approach only.

Figure 5.33 shows the denoised signal using MODWTMRA with the highest accuracy (92%) for the supine position with a normal mattress.

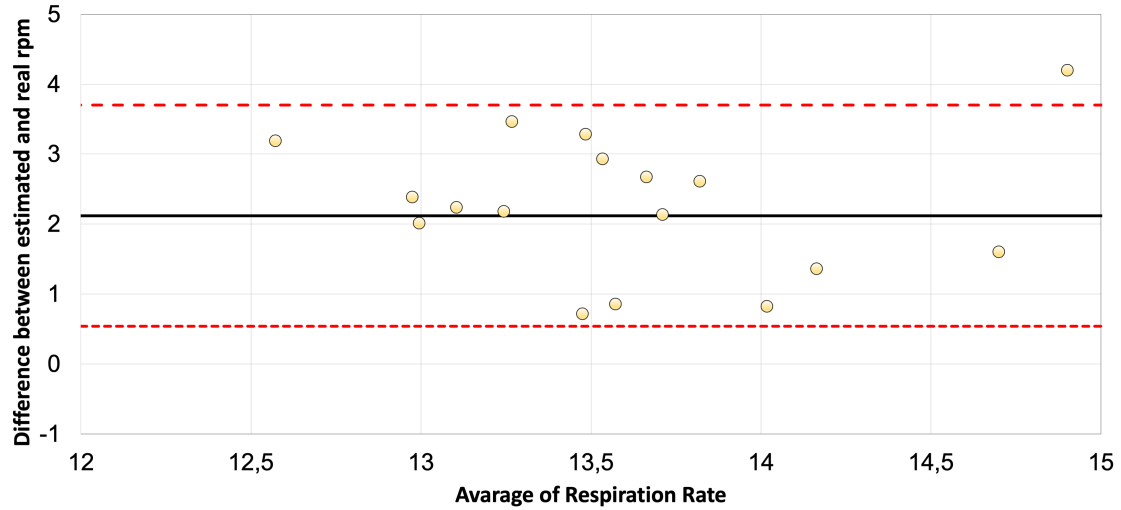


Figure 5.14: Bland Altman Plot of estimated rpm from the pipeline compared to the value of the ground truth - Normal bed and supine position

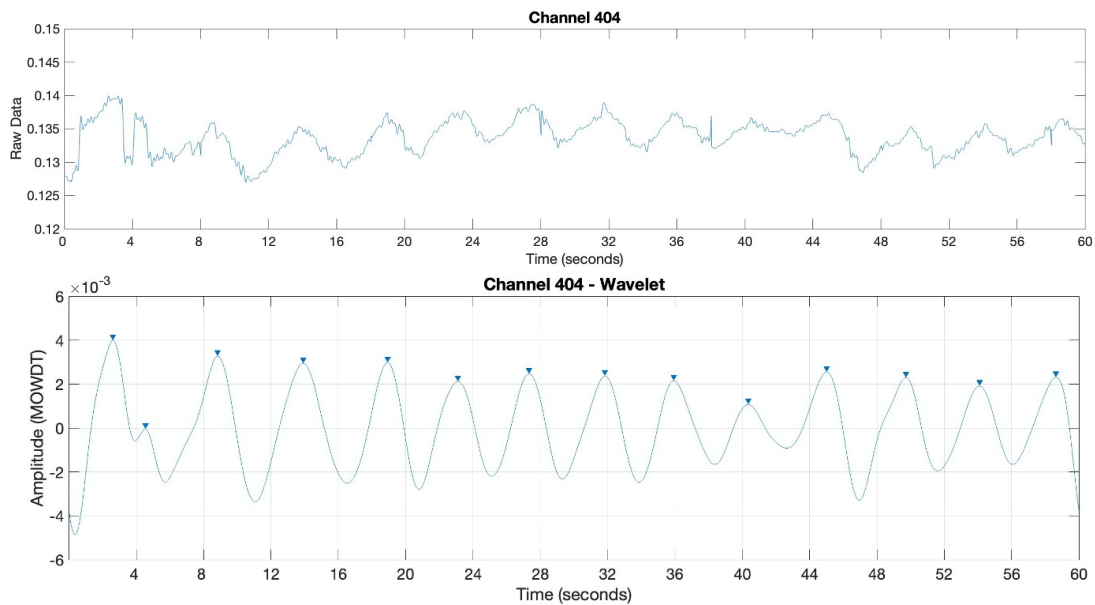


Figure 5.15: Raw data and denoised signal using MODWTMRA of the channel with the highest percentage of confidence (92%) - Normal bed and supine position

Result Rocking Bed in Right Side

The estimated respiratory rate per minute (rpm) while the participants are in right side position with the mattress placed on a rocking bed is further presented.

Table 5.31 presented the estimated rpm using binary and weighted approach compared with the rpm given by the ground truth. The approaches retrieve an almost identical rpm.

Binary	Weighed	RPM (NOXA1)
15.8095	15.8095	11.7955
15.2105	15.1	11.9185
15.5652	15.5652	11.8639
15.8261	15.8261	12.28
15.6667	15.6667	12.0136
15.1176	15.1176	12.8838
15.3571	15.3571	11.5695
15	14.8696	12.8922
15.1176	15.1176	11.587
15.2857	15.2857	11.2449
15.3333	15.3333	11.7082
15.3684	15.35	13.9497
15.6154	15.4286	11.6145
15.4286	15.4286	13.9913
15.2727	15.2727	11.6172
15.3	15.3	13.3257
15.1667	15.1667	13.5179
14.9231	14.9286	13.5767

Table 5.15: Estimated rpm using binary and weighted approach of the pipeline compared with the rpm given by the ground truth - Rocking bed and right side position

Table 5.31 present the average rpm for both approaches and the relative mean absolute error (MAE) and mean absolute percentage error (MAPE). As just discussed in the previous paragraph there is no substantial difference between the two different approaches. The data on which to focus more is the number of breaths that the algorithm misses, represented by MAE and expressed in percentage by MAPE. The average number is 2.9rpm, which means that if we consider the

	Binary	Weighed
rpm mean	15.3536	15.3291
MAE resp	2.9452	2.9208
MAPE	24.4008 %	24.1986%

Table 5.16: Evarage number of breath for each approach with the relative mean absolute error (MAE) and mean absolute percentage error (MAE) - Rocking bed and right side

estimated average of 15.3rpm the error is almost 24%, which is too high for an approach that must be used in the medical field.

Figure 5.32 show the Bland–Altman plot, presented in section 5.1.3, of the estimated rpm from the pipeline compared to the value of the ground truth. It helps to visualize the data from Table 5.32 in respect of the error. Since the result for the approaches is similar the data presented with this plot refers to the weighted approach only.

Figure 5.33 shows the denoised signal using MODWTMRA with the highest accuracy (92%) for the supine position with a normal mattress.

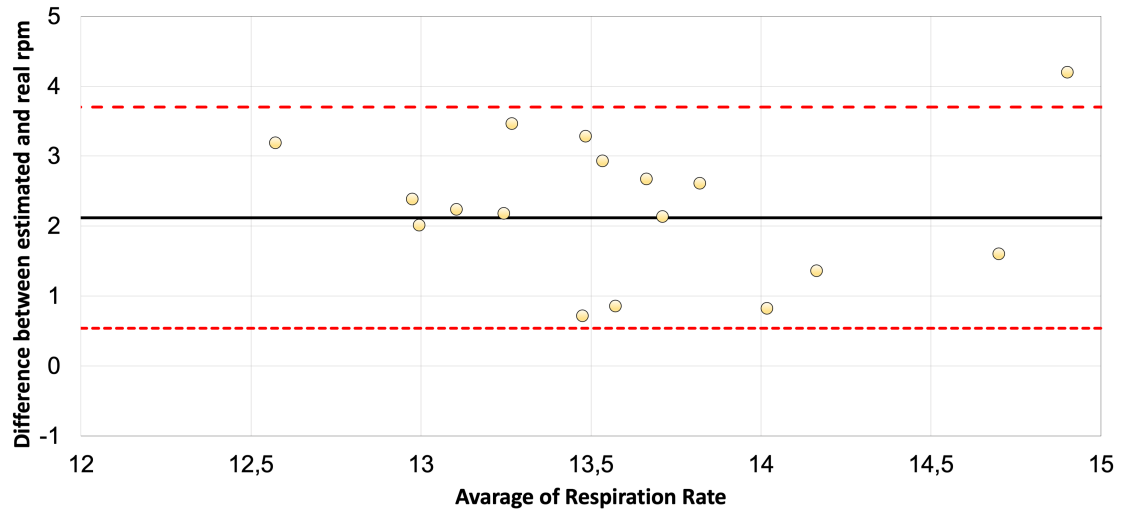


Figure 5.16: Bland Altman Plot of estimated rpm from the pipeline compared to the value of the ground truth - Normal bed and supine position

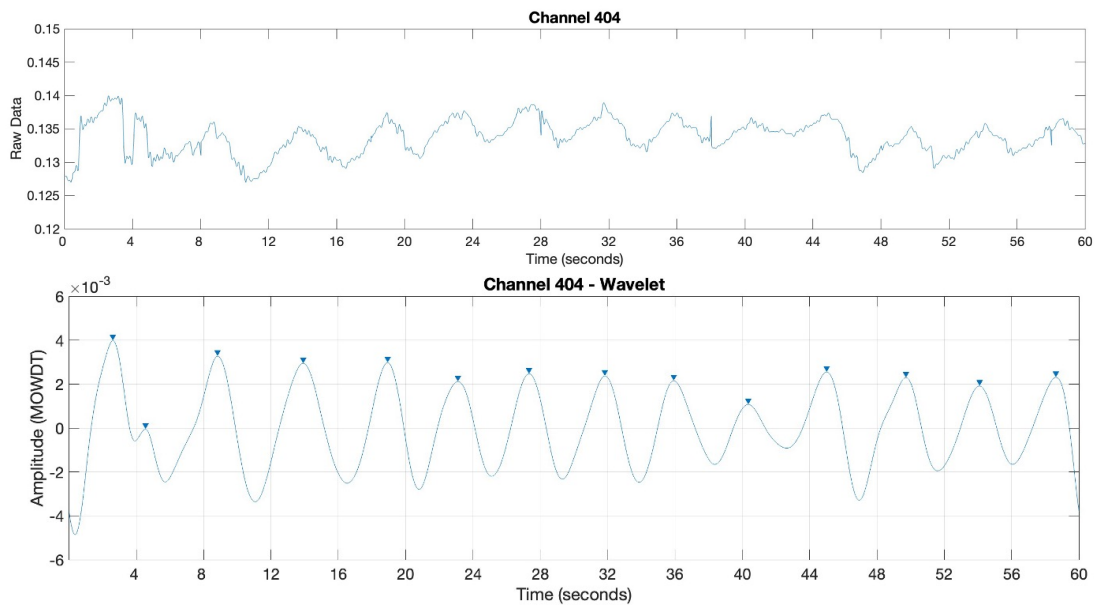


Figure 5.17: Raw data and denoised signal using MODWTMRA of the channel with the highest percentage of confidence (92%) - Normal bed and supine position

5.3 Result for Savitzky–Golay filter

The result presented in this section are denoised with Savitzky–Golay filter and are divided into normal bed, section 5.3.1, and rocking bed 5.3.2. Inside both sections are presented the result for each position for the binary and weighted approach.

5.3.1 Normal Bed

The participant in this phase has to perform a series of jumps before lying on the mattress due to recreating the increase or decrease of the breath rate between the different sleep stages. This phase aims to understand the feasibility of extracting breath rate from the mat. For this phase, the mattress is placed on a standard bed.

Result Normal Bed in Supine Position

The estimated respiratory rate per minute (rpm) while the participants are supine with the mattress placed on a normal bed is further presented. Table 5.17 presented the estimated rpm using binary and weighted approach compared with the rpm given by the ground truth. The approaches retrieve an almost identical rpm, this result may be due to the choice of the minimum confidence value at 80% that allows keeping only the best signal, maybe with higher confidence can be seen a higher difference between the two approaches.

Table 5.18 present the average rpm for both approaches and the relative mean absolute error (MAE) and mean absolute percentage error (MAPE). As just discussed in the previous paragraph there is no substantial difference between the two different approaches. The data on which to focus more is the number of breaths that the algorithm misses, represented by MAE and expressed in percentage by MAPE. The average number is 2rpm, which means that if we consider the estimated average of 14.5rpm the error is almost 20%, quite high for an approach that must be used in the medical field.

Binary	Weighted	RPM (NOXA1)
14.8438	14.7353	13.485
14	14	13.1443
15.125	15.125	12.5154
13.8333	13.8333	13.117
14.4286	14.4286	13.6077
15.5	15.5	13.8993
15	15	12.0681
11	11	11.4768
14.3333	14.3333	12.1549
17	17	12.8028
15	15	12.3275
14.1667	14.1667	10.9785
15.125	15.125	11.8441
14.7778	14.7778	12.6438
15	15	11.5351
14	14	11.99
14.2222	14.2222	11.9868
14.1667	13.8571	11.7824

Table 5.17: Estimated rpm using binary and weighted approach of the pipeline compared with the rpm given by the ground truth - Normal bed and supine position

	Binary	Weighted
rpm mean	14.529	14.506
MAE rpm	2.1731	2.1499
MAPE	17.8104%	17.6198%

Table 5.18: Avarage number of breath for each approach with the relative mean absolute error (MAE) and mean absolute percentage error (MAE) - Normal bed and supine position

Figure 5.32 show the Bland–Altman plot, presented in section 5.1.3, of the estimated rpm from the pipeline compared to the value of the ground truth. It helps to visualize the data from Table 5.18 in respect of the error. Since the result for the approaches is similar the data presented with this plot refers to the weighted approach only.

Figure 5.33 shows the denoised signal using MODWTMRA with the highest accuracy (92%) for the supine position with a normal mattress.

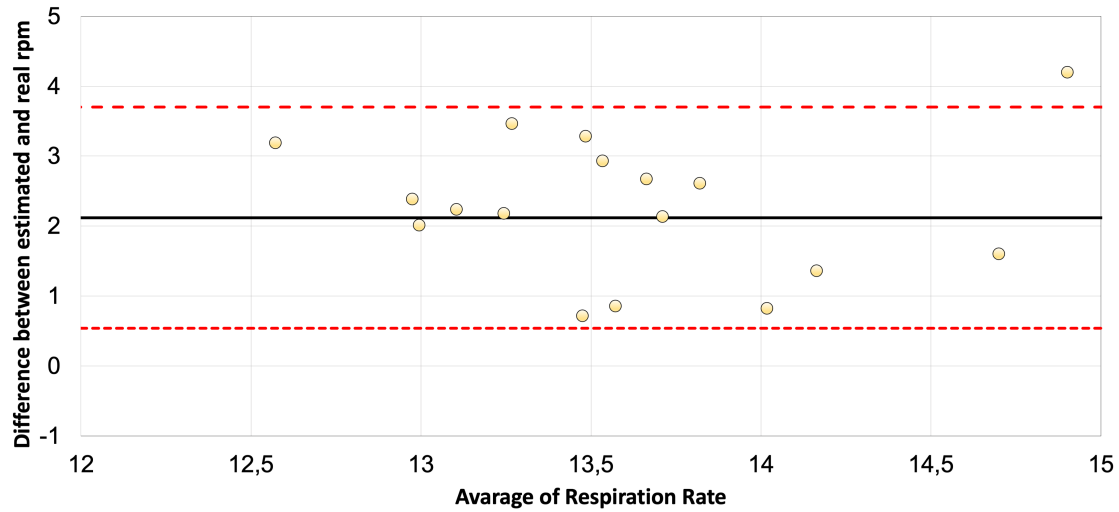


Figure 5.18: Bland Altman Plot of estimated rpm from the pipeline compared to the value of the ground truth - Normal bed and supine position

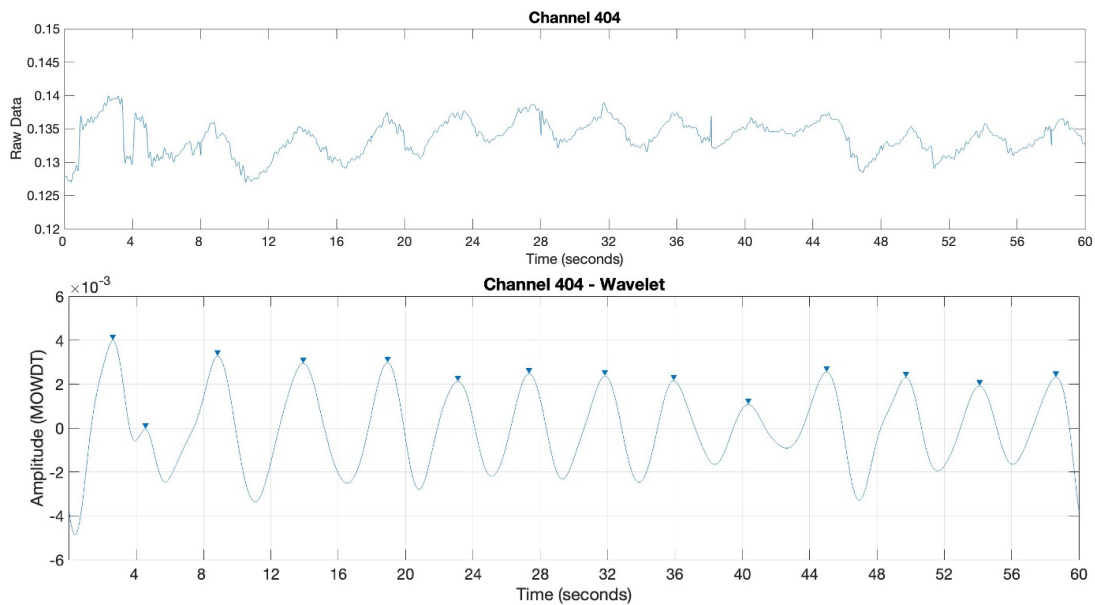


Figure 5.19: Raw data and denoised signal using MODWTMRA of the channel with the highest percentage of confidence (92%) - Normal bed and supine position

Result Normal Bed in Left Side Position

The estimated respiratory rate per minute (rpm) while the participants are on the left side with the mattress placed on a normal bed is further presented. Table 5.19 presented the estimated rpm using binary and weighted approach compared with the rpm given by the ground truth. The approaches retrieve an almost identical rpm, this result may be due to the choice of the minimum confidence value at 80% that allows keeping only the best signal, maybe with higher confidence can be seen a higher difference between the two approaches.

Binary	Weighed	RPM (NOXA1)
14.6364	14.6364	11.2045
15	15	12.7397
16	15.25	13.0613
14.2	14.2	12.2669
19	19	12.1628
15	14.5	13.6039
14.2222	14.2222	13.1398
15.6667	15.6667	11.5445
+ 14.7	14.7	10.77
15.8571	15.8571	14.2216
15.5556	15.5556	13.1656
16.5714	16.5714	12.9764
15	15	10.9055
15.125	15.125	13.2294
15.7143	15.5	12.8524
15.2	15.2	11.3824
14.6	14.6	13.5579
15.8889	15.8889	11.6069

Table 5.19: Estimated rpm using binary and weighted approach of the pipeline compared with the rpm given by the ground truth - - Normal bed and left side

Table 5.20 present the average rpm for both approaches and the relative mean absolute error (MAE) and mean absolute percentage error (MAPE). As just discussed in the previous paragraph there is no substantial difference between

the two different approaches. The data on which to focus more is the number of breaths that the algorithm misses, represented by MAE and expressed in percentage by MAPE. The average number is 2.5rpm, which means that if we consider the estimated average of 15.3rpm the error is over 24%, worst than in the supine position, probably due to the smaller contact area between the body and the mattress.

	Binary	Weighed
rpm mean	15.441	15.360
MAE resp	2.4545	2.8934
MAPE	24.62%	24.0041%

Table 5.20: varage number of breath for each approach with the relative mean absolute error (MAE) and mean absolute percentage error (MAE) - Normal bed and left side

Figure 5.22 show the Bland–Altman plot, presented in section 5.1.3, of the estimated rpm from the pipeline compared to the value of the ground truth. It helps to visualize the data from Table 5.20 in respect of the error. Since the result for the approaches is similar the data presented with this plot refers to the weighted approach only.

Figure 5.33 shows the denoised signal using MODWTMRA with the highest accuracy (92%) for the supine position with a normal mattress.

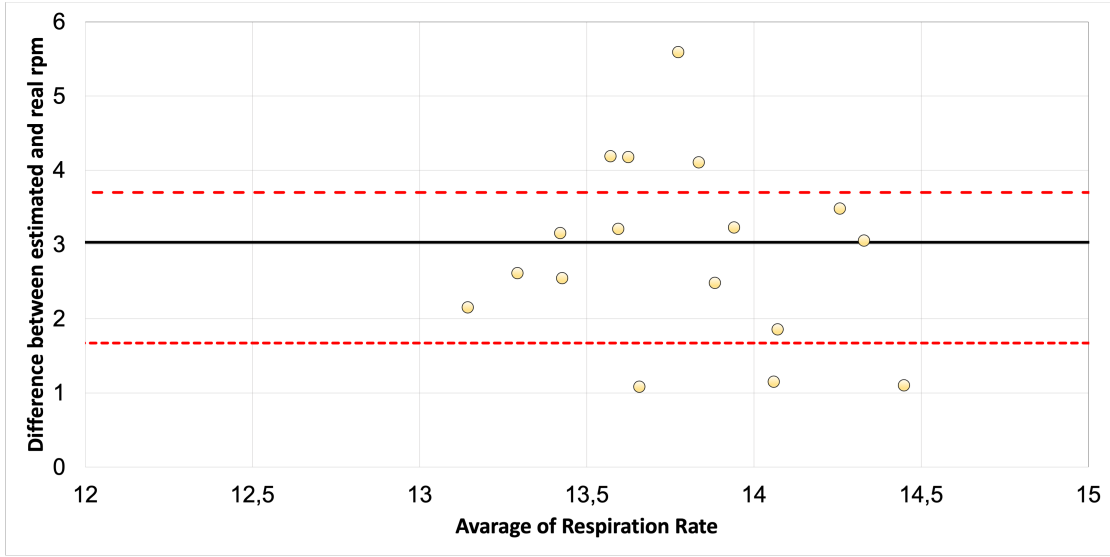


Figure 5.20: Bland Altman Plot of estimated rpm from the pipeline compared to the value of the ground truth - Normal bed and left side

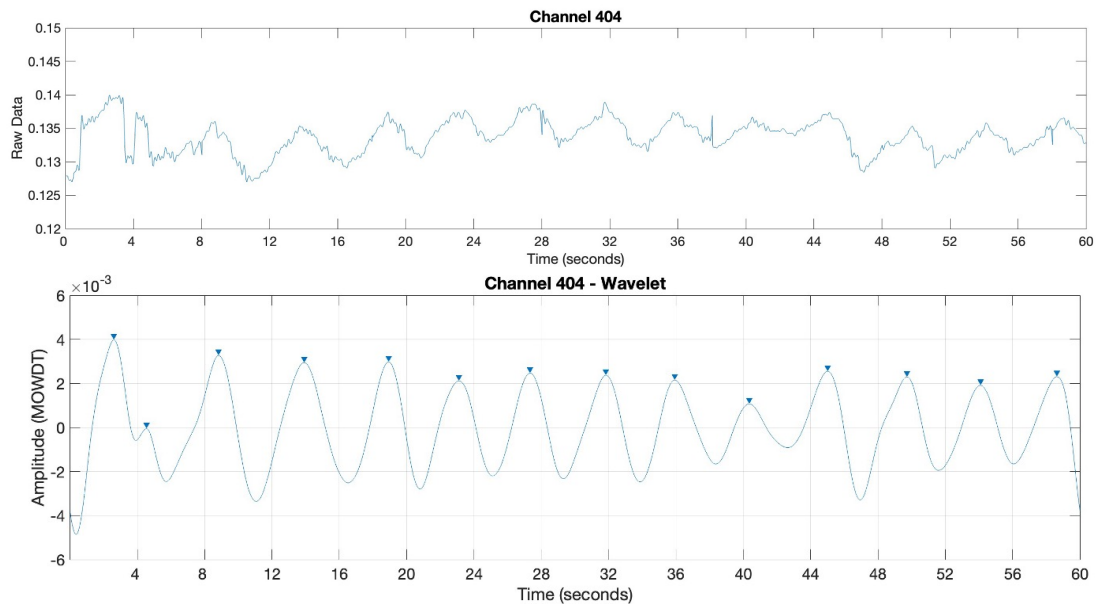


Figure 5.21: Raw data and denoised signal using MODWTMRA of the channel with the highest percentage of confidence (92%) - Normal bed and supine position

Result Normal Bed in Prone Side Position

The estimated respiratory rate per minute (rpm) while the participants are in the prone position with the mattress placed on a normal bed is further presented. Table 5.21 presented the estimated rpm using binary and weighted approach compared with the rpm given by the ground truth. The approaches retrieve an almost identical rpm, this result may be due to the choice of the minimum confidence value at 80% that allows keeping only the best signal, maybe with higher confidence can be seen a higher difference between the two approaches.

Binary	Weighed SGf	RPM (NOXA1)
15.7	15.7	11.5949
15.7333	15.7333	11.1628
16.1	16.1	11.0005
15.6667	15.6667	10.4762
15.25	15.25	10.4723
14.5714	14.5714	9.5345
15.5714	15.5714	9.5467
15.875	15.875	13.5758
14	14	11.1779
14.375	14.375	9.5345
14.4667	14.4667	9.5841
14.5	14.5	11.8196
14.2143	14.2143	11.8153
13.9474	13.9474	9.5223
15.037	15.037	10.8508
14.931	14.931	10.8876
15.25	15.25	10.9705
15.3333	15.3333	11.237

Table 5.21: Estimated rpm using binary and weighted approach of the pipeline compared with the rpm given by the ground truth - Normal bed and supine position

Table 5.22 present the average rpm for both approaches and the relative mean absolute error (MAE) and mean absolute percentage error (MAPE). As just discussed in the previous paragraph there is no substantial difference between

the two different approaches. The data on which to focus more is the number of breaths that the algorithm misses, represented by MAE and expressed in percentage by MAPE. The average number is 2.8rpm, which means that if we consider the estimated average of 15rpm the error is over 36%, worst worse than the two previous results it may depend on the movement of the chest in the prone position changes.

	Binary	Weighed
rpm mean	15.029	15.029
MAE rpm	2.8957 %	2.8957%
MAPE tool	36.5982	36.5982

Table 5.22: Metrics to evaluate the participant in belly position with moving mattress

Figure 5.22 show the Bland–Altman plot, presented in section 5.1.3, of the estimated rpm from the pipeline compared to the value of the ground truth. It helps to visualize the data from Table 5.22 in respect of the error. Since the result for the approaches is similar the data presented with this plot refers to the weighted approach only.

Figure 5.33 shows the denoised signal using MODWTMRA with the highest accuracy (92%) for the supine position with a normal mattress.

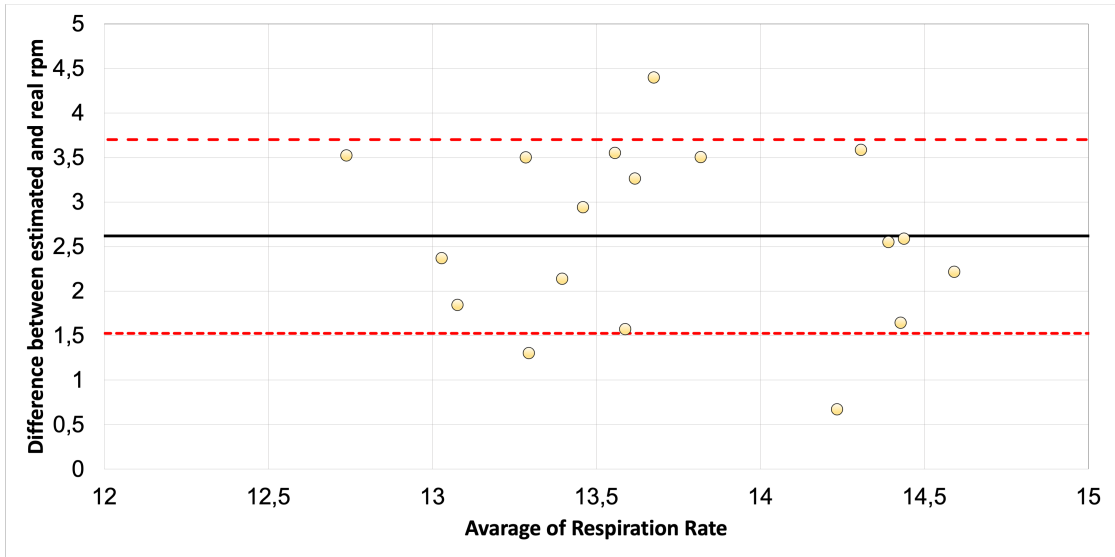


Figure 5.22: Bland Altman Plot of estimated rpm from the pipeline compared to the value of the ground truth - Normal bed and prone position

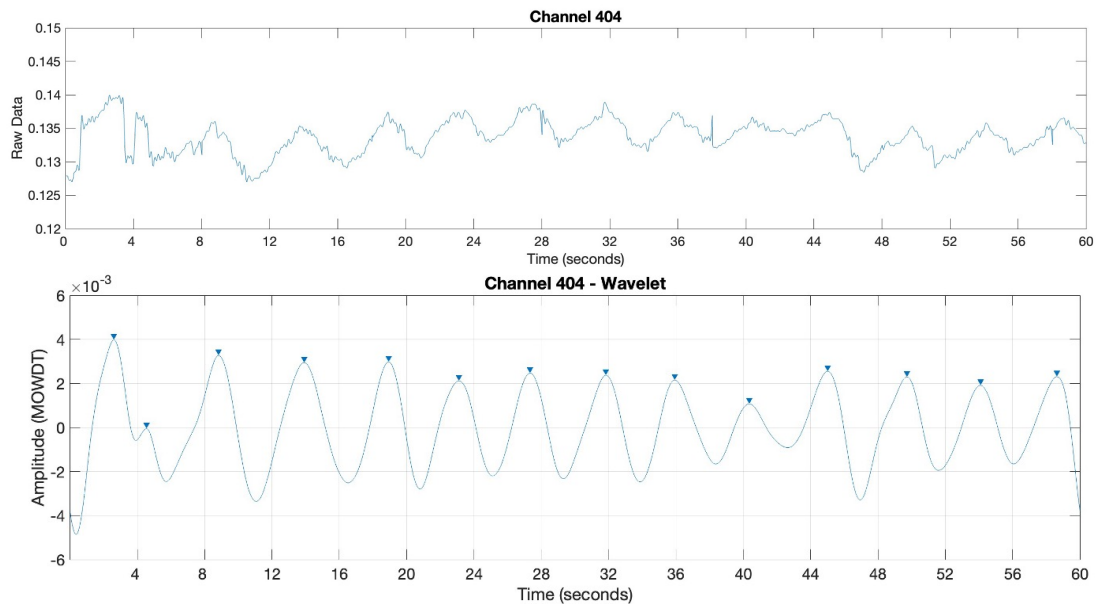


Figure 5.23: Raw data and denoised signal using MODWTMRA of the channel with the highest percentage of confidence (92%) - Normal bed and supine position

Result Normal Bed in Right Side Position

The estimated respiratory rate per minute (rpm) while the participants are on the right side with the mattress placed on a normal bed is further presented. Table 5.23 presented the estimated rpm using binary and weighted approach compared with the rpm given by the ground truth. The approaches retrieve an almost identical rpm, this result may be due to the choice of the minimum confidence value at 80% that allows keeping only the best signal, maybe with higher confidence can be seen a higher difference between the two approaches.

Binary	Weighed	RPM (NOXA1)
16.1667	16.1667	12.4771
17.75	17.75	13.0835
16.5	16.5	14.3858
15.25	15.25	12.7261
15.8333	15.8333	13.4867
15	15	12.9816
15.2353	15.2353	14.0566
15.1667	15.1667	12.038
15.5	15.5	11.4923
13	13	11.9625
13.3333	13.3333	11.0151
15.5	15.5	11.9016
14.3333	14.3333	11.4255
13.8333	13.8333	12.5227
15.2	15.2	11.5945
14.0909	14.0909	13.4141
14.5	14.4286	13.5282
15.2308	15.2308	12.9839

Table 5.23: Estimated rpm using binary and weighted approach of the pipeline compared with the rpm given by the ground truth - Normal bed and right side

Table 5.24 present the average rpm for both approaches and the relative mean absolute error (MAE) and mean absolute percentage error (MAPE). As just discussed in the previous paragraphs there is no substantial difference between

the two different approaches. The data on which to focus more is the number of breaths that the algorithm misses, represented by MAE and expressed in percentage by MAPE. The average number is 2.5rpm, which means that if we consider the estimated average of 15rpm the error is almost 20%, worst than in the supine position but better than in the prone position and left side.

	Binary	Weighed
rpm mean	15.015	15.020
MAE resp	2.4638	2.4691
MAPE	19.9146 %	19.9693 %

Table 5.24: Evarage number of breath for each approach with the relative mean absolute error (MAE) and mean absolute percentage error (MAE) - Normal bed and right side

Figure 5.24 show the Bland–Altman plot, presented in section 5.1.3, of the estimated rpm from the pipeline compared to the value of the ground truth. It helps to visualize the data from Table 5.24 in respect of the error. Since the result for the approaches is similar the data presented with this plot refers to the weighted approach only.

Figure 5.25 shows the denoised signal using MODWTMRA with the highest accuracy (92%) for the supine position with a normal mattress.

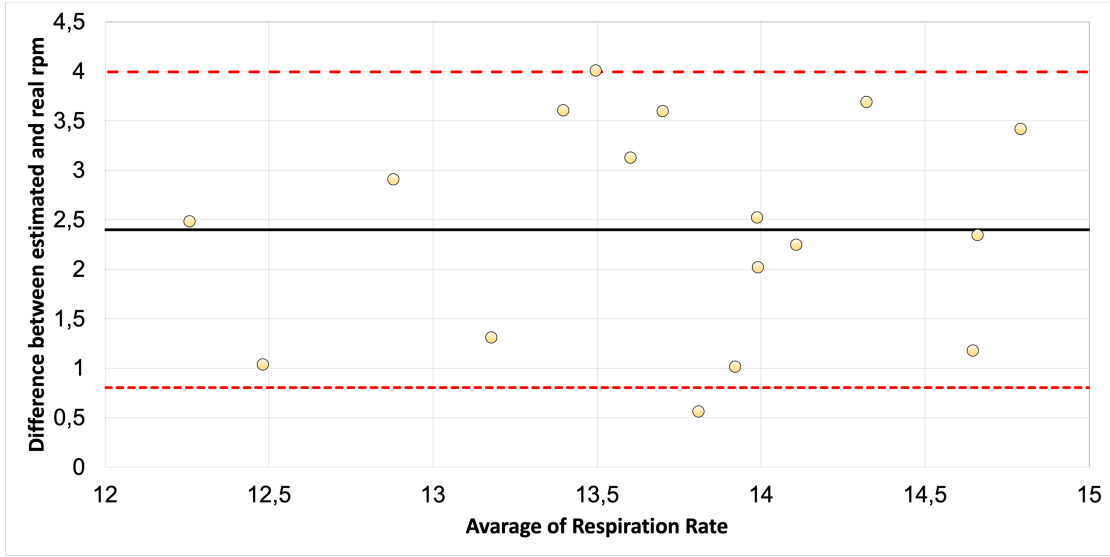


Figure 5.24: Bland Altman Plot of estimated rpm from the pipeline compared to the value of the ground truth - Normal bed and left side

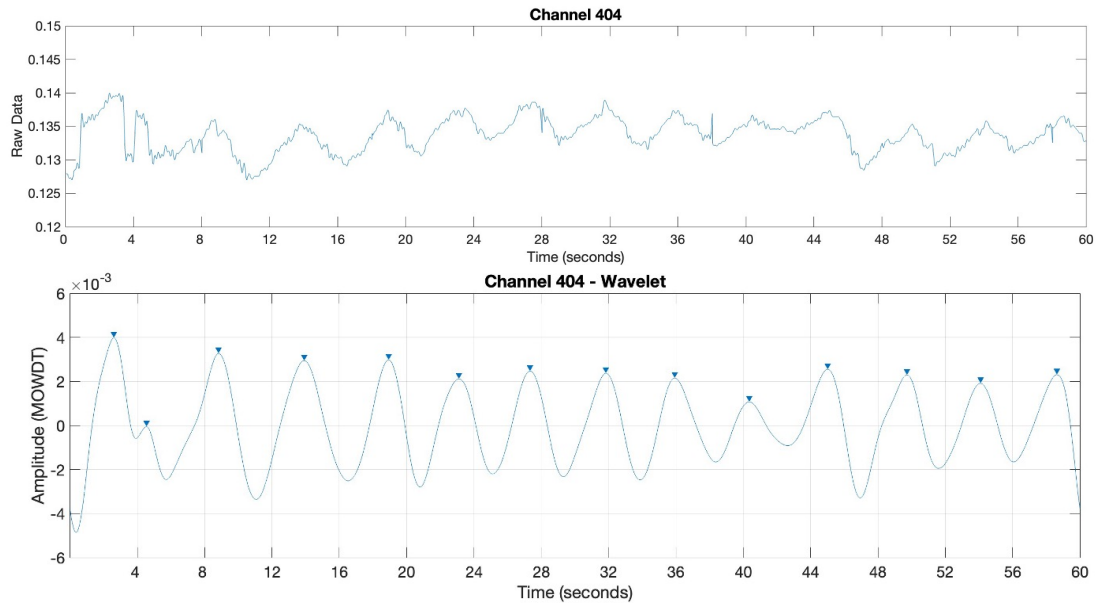


Figure 5.25: Raw data and denoised signal using MODWTMRA of the channel with the highest percentage of confidence (92%) - Normal bed and supine position

5.3.2 Rocking Bed

The second part of the data collection aims to understand if the movement of the rocking bed could influence the signal. The participant has to lie on the mattress without jumps, to have less variability in the data. For this phase, the mattress is placed on a rocking bed, which periods have been fixed at 4 seconds (15 periods in a minute) with an acceleration of 0.25 m/s^2 .

Result Rocking Bed in Supine Position

The estimated respiratory rate per minute (rpm) while the participants are supine with the mattress placed on a rocking bed is further presented.

Table 5.25 presented the estimated rpm using binary and weighted approach compared with the rpm given by the ground truth. The approaches retrieve an almost identical rpm.

Binary	Weighed	RPM (NOXA1)
15.5	15.5	10.7609
16.1333	16.1333	11.3077
15.3333	15.3333	13.1449
14.9474	14.9474	11.3366
15.1	15.1	12.7314
15.6364	15.6364	11.8892
14.6923	14.6923	11.42
15.2222	15.2222	13.0092
15.1667	15.1667	13.2539
14.6667	14.6667	11.6391
15	15	12.2165
14.75	14.75	11.9216
15	15	11.3091
14.625	14.625	13.8905
15.6154	15.6154	11.3344
15	14.8182	11.4474
15.1765	15.1765	11.6675
14.6154	14.6154	13.4799

Table 5.25: Estimated rpm using binary and weighted approach of the pipeline compared with the rpm given by the ground truth - Rocking bed and supine position

Table 5.25 present the average rpm for both approaches and the relative mean absolute error (MAE) and mean absolute percentage error (MAPE). As just discussed in the previous paragraph there is no substantial difference between the two different approaches. The data on which to focus more is the number of breaths that the algorithm misses, represented by MAE and expressed in percentage by MAPE. The average number is 3rpm, which means that if we consider the estimated average of 15.1rpm the error is almost 25%, is too high for an approach that must be used in the medical field.

Figure 5.32 show the Bland–Altman plot, presented in section 5.1.3, of the estimated rpm from the pipeline compared to the value of the ground truth. It helps to visualize the data from Table 5.26 in respect of the error. Since the result for the approaches is similar the data presented with this plot refers to the weighted approach only.

	Binary	Weighed
rpm mean	15.1211	15.1110
MAE resp	3.0234	3.0133
MAPE resp	25.7324%	25.6442%

Table 5.26: Evarage number of breath for each approach with the relative mean absolute error (MAE) and mean absolute percentage error (MAE) - Rocking bed and right side

Figure 5.33 shows the denoised signal using MODWTMRA with the highest accuracy (92%) for the supine position with a normal mattress.

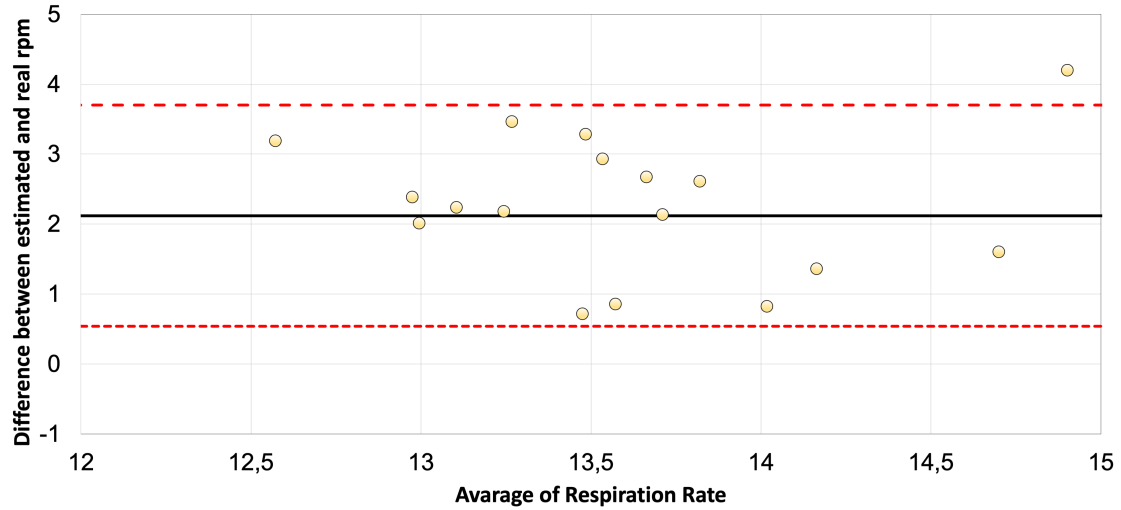


Figure 5.26: Bland Altman Plot of estimated rpm from the pipeline compared to the value of the ground truth - Rocking bed and supine position

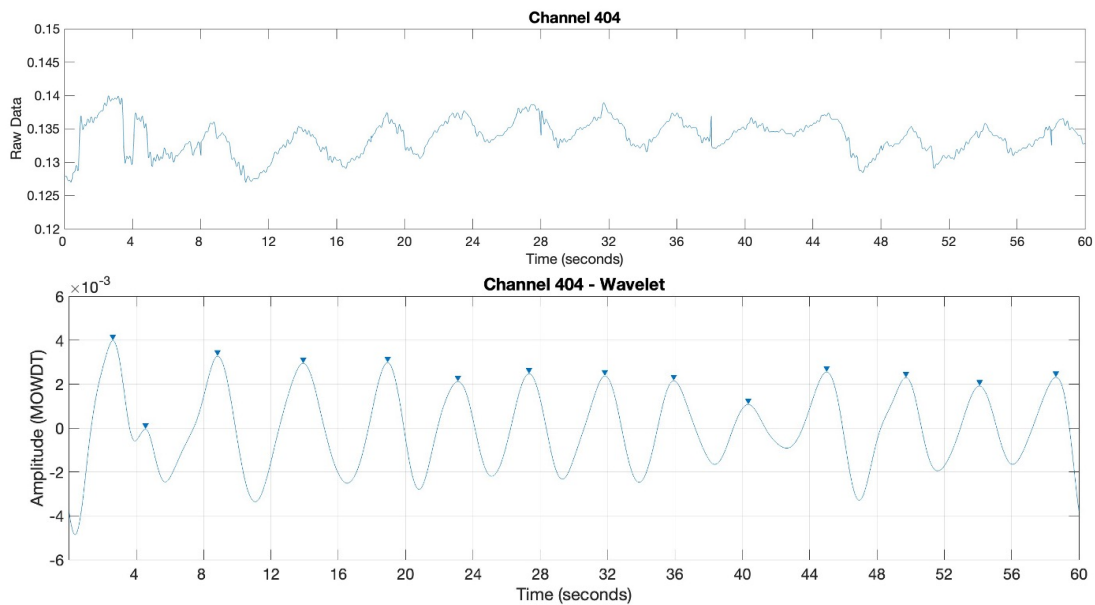


Figure 5.27: Raw data and denoised signal using MODWTMRA of the channel with the highest percentage of confidence (92%) - Normal bed and supine position

Result Rocking Bed in Left Side Position

The estimated respiratory rate per minute (rpm) while the participants are in left side position with the mattress placed on a rocking bed is further presented.

Table 5.27 presented the estimated rpm using binary and weighted approach compared with the rpm given by the ground truth. The approaches retrieve an almost identical rpm.

Binary	Weighed	RPM (NOXA1)
15.0625	15.0625	13.6613
15.5556	15.5556	11.4545
15.8824	15.8824	12.3288
16.1176	16.1176	10.8865
15.2083	15.2083	11.4082
15.3214	15.3103	12.2589
15.4583	15.4583	13.7093
15.4375	15.4375	12.7019
15.2353	15.2353	13.3305
15.5556	15.5556	13.7078
15.2143	15.2143	13.5674
15.2	15.1538	11.8694
15.5556	15.5556	13.4086
14.75	14.75	13.9781
14.5	14.5	12.4749
15.25	15.25	12.4049
14.625	14.7273	13.4108
14.2857	14.3333	13.4716

Table 5.27: Estimated rpm using binary and weighted approach of the pipeline compared with the rpm given by the ground truth - Rocking bed and left side

Table 5.27 present the average rpm for both approaches and the relative mean absolute error (MAE) and mean absolute percentage error (MAPE). As just discussed in the previous paragraph there is no substantial difference between the two different approaches. The data on which to focus more is the number of breaths that the algorithm misses, represented by MAE and expressed in percentage by MAPE. The average number is 2.5rpm, which means that if we consider the

estimated average of 15.2rpm the error is almost 20%, which is too high for an approach that must be used in the medical field.

	Binary	Weighed
rpm mean	15.2342	15.2393
MAE resp	2.4545	2.4597
MAPE resp	19.9605 %	19.9959 %

Table 5.28: Evarage number of breath for each approach with the relative mean absolute error (MAE) and mean absolute percentage error (MAE) - Rocking bed and left side

Figure 5.32 show the Bland–Altman plot, presented in section 5.1.3, of the estimated rpm from the pipeline compared to the value of the ground truth. It helps to visualize the data from Table 5.28 in respect of the error. Since the result for the approaches is similar the data presented with this plot refers to the weighted approach only.

Figure 5.33 shows the denoised signal using MODWTMRA with the highest accuracy (92%) for the supine position with a normal mattress.

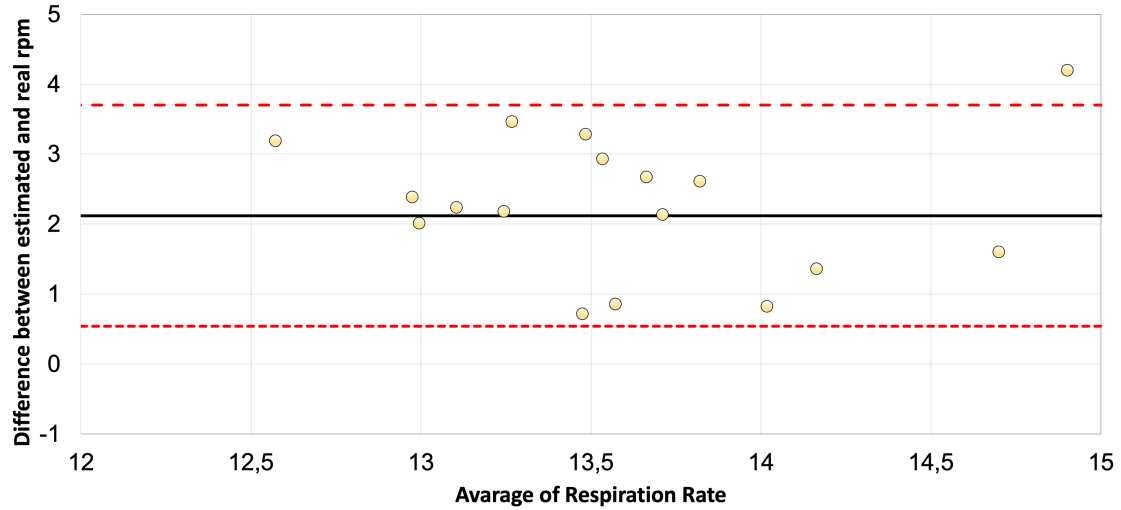


Figure 5.28: Bland Altman Plot of estimated rpm from the pipeline compared to the value of the ground truth - Normal bed and supine position

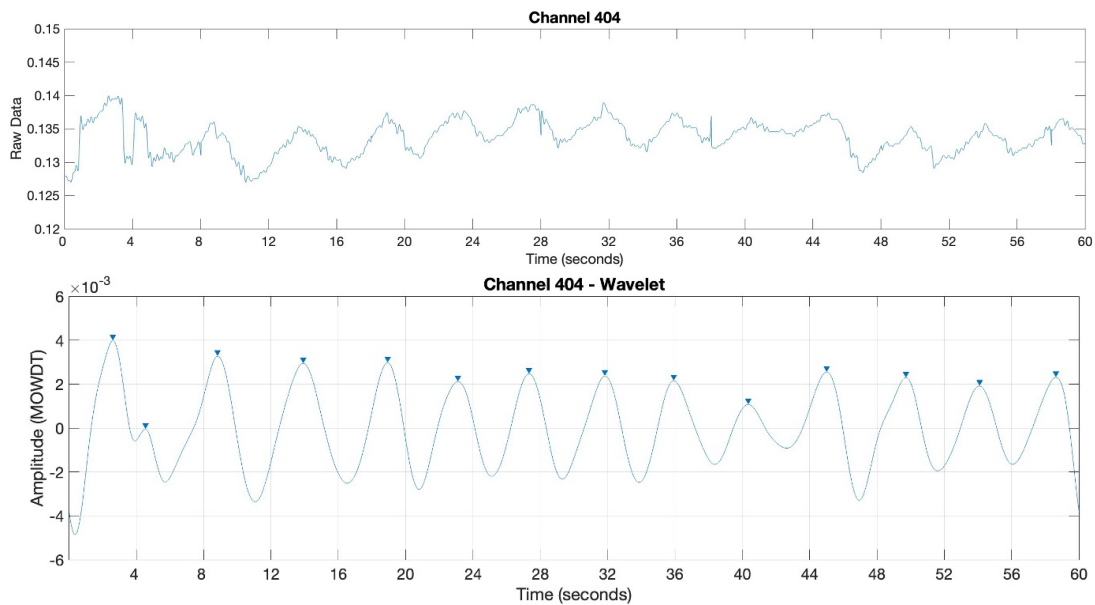


Figure 5.29: Raw data and denoised signal using MODWTMRA of the channel with the highest percentage of confidence (92%) - Normal bed and supine position

Result Rocking Bed in Prone Position

The estimated respiratory rate per minute (rpm) while the participants are in prone position with the mattress placed on a rocking bed is further presented.

Table 5.27 presented the estimated rpm using binary and weighted approach compared with the rpm given by the ground truth. The approaches retrieve an almost identical rpm.

Binary	Weighed	RPM (NOXA1)
16	16	12.6296
15.3684	15.3684	14.168
15.6818	15.6818	13.2588
15.5	15.4286	13.8107
15.8333	15.8333	13.485
16	16	12.6052
16	16	11.0417
15.7059	15.7059	12.9088
15.5333	15.5333	13.0502
16.3333	16.3333	11.1723
14.5625	14.5625	14.6869
15.5294	15.5294	11.3484
14.7273	14.7273	13.0399
14.7778	14.7778	9.54872
15.4444	15.4444	11.7918
14.9286	14.9286	12.8182
15.8333	15.8333	9.53453
14.619	14.619	9.5416

Table 5.29: Estimated rpm using binary and weighted approach of the pipeline compared with the rpm given by the ground truth - Rocking bed and prone position

Table 5.30 present the average rpm for both approaches and the relative mean absolute error (MAE) and mean absolute percentage error (MAPE). As just discussed in the previous paragraph there is no substantial difference between the two different approaches. The data on which to focus more is the number of breaths that the algorithm misses, represented by MAE and expressed in percentage by MAPE. The average number is 2.5rpm, which means that if we consider the estimated average of 15.2rpm the error is almost 20%, which is too high for an

approach that must be used in the medical field.

	Binary	Weighed
rpm mean	15.4655	15.4615
MAE resp	3.2326	3.2286
MAPE resp	28.5509	28.5221

Table 5.30: Evarage number of breath for each approach with the relative mean absolute error (MAE) and mean absolute percentage error (MAE) - Rocking bed and prone position

Figure 5.32 show the Bland–Altman plot, presented in section 5.1.3, of the estimated rpm from the pipeline compared to the value of the ground truth. It helps to visualize the data from Table 5.30 in respect of the error. Since the result for the approaches is similar the data presented with this plot refers to the weighted approach only.

Figure 5.33 shows the denoised signal using MODWTMRA with the highest accuracy (92%) for the supine position with a normal mattress.

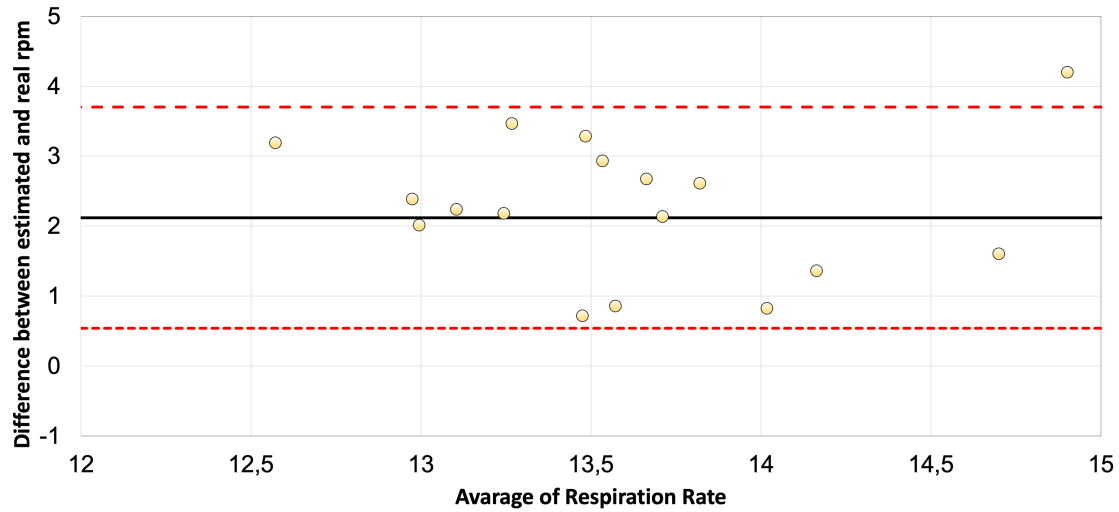


Figure 5.30: Bland Altman Plot of estimated rpm from the pipeline compared to the value of the ground truth - Normal bed and supine position

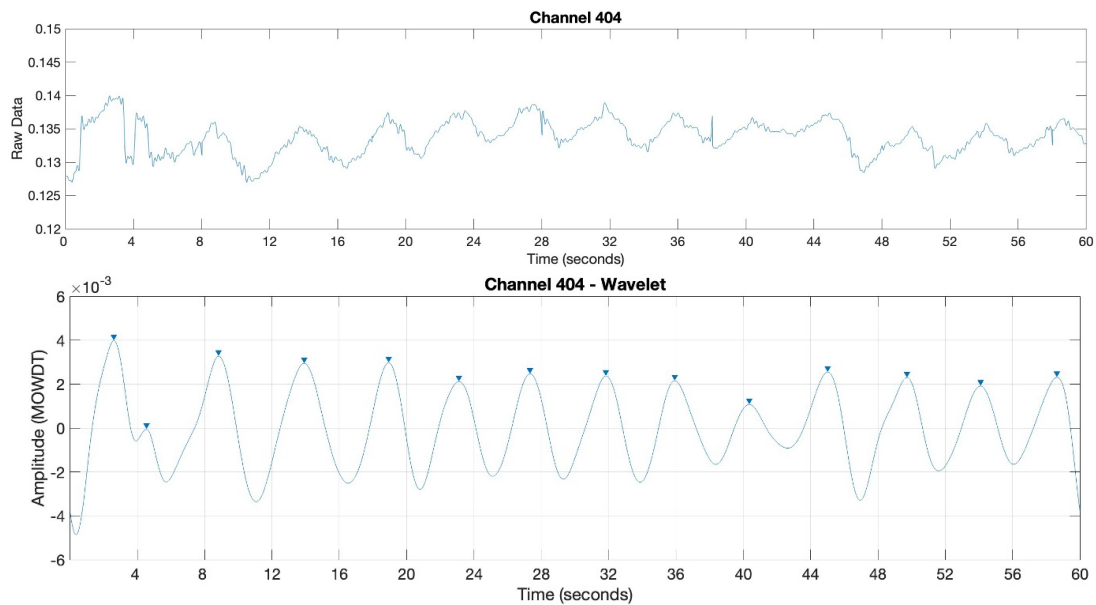


Figure 5.31: Raw data and denoised signal using MODWTMRA of the channel with the highest percentage of confidence (92%) - Normal bed and supine position

Result Rocking Bed in Right Side

The estimated respiratory rate per minute (rpm) while the participants are in right side position with the mattress placed on a rocking bed is further presented.

Table 5.31 presented the estimated rpm using binary and weighted approach compared with the rpm given by the ground truth. The approaches retrieve an almost identical rpm.

Binary	Weighed	RPM (NOXA1)
15.8095	15.8095	11.7955
15.2105	15.1	11.9185
15.5652	15.5652	11.8639
15.8261	15.8261	12.28
15.6667	15.6667	12.0136
15.1176	15.1176	12.8838
15.3571	15.3571	11.5695
15	14.8696	12.8922
15.1176	15.1176	11.587
15.2857	15.2857	11.2449
15.3333	15.3333	11.7082
15.3684	15.35	13.9497
15.6154	15.4286	11.6145
15.4286	15.4286	13.9913
15.2727	15.2727	11.6172
15.3	15.3	13.3257
15.1667	15.1667	13.5179
14.9231	14.9286	13.5767

Table 5.31: Estimated rpm using binary and weighted approach of the pipeline compared with the rpm given by the ground truth - Rocking bed and right side position

Table 5.31 present the average rpm for both approaches and the relative mean absolute error (MAE) and mean absolute percentage error (MAPE). As just discussed in the previous paragraph there is no substantial difference between the two different approaches. The data on which to focus more is the number of breaths that the algorithm misses, represented by MAE and expressed in percentage by MAPE. The average number is 2.9rpm, which means that if we consider the

	Binary	Weighed
rpm mean	15.3536	15.3291
MAE resp	2.9452	2.9208
MAPE	24.4008 %	24.1986%

Table 5.32: Everage number of breath for each approach with the relative mean absolute error (MAE) and mean absolute percentage error (MAE) - Rocking bed and right side

estimated average of 15.3rpm the error is almost 24%, which is too high for an approach that must be used in the medical field.

Figure 5.32 show the Bland–Altman plot, presented in section 5.1.3, of the estimated rpm from the pipeline compared to the value of the ground truth. It helps to visualize the data from Table 5.32 in respect of the error. Since the result for the approaches is similar the data presented with this plot refers to the weighted approach only.

Figure 5.33 shows the denoised signal using MODWTMRA with the highest accuracy (92%) for the supine position with a normal mattress.

5.4 Final Remarks on the Results

This chapter presented the results of the pipeline. Since it has several parameters that can be chosen and they influence the outcome, they are commented on.

The pipeline allows choosing which approach to use to denoise the signal, in order to be able to give it as input to a peak finder. The different approaches are Multiresolution Overlap Discrete Wavelet Transform (described in Chapter 4.2.4) and Savitzky–Golay filter (described in Chapter 4.2.5). Both approaches are used in the context of the estimation of respiratory rate [43, 48], for this reason, it has been very important to have the possibility to compare them to understand which one could perform better in the context of this thesis.

The result presented in the previous section highlighted how the Savitzky–Golay filter has a lower error in respect of the wavelet approach. In fact, focusing on the MAPE it is 10% lower in most of the positions and in both settings. The average error is 1 breath in respect of MODWTMRA which arrive up to 4 in the case of a

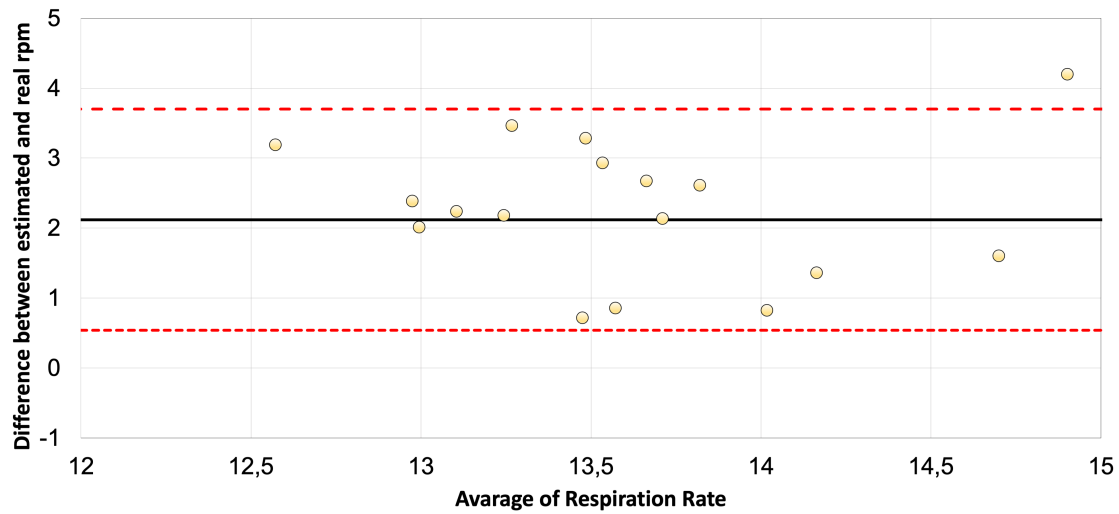


Figure 5.32: Bland Altman Plot of estimated rpm from the pipeline compared to the value of the ground truth - Normal bed and supine position

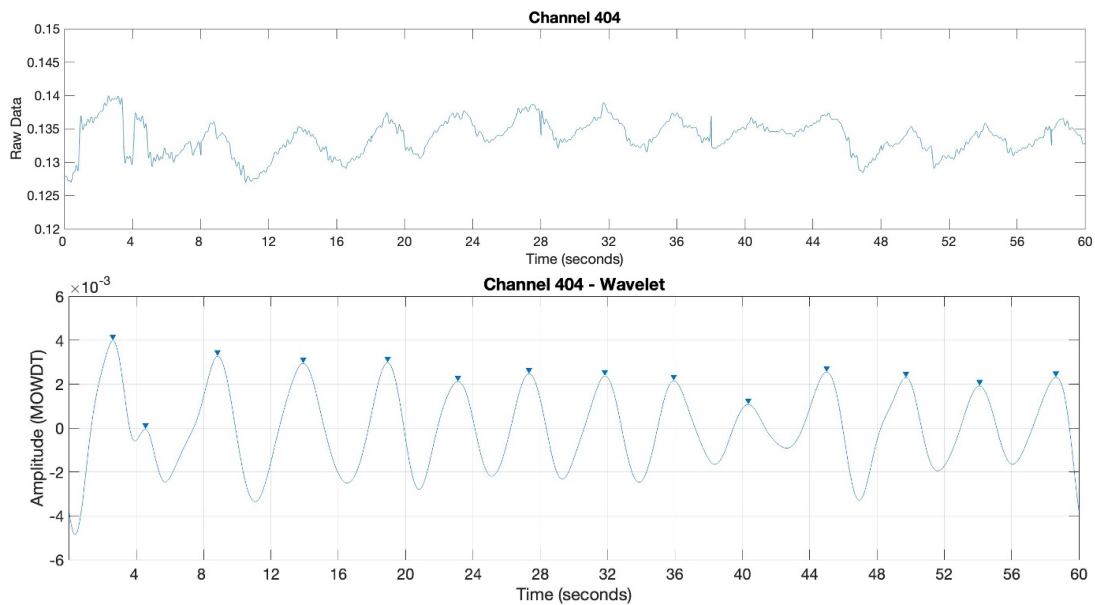


Figure 5.33: Raw data and denoised signal using MODWTMRA of the channel with the highest percentage of confidence (92%) - Normal bed and supine position

prone position with a rocking bed.

One of the aims of the data collection conducted during this study, described in Chapter 3.2, has been to understand if the movement of the rocking bed could influence the signal from the mattress. Even if the bed is designed to have an inaudible rocking mechanism, it is reasonable to expect that the movement could influence the data acquisition. The raw data visually present more noise, but the denoise approaches are able to exclude it and estimate the respiratory rate. This can be seen in the reconstruction of the data, as shown in figure [PLACEHOLDER], and also in the result of the metrics that have a slight increase of the error but not higher as expected. From the respiratory rate point of view, the influence on the error is mostly given by the chosen approach rather than the bed set.

The position of the participant on the bed also seems to be decisive, in the prone position the error increases particularly and in the supine has the minimum error. It may depend on the movement of the chest that in the prone position changes.

Chapter 6

Conclusion

This thesis's projects have been focused to investigate the possibility of estimating a patient's respiratory rate using a sensor pressure mattress.

In order to understand this possibility has been conducted a preliminary study of Sensomative mattress data, already available from previous data collection. This has highlighted the possibility, of using a multiresolution overlap discrete wavelet transform to denoise the data to recreate a clean wave to then apply a peak finder algorithm. Consequently having defined as breath the moment between inhaling and exhaling, has been possible to asset the respiration rate per minute as the number of peaks in a minute, retrieved from the signals of the mattress but also visible in the nasal pressure of the cardiopulmonary polysomnography.

The project concentrates on the SensingTex mattress whose data were not available and leading to the necessity to conduct a data collection. In the course of that, it has been recreated the condition to have variability in the data and also collected while the Somnomat Casa was moving. The second phase aims to understand if the movement of the rocking bed could influence the signals.

Seen the number of SensingTex sensors has been necessary to design a pipeline that discriminates the ones that represent a respiratory pattern from the others, through the definition of a metric that asset the percentage of confidence to have a respiratory pattern in that specific signal for that window. Within the pipeline is it possible to choose: the approach with whom use the criteria, binary or weighted, and the methods to denoise the raw data, such as multiresolution overlap discrete

wavelet or Savitzky–Golay filter. The best channels retrieved with the pipeline are analysed with a peak finder to asset the respiration rate per minute estimated from that sensor. The result is an average of the estimated respiratory rate per minute between the best sensors.

Looking at the mean average error of the result for each position, the Savitzky–Golay filter has a lower error in almost every position of 10%. Although the error also seems to be determined by the position of the person on the mattress, in the prone position this may be due to different movements of the chest that is in direct contact with the bed. Even if with a not negligible error of average 2 breaths, the first aim of this thesis, i.e. to understand the feasibility to estimate respiratory rate from a sensor pressure mattress, has been addressed.

The data collected while the bed is moving are slightly worse in respect of the data collected on a normal bed. However, this increase is not as consistent as we would have expected. This knowledge leads to accomplishing the second goal of the data collection and of this project, i.e. to understand if the movement of the rocking bed affects the signal. There is a slight effect but not to be prevented from estimating the respiratory rate. The objectives of the thesis are then achieved.

The limitation of this thesis is the small number of participants in the data collection, that are in the same age group even if well balanced between genders. Since different age groups have different respiratory rates at rest, exploring them could be significant to improve the pipeline. A further limitation is a mean average error that is too high to use this approach in the medical context, such as in the study of sleep stages which requires more accurate estimation. Although in domestic use, to satisfy a person’s desire to track respiratory rhythm, this error is not a issue.

List of Tables

5.1	Estimated rpm using binary and weighted approach of the pipeline compared with the rpm given by the ground truth - Normal bed and supine position	52
5.2	Average number of breath for each approach with the relative mean absolute error (MAE) and mean absolute percentage error (MAE) - Normal bed and supine position	52
5.3	Estimated rpm using binary and weighted approach of the pipeline compared with the rpm given by the ground truth - - Normal bed and left side	55
5.4	varage number of breath for each approach with the relative mean absolute error (MAE) and mean absolute percentage error (MAE) - Normal bed and left side	55
5.5	Estimated rpm using binary and weighted approach of the pipeline compared with the rpm given by the ground truth - Normal bed and supine position	58
5.6	Metrics to evaluate the participant in belly position with moving mattress	59
5.7	Estimated rpm using binary and weighted approach of the pipeline compared with the rpm given by the ground truth - Normal bed and right side	61
5.8	Evarage number of breath for each approach with the relative mean absolute error (MAE) and mean absolute percentage error (MAE) - Normal bed and right side	62

5.9	Estimated rpm using binary and weighted approach of the pipeline compared with the rpm given by the ground truth - Rocking bed and supine position	65
5.10	Evarage number of breath for each approach with the relative mean absolute error (MAE) and mean absolute percentage error (MAE) - Rocking bed and right side	66
5.11	Estimated rpm using binary and weighted approach of the pipeline compared with the rpm given by the ground truth - Rocking bed and left side	68
5.12	Evarage number of breath for each approach with the relative mean absolute error (MAE) and mean absolute percentage error (MAE) - Rocking bed and left side	69
5.13	Estimated rpm using binary and weighted approach of the pipeline compared with the rpm given by the ground truth - Rocking bed and prone position	71
5.14	Evarage number of breath for each approach with the relative mean absolute error (MAE) and mean absolute percentage error (MAE) - Rocking bed and prone position	72
5.15	Estimated rpm using binary and weighted approach of the pipeline compared with the rpm given by the ground truth - Rocking bed and right side position	74
5.16	Evarage number of breath for each approach with the relative mean absolute error (MAE) and mean absolute percentage error (MAE) - Rocking bed and right side	75
5.17	Estimated rpm using binary and weighted approach of the pipeline compared with the rpm given by the ground truth - Normal bed and supine position	78
5.18	Avarage number of breath for each approach with the relative mean absolute error (MAE) and mean absolute percentage error (MAE) - Normal bed and supine position	78
5.19	Estimated rpm using binary and weighted approach of the pipeline compared with the rpm given by the ground truth - - Normal bed and left side	80

5.20	varage number of breath for each approach with the relative mean absolute error (MAE) and mean absolute percentage error (MAE) - Normal bed and left side	81
5.21	Estimated rpm using binary and weighted approach of the pipeline compared with the rpm given by the ground truth - Normal bed and supine position	83
5.22	Metrics to evaluate the participant in belly position with moving mattress	84
5.23	Estimated rpm using binary and weighted approach of the pipeline compared with the rpm given by the ground truth - Normal bed and right side	86
5.24	Evarage number of breath for each approach with the relative mean absolute error (MAE) and mean absolute percentage error (MAE) - Normal bed and right side	87
5.25	Estimated rpm using binary and weighted approach of the pipeline compared with the rpm given by the ground truth - Rocking bed and supine position	90
5.26	Evarage number of breath for each approach with the relative mean absolute error (MAE) and mean absolute percentage error (MAE) - Rocking bed and right side	91
5.27	Estimated rpm using binary and weighted approach of the pipeline compared with the rpm given by the ground truth - Rocking bed and left side	93
5.28	Evarage number of breath for each approach with the relative mean absolute error (MAE) and mean absolute percentage error (MAE) - Rocking bed and left side	94
5.29	Estimated rpm using binary and weighted approach of the pipeline compared with the rpm given by the ground truth - Rocking bed and prone position	96
5.30	Evarage number of breath for each approach with the relative mean absolute error (MAE) and mean absolute percentage error (MAE) - Rocking bed and prone position	97

5.31 Estimated rpm using binary and weighted approach of the pipeline compared with the rpm given by the ground truth - Rocking bed and right side position	99
5.32 Evarage number of breath for each approach with the relative mean absolute error (MAE) and mean absolute percentage error (MAE) - Rocking bed and right side	100

List of Figures

2.1	Sleep Cycles	10
2.2	Respiratory sistem	12
2.3	Polysomnography	15
2.4	Cardiorespiratory Polysomnography	16
2.5	Pressure Sensor Array	17
2.6	Sensing Mat (optic fiber sensors)	17
2.7	Inflatable Mattress	18
2.8	Sensomatic textile sensors	18
3.1	Sensomatic over a bed	20
3.2	Sensomatic data	21
3.3	SensigTex over a bed	22
3.4	SensigTex Data	23
3.5	Nox A1™ PSG System device of NoxMedical	24
3.6	Somnomat	25
3.7	Place holder normal bed	27
3.8	Place holder rocking bed	27
3.9	Full recording of a participant - 42 minutes long	28
4.1	Breath pattern	30
4.2	MODWTMRA reconstruction	30
4.3	4 minute	31
4.4	1 minute	32
4.5	Pipeline	33
4.6	Raw Data - Channel 500 - Stationary on a Value	34
4.7	Raw Data - Channel 100 - Partial Stationary Signal	34

4.8	Raw Data - Channel 121 - Small amplitude	35
4.9	Raw Data - Channel 322 - Massive presence of Spike	36
4.10	Raw Data - Channel 404 - Small presence of spikes	36
4.11	Daubechies wavelet with two vanishing moments	38
4.12	Stationary Signal	39
4.13	Raw Data - Channel 579 - Massive presence of Spike	40
4.14	Channel 404 Filtered - with Wavelet	40
4.15	Savitzky-Golay filter	42
4.16	Channel 404 Filtered - with Savitz-Golay filter	43
4.17	Euclidean	44
4.18	Length	45
4.19	Heatmap of channels with the highest confidence	47
5.1	Example of Bland Altman Plot	50
5.2	Bland Altman Plot of estimated rpm from the pipeline compared to the value of the ground truth - Normal bed and supine position . . .	54
5.3	Raw data and denoised signal using MODWTMRA of the channel with the highest percentage of confidence (92%) - Normal bed and supine position	54
5.4	Bland Altman Plot of estimated rpm from the pipeline compared to the value of the ground truth - Normal bed and left side	57
5.5	Raw data and denoised signal using MODWTMRA of the channel with the highest percentage of confidence (92%) - Normal bed and supine position	57
5.6	Bland Altman Plot of estimated rpm from the pipeline compared to the value of the ground truth - Normal bed and prone position . . .	60
5.7	Raw data and denoised signal using MODWTMRA of the channel with the highest percentage of confidence (92%) - Normal bed and supine position	60
5.8	Bland Altman Plot of estimated rpm from the pipeline compared to the value of the ground truth - Normal bed and left side	63
5.9	Raw data and denoised signal using MODWTMRA of the channel with the highest percentage of confidence (92%) - Normal bed and supine position	63

5.10 Bland Altman Plot of estimated rpm from the pipeline compared to the value of the ground truth - Rocking bed and supine position	67
5.11 Raw data and denoised signal using MODWTMRA of the channel with the highest percentage of confidence (92%) - Normal bed and supine position	67
5.12 Bland Altman Plot of estimated rpm from the pipeline compared to the value of the ground truth - Normal bed and supine position	70
5.13 Raw data and denoised signal using MODWTMRA of the channel with the highest percentage of confidence (92%) - Normal bed and supine position	70
5.14 Bland Altman Plot of estimated rpm from the pipeline compared to the value of the ground truth - Normal bed and supine position	73
5.15 Raw data and denoised signal using MODWTMRA of the channel with the highest percentage of confidence (92%) - Normal bed and supine position	73
5.16 Bland Altman Plot of estimated rpm from the pipeline compared to the value of the ground truth - Normal bed and supine position	76
5.17 Raw data and denoised signal using MODWTMRA of the channel with the highest percentage of confidence (92%) - Normal bed and supine position	76
5.18 Bland Altman Plot of estimated rpm from the pipeline compared to the value of the ground truth - Normal bed and supine position	79
5.19 Raw data and denoised signal using MODWTMRA of the channel with the highest percentage of confidence (92%) - Normal bed and supine position	79
5.20 Bland Altman Plot of estimated rpm from the pipeline compared to the value of the ground truth - Normal bed and left side	82
5.21 Raw data and denoised signal using MODWTMRA of the channel with the highest percentage of confidence (92%) - Normal bed and supine position	82
5.22 Bland Altman Plot of estimated rpm from the pipeline compared to the value of the ground truth - Normal bed and prone position	85

5.23 Raw data and denoised signal using MODWTMRA of the channel with the highest percentage of confidence (92%) - Normal bed and supine position	85
5.24 Bland Altman Plot of estimated rpm from the pipeline compared to the value of the ground truth - Normal bed and left side	88
5.25 Raw data and denoised signal using MODWTMRA of the channel with the highest percentage of confidence (92%) - Normal bed and supine position	88
5.26 Bland Altman Plot of estimated rpm from the pipeline compared to the value of the ground truth - Rocking bed and supine position . . .	92
5.27 Raw data and denoised signal using MODWTMRA of the channel with the highest percentage of confidence (92%) - Normal bed and supine position	92
5.28 Bland Altman Plot of estimated rpm from the pipeline compared to the value of the ground truth - Normal bed and supine position . . .	95
5.29 Raw data and denoised signal using MODWTMRA of the channel with the highest percentage of confidence (92%) - Normal bed and supine position	95
5.30 Bland Altman Plot of estimated rpm from the pipeline compared to the value of the ground truth - Normal bed and supine position . . .	98
5.31 Raw data and denoised signal using MODWTMRA of the channel with the highest percentage of confidence (92%) - Normal bed and supine position	98
5.32 Bland Altman Plot of estimated rpm from the pipeline compared to the value of the ground truth - Normal bed and supine position . . .	101
5.33 Raw data and denoised signal using MODWTMRA of the channel with the highest percentage of confidence (92%) - Normal bed and supine position	101

Bibliography

- [1] T. Penzel, J. W. Kantelhardt, R. P. Bartsch, M. Riedl, J. F. Kraemer, N. Wessel, C. Garcia, M. Glos, I. Fietze, and C. Schöbel, “Modulations of Heart Rate, ECG, and Cardio-Respiratory Coupling Observed in Polysomnography,” *Frontiers in physiology*, vol. 7, 10 2016.
- [2] J. M. Calleja, S. Esnaola, R. Rubio, and J. Durá, “Comparison of a cardiorespiratory device versus polysomnography for diagnosis of sleep apnoea,”
- [3] Z. Wang, Z. Sui, A. Zhang, R. Wang, Z. Zhang, F. Lin, J. Chen, and S. Gao, “A piezoresistive array based force sensing technique for sleeping posture and respiratory rate detection for sas patients,” *IEEE Sensors Journal*, pp. 1–1, 2021.
- [4] A. Gasmi, V. Augusto, P. A. Beaudet, J. Faucheu, C. Morin, X. Serpaggi, and F. Vassel, “Sleep stages classification using cardio-respiratory variables,” *IEEE International Conference on Automation Science and Engineering*, vol. 2020-August, pp. 1031–1036, 8 2020.
- [5] A. Pal, F. Martinez, M. A. Akey, R. S. Aysola, L. A. Henderson, A. Malhotra, and P. M. Macey, “Breathing rate variability in obstructive sleep apnea during wakefulness,” *Journal of clinical sleep medicine : JCSM : official publication of the American Academy of Sleep Medicine*, vol. 18, pp. 825–833, 3 2022.
- [6] D. Zito, D. Pepe, M. Mincica, F. Zito, A. Tognetti, A. Lanata, and D. De Rossi, “Soc cmos uwb pulse radar sensor for contactless respiratory rate monitoring,” *IEEE Transactions on Biomedical Circuits and Systems*, vol. 5, no. 6, pp. 503–510, 2011.
- [7] T. Lauteslager, M. Maslik, F. Siddiqui, S. Marfani, G. D. Leschziner, and A. J. Williams, “Validation of a new contactless and continuous respiratory

- rate monitoring device based on ultra-wideband radar technology,” *Sensors*, vol. 21, p. 4027, Jun 2021.
- [8] M. van Gastel, S. Stuijk, S. Overeem, J. P. van Dijk, M. M. van Gilst, and G. de Haan, “Camera-based vital signs monitoring during sleep – a proof of concept study,” *IEEE Journal of Biomedical and Health Informatics*, vol. 25, no. 5, pp. 1409–1418, 2021.
- [9] “Garmin.” <https://www.garmin.com>. visited on 20.02.2023.
- [10] E. D. Chinoy, J. A. Cuellar, K. E. Huwa, J. T. Jameson, C. H. Watson, S. C. Bessman, D. A. Hirsch, A. D. Cooper, S. P. A. Drummond, and R. R. Markwald, “Performance of seven consumer sleep-tracking devices compared with polysomnography,” *Sleep*, vol. 44, 12 2020.
- [11] M. Tenhunen, E. Elomaa, H. Sistonen, E. Rauhala, and S. L. Himanen, “Emfit movement sensor in evaluating nocturnal breathing,” *Respiratory Physiology & Neurobiology*, vol. 187, pp. 183–189, 6 2013.
- [12] “Emfit.” <https://www.emfit.com>. visited on 19.02.2023.
- [13] “Developing a robotic platform to improve the quality of sleep.” <https://www.news-medical.net/news/20220318/Developing-an-autonomous-robotic-platform-to-improve-the-quality-of-sleep.aspx>. visited on 12.02.2023.
- [14] “Sensomative.” <https://sensomative.com/en/>. visited on 13.10.2022.
- [15] “Sensing Tex.” <https://sensingtex.com/>. visited on 13.10.2022.
- [16] “Wireless and Portable Polysomnography Device: Nox A1 PSG System.” <https://noxmedical.com/products/nox-a1-psg-system/>. visited on 13.02.2023.
- [17] C. Chourpiliadis and A. Bhardwaj, “Physiology, Respiratory Rate,” *StatPearls*, 9 2022.
- [18] G. Yuan, N. A. Drost, and R. A. McIvor, “Respiratory rate and breathing pattern,” *McMaster Univ. Med. J*, vol. 10, no. 1, pp. 23–25, 2013.
- [19] “Manuel Fujs – Sensory-Motor Systems Lab — ETH Zurich.” https://sms.hest.ethz.ch/the-group/team/manuel_fujs.html.
- [20] H. R. Colten and B. M. Altevogt, “Sleep Disorders and Sleep Deprivation: An

- Unmet Public Health Problem,” *Sleep Disorders and Sleep Deprivation: An Unmet Public Health Problem*, pp. 1–404, 10 2006.
- [21] A. K. Patel, V. Reddy, K. R. Shumway, and J. F. Araujo, “Physiology, Sleep Stages,” *StatPearls*, 9 2022.
 - [22] “Stages of Sleep: What Happens in a Sleep Cycle — Sleep Foundation.” <https://www.sleepfoundation.org/stages-of-sleep#references-175856>. visited on 10.03.2023.
 - [23] J. Yordanova, V. Kolev, U. Wagner, and R. Verleger, “Differential associations of early- and late-night sleep with functional brain states promoting insight to abstract task regularity,” *PloS one*, vol. 5, 2 2010.
 - [24] B. Baran, E. F. Pace-Schott, C. Ericson, and R. M. Spencer, “Processing of Emotional Reactivity and Emotional Memory over Sleep,” *Journal of Neuroscience*, vol. 32, pp. 1035–1042, 1 2012.
 - [25] C. J. Fisher, “Physiology of respiration,” *Emergency Medicine Clinics of North America*, vol. 1, no. 2, pp. 223–239, 1983.
 - [26] C. A. Del Negro, G. D. Funk, and J. L. Feldman, “Breathing matters,” *Nature Reviews Neuroscience* 2018 19:6, vol. 19, pp. 351–367, 5 2018.
 - [27] K. E. Barrett, S. Boitano, S. M. Barman, and H. L. Brooks, “Ganong’s review of medical physiology twenty,” p. 588, 2010.
 - [28] W. Hong, A. Earnest, P. Sultana, Z. Koh, N. Shahidah, and M. E. H. Ong, “How accurate are vital signs in predicting clinical outcomes in critically ill emergency department patients,” *European Journal of Emergency Medicine*, vol. 20, pp. 27–32, 2 2013.
 - [29] J. F. Fieselmann, M. S. Hendryx, C. M. Helms, and D. S. Wakefield, “Respiratory rate predicts cardiopulmonary arrest for internal medicine inpatients,” *Journal of General Internal Medicine*, vol. 8, pp. 354–360, 7 1993.
 - [30] C. P. Subbe, R. G. Davies, E. Williams, P. Rutherford, and L. Gemmell, “Effect of introducing the Modified Early Warning score on clinical outcomes, cardiopulmonary arrests and intensive care utilisation in acute medical admissions*,” *Anaesthesia*, vol. 58, pp. 797–802, 8 2003.
 - [31] J. V. Rundo and R. Downey, “Chapter 25 - polysomnography,” in *Clinical*

- Neurophysiology: Basis and Technical Aspects* (K. H. Levin and P. Chauvel, eds.), vol. 160 of *Handbook of Clinical Neurology*, pp. 381–392, Elsevier, 2019.
- [32] “Electroencephalogram (EEG) — Johns Hopkins Medicine.” <https://www.hopkinsmedicine.org/health/treatment-tests-and-therapies/electroencephalogram-eeg>. visited on 14.03.2023.
- [33] D. J. Creel, “Chapter 33 - the electrooculogram,” in *Clinical Neurophysiology: Basis and Technical Aspects* (K. H. Levin and P. Chauvel, eds.), vol. 160 of *Handbook of Clinical Neurology*, pp. 495–499, Elsevier, 2019.
- [34] “Electromyography (EMG) — Mayo Clinic.” <https://www.mayoclinic.org/tests-procedures/emg/about/pac-20393913>. visited on 13.03.2023.
- [35] “Electrocardiogram (ECG) - NHS.” visited on 17.03.2023.
- [36] “Pulse Oximetry — Johns Hopkins Medicine.” visited on 17.03.2023.
- [37] S. J. Heitman, R. S. Atkar, E. A. Hajduk, R. A. Wanner, and W. W. Flemons, “Validation of nasal pressure for the identification of apneas/hypopneas during sleep,” *American journal of respiratory and critical care medicine*, vol. 166, no. 3, pp. 386–391, 2002.
- [38] G. Brüllmann, K. Fritsch, R. Thurnheer, and K. E. Bloch, “Respiratory Monitoring by Inductive Plethysmography in Unrestrained Subjects Using Position Sensor-Adjusted Calibration,” *Respiration*, vol. 79, pp. 112–120, 12 2010.
- [39] J. Calleja, S. Esnaola, R. Rubio, and J. Durán, “Comparison of a cardiorespiratory device versus polysomnography for diagnosis of sleep apnoea,” *European Respiratory Journal*, vol. 20, no. 6, pp. 1505–1510, 2002.
- [40] A. Tataraidze, L. Anishchenko, L. Korostovtseva, B. J. Kooij, M. Bochkarev, and Y. Sviryaev, “Sleep stage classification based on respiratory signal,” in *2015 37th Annual International Conference of the IEEE Engineering in Medicine and Biology Society (EMBC)*, pp. 358–361, 2015.
- [41] S. Redmond and C. Heneghan, “Cardiorespiratory-based sleep staging in subjects with obstructive sleep apnea,” *IEEE Transactions on Biomedical Engineering*, vol. 53, no. 3, pp. 485–496, 2006.
- [42] M. Holtzman, D. Townsend, R. Goubran, and F. Knoefel, “Validation of

BIBLIOGRAPHY

- pressure sensors for physiological monitoring in home environments,” *2010 IEEE International Workshop on Medical Measurements and Applications, MeMeA 2010 - Proceedings*, pp. 38–42, 2010.
- [43] I. Sadek, E. Seet, J. Biswas, B. Abdulrazak, and M. Mokhtari, “Nonintrusive Vital Signs Monitoring for Sleep Apnea Patients: A Preliminary Study,” *IEEE Access*, vol. 6, pp. 2506–2514, 12 2017.
- [44] P. Chow, G. Nagendra, J. Abisheganaden, and Y. Wang, “Respiratory monitoring using an air-mattress system,” *Physiological measurement*, vol. 21, pp. 345–54, 09 2000.
- [45] K. J. Hunt, S. E. Fankhauser, and J. Saengsuwan, “Identification of heart rate dynamics during moderate-to-vigorous treadmill exercise,” *BioMedical Engineering Online*, vol. 14, pp. 1–13, 12 2015.
- [46] C. Hoog Antink, Y. Mai, R. Aalto, C. Bruser, S. Leonhardt, N. Oksala, and A. Vehkaoja, “Ballistocardiography can estimate beat-to-beat heart rate accurately at night in patients after vascular intervention,” *IEEE Journal of Biomedical and Health Informatics*, vol. 24, pp. 2230–2237, 8 2020.
- [47] I. Sadek, T. Tan Soon Heng, E. Seet, and B. Abdulrazak, “A New Approach for Detecting Sleep Apnea Using a Contactless Bed Sensor: Comparison Study,” *J Med Internet Res* 2020;22(9):e18297 <https://www.jmir.org/2020/9/e18297>, vol. 22, p. e18297, 9 2020.
- [48] W. Chen, X. Zhu, T. Nemoto, K. I. Kitamura, K. Sugitani, and D. Wei, “Unconstrained monitoring of long-term heart and breath rates during sleep,” *Physiological Measurement*, vol. 29, p. N1, 1 2008.